UDK 621.3:(53+54+621+66)(05)(497.1)=00 ISSN 0352-9045

INFORMACIJE MIDEM 2 ◦ 1994

Strokovno društvo za mikroelektroniko elektronske sestavne dele in materiale

Časopis za mikroelektroniko, elektronske sestavne dele in materiale
Časopis za mikroelektroniku, elektronske sastavne dijelove i materijale
Journal of Microelectronics, Electronic Components and Materials

INFORMACIJE MIDEM, LETNIK 24, ŠT. 2(70), LJUBLJANA, junij 1994

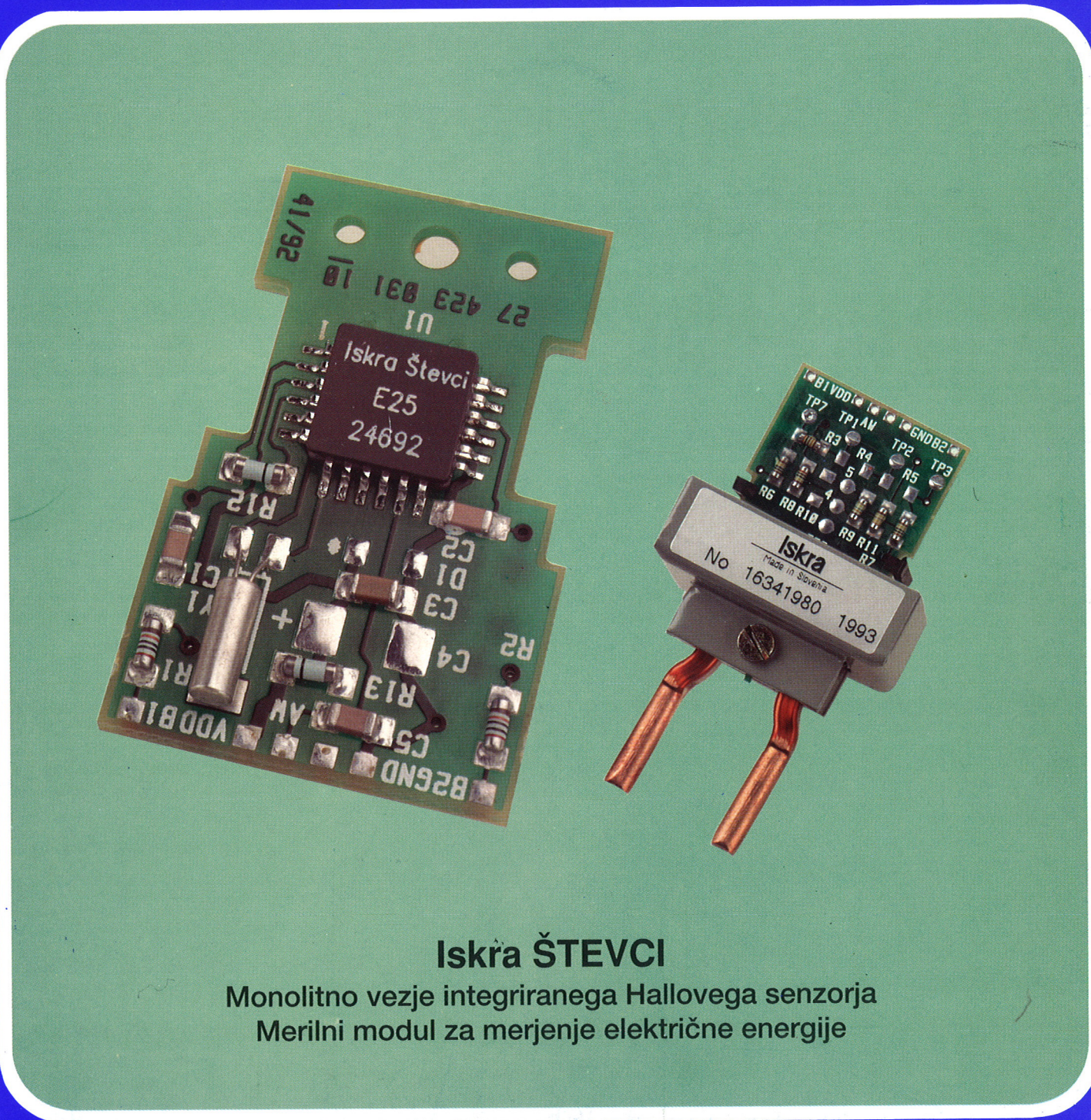

Iskra ŠTEVCI

Monolitno vezje integriranega Hallovega senzorja
Merilni modul za merjenje električne energije

INFORMACIJE MIDEM 2 ° 1994

INFORMACIJE MIDEM	LETNIK 24, ŠT. 2(70), LJUBLJANA,	JUNIJ 1994
INFORMACIJE MIDEM	GODINA 24, BR. 2(70), LJUBLJANA,	JUN 1994
INFORMACIJE MIDEM	VOLUME 24, NO. 2(70), LJUBLJANA,	JUNE 1994

Izdaja trimesečno (marec, junij, september, december) Strokovno društvo za mikroelektroniko, elektronske sestavne dele in materiale.
Izdaja tromjesečno (mart, jun, septembar, decembar) Stručno društvo za mikroelektroniku, elektronske sastavne dijelove i materiale.
Published quarterly (march, june, september, december) by Society for Microelectronics, Electronic Components and Materials - MIDEM.

Naslov uredništva
Adresa redakcije
Headquarters
Uredništvo Informacije MIDEM
Elektrotehniška zveza Slovenije
Dunajska 10, 61000 Ljubljana, Slovenija
(0)61 - 316 886

Letna naročnina znaša 7000,00 SIT, cena posamezne številke je 1750,00 SIT. Člani in sponzorji MIDEM prejemajo Informacije MIDEM brezplačno.
Godišnja pretplata iznosi 7000,00 SIT, cijena pojedinog broja je 1750,00 SIT. Članovi i sponzori MIDEM primaju Informacije MIDEM besplatno.
Annual subscription rate is DEM 100, separate issue is DEM 25. MIDEM members and Society sponsors receive Informacije MIDEM for free.

Znanstveni svet za tehnične vede l je podal pozitivno mnenje o časopisu kot znanstveno strokovni reviji za mikroelektroniko, elektronske sestavne dele in materiale. Izdajo revije sofinanci rajo Ministrstvo za znanost in tehnologijo in sponzorji društva.
Scientific Council for Technical Sciences of Slovene Ministry of Science and Technology has recognized Informacije MIDEM as scientific Journal for microelectronics, electronic components and materials.
Publishing of the Journal is financed by Slovene Ministry of Science and Technology and by Society sponsors.

Znanstveno strokovne prispevke objavljene v Informacijah MIDEM zajemamo v:
* domačo bazo podatkov ISKRA SAIDC-el, kakor tudi
* v tujo bazo podatkov INSPEC
Scientific and professional papers published in Informacije MIDEM are assessed into:
* domestic data base ISKRA SAIDC-el and
* foreign data base INSPEC

Po mnenju Ministrstva za informiranje št.23/300-92 šteje glasilo Informacije MIDEM med proizvode informativnega značaja, za katere se plačuje davek od prometa proizvodov po stopnji 5 %.

Grafična priprava in tisk
Grafička priprema i štampa
Printed by
BIRO M, Ljubljana

Naklada
Tiraž
Circulation
1000 izvodov
1000 primjeraka
1000 issues

UDK621.3:(53+54+621+66),ISSN0352-9045 Informacije MIDEM 24(1994)2,Ljubljana

VSEBINA CONTENT

SLOVENIAN PROJECT "YOUNG RESEARCHERS"

As early as in the 1985 Slovenian Ministry for Science and Technology started a project "Young researchers". The main scope of the project was to stimulate the introduction of young industrial researchers in the scientific field of Slovenia. This project, after nearly 10 years, is probably the most successful project in Slovenia.

Ministry grants to the scientific organisation in which the young researcher makes his stage the expenses of his salary. After the scientific stage the researcher is supposed to work for the company where he came from.

There are three different levels of the stage. A two year stage in a scientific or research organisation with no academic title reached after the stage. Only an internal "specialist" nomination is given. A three year Slovenian master of science stage is the next possibility related also to formal study on one of the faculties, with reaching the Slovenian title "magister of science". Another two year stage in connection with the university can bring the researcher to the title of "doctor of science".

In the field of Electronic components and technology, 61 researchers participated in the project. 34 of them reached their goal, no one missed it. 7 researchers were given the doctor's title, 20 the master's one and 7 specialist nomination. 27 stages are still running.

Where are working the researchers who finished the project? 19 remain in the research institute, 13 are employed in the industry and 2 are abroad. This means 50% of the final scope was reached but it is to mention that this result is influenced by the crises in Slovenian industry which is not able to receive all researchers back. (For example Iskra reduced employment from 36.000 units to less than 12.000).

There are four research institutions acting on the project in the electronic components and technology field: Faculty for Electronic and computer sciences with five laboratories (FER), Faculty for machine engineering, Institute for electronic and vacuum technology (IEVT) and Mikroiks (a private research company). Most of the young researchers are doing or they made their stage in the laboratories leading by L. Trontelj and J.Furlan on the FER and B.Jenko on the IEVT.

The data given here are published for the first time and I hope you find them at least interesting. Personally I hope the project will continue with the same success.

MIDEM Society President
Dr. Rudolf Ročak

OPTICAL AMPLIFIER IN COMMUNICATION NETWORKS. CURRENT APPLICATIONS AND PERSPECTIVES

S. Cecchi, G. Randone and S. Rotolo
Italtel, Central Research Laboratories
Castelletto di Settimo Milanese, Milano (Italy)

Keywords: communication networks, optical networks, optical technologies, optical amplifiers, basic principles, state of the art, practical applications, EDFA amplifiers, SOA amplifiers

Abstract: Optical amplifiers may be considered one of the most significant innovation in the field of optical communication technologies, as they will allow to overcome in principle several current bottlenecks in the evolution of optical networks. In this paper, basic aspects of optical amplifier operation will be reviewed, and their use in different network applications will be discussed.[1]

Optični ojačevalnik v komunikacijskih omrežjih. Uporaba in bodočnost

Ključne besede: omrežja komunikacijska, omrežja optična, tehnologije optične, ojačevalnik optični, osnove, stanje razvoja, aplikacije praktične, EDFA ojačevalniki, SOA ojačevalniki

Povzetek: Optični ojačevalniki so ena najbolj pomembnih inovacij na področju optičnih komunikacijskih tehnologij, saj bodo v principu omogočili premagovanje nekaj ozkih grl pri razvoju optičnih omrežij. V tem prispevku smo opisali osnovne principe delovanja optičnih ojačevalnikov, kakor tudi njihovo praktično uporabo v različnih komunikacijskih omrežjih.

1. INTRODUCTION

After more than 20 years of continuous progress, optical fibre transmission systems have become the dominant technology for telecommunication networks. At present, more than 50% of long haul traffic in high developed industrial countries is routed through optical cables; the overall volume of optical fibres already installed world-wide is approximately 50 million-km.

In spite of the fact that optical communications can be considered a well established and mature technology, a strong evolution is still taking place both as regards new devices development and proposals for new system concepts; the reason is that, for the time being, only Long Distance Transmission, among the main sectors of a communication network, has been fully involved in taking advantage from optical technology; while the others (Switching and Customer Access) still remain quite far from achieving similar results, and strong interest exists to bridge this gap.

Extending the penetration of optical technologies to switching functions and access systems may in fact trigger a potential revolution in the network performance and effectiveness, resulting from a very high increase in data throughput and from an overall optical compatibility. In particular, penetration of optical fibres in the local loop will create access for everybody to a cost-effective almost unlimited bandwidth.

The ultimate objective of a fully optical network cannot be considered of course within easy reach of currently available technologies: optical switching, for instance, still requires some fundamental advance in optical processing to become a practical opportunity. Other constraints, not less important than technical problems, are limiting the growth of optical technologies in the access network, as cost, market competitions, lack of international standards, and it is beyond the scope of this paper to discuss these aspects in more detail.

Even if the progress route may be still very long, the development of the optical amplifier can be considered a major milestone along this route, similar in nature to other fundamental breakthrough, like the CW operation of the semiconductor laser and the development of a low loss optical fibre, at the beginning of years '70. The use of the Erbium-Doped-Fibre-Amplifier (EDFA) high gain and low noise properties result in a dramatic improvement in performances of optical links; but in addition the optical amplification principle makes possible to forecast

[1]This paper is the first of a series, which will be presented on MIDEM during 1994, concerning advanced topics in optical technologies and systems. The next contribution will deal with optical interconnections and integrated optics, and the last one will discuss a specific application to multiwavelength transport networks

the practical implementation of a number of optical network architectures, which were considered until now only in terms of theoretical or laboratory feasibility.

In the following, operating characteristics, design criteria and different applications for optical amplifiers will be reviewed.

2. OPTICAL AMPLIFIER CHARACTERISTICS

Optical gain in an inverted population medium is a well-known process; when the gain is controlled by the optical feedback of a resonant cavity, a laser oscillation sets up; when the feedback mechanism is suppressed, the active medium is able to amplify an incoming optical signal. The amplification process depends on several parameters: the spectral gain profile, the optical signal wavelength, the structure and relaxation time of excited levels in the active material and the excitation mechanism for the population inversion.

The structure of a very high power laser (in nuclear fusion research, for instance) is based actually on a master laser oscillator and a cascade of several bulk amplifier stages, which are able to reach optical pulse power in excess of GWatts.

The optical amplifier for communication applications is based on the same principles, but includes a specific important feature, which makes possible to control very precisely the amplification parameters like gain and noise with high overall efficiency. This result has been obtained by using a dielectric waveguide for optical confinement of the active medium. In particular the waveguide can be realised by an optical fibre or by the active region of a semiconductor laser. The optical confinement in the core region of the waveguide is very effective in allowing a high degree of control in the design parameters of the amplifier, like the active material volume, the overall gain, the coupling of the excitation pump. Moreover, the nearly ideal matching of the active fibre with the fibre used in the communication network makes almost straightforward the add-on of this new device into the existing equipment.

The careful optimisation and matching of these parameters, which has been the subject of an intense development activity in the past 5 years /1/ /2/, has given finally to the communication engineers the real opportunity to achieve, for the first time, the control of the optical carrier in the electromagnetic regime, without being obliged to step back and forth to the low frequency scalar components of the field (voltage and current) for signal amplification purposes. This is the real meaning of the conceptual innovation introduced by the guided optical amplifier, which opens the way to implement a wide range of new data processing methods in the optical domain.

To discuss the amplifier characteristics in more detail let focus on the fibre structure first.

2.1 Fibre amplifier

The structure of an Optical Fibre Amplifier (OFA, Fig. 1) is very simple in principle; it includes a short length (a few meters) of active fibre, a wavelength division multiplexer to couple into the active fibre the signal optical carrier and the pump intensity, an optical isolator on the output port, in order to avoid any parasitic light reflection which may cause spurious laser oscillation in the active medium and a pump source; due to the high gain available, isolation in the range of 50 ÷ 60 dB is usually required, and therefore the isolator is quite critical for a correct operation of the amplifier.

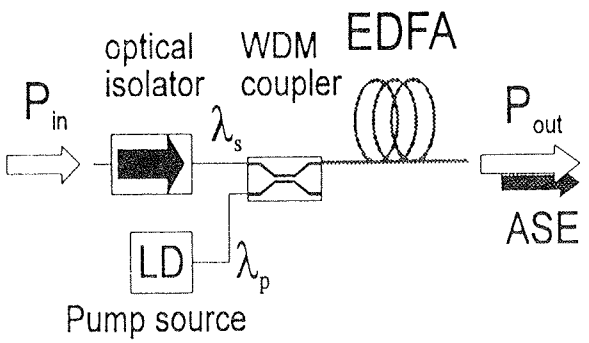

Fig. 1: Optical fibre amplifier: schematic block diagram

Let discuss in some detail the OFA components:

– active fibre

The principle of using a guided structure for increasing the efficiency of the optical gain in an inverted medium is indeed very old. As early as in 1963 /3/, for instance, well before the introduction of fibres for communication purposes, a Nd doped fibre was realised to demonstrate the possibility of high optical gain at λ = 1060 nm.

At present, two wavelength bands are considered for optical amplifiers, at λ = 1300 and 1550 nm; a number of so called Rare Earth Elements in the Periodic Table can have the appropriate electronic levels structure to allow for stimulated emission at the required wavelengths: most popular examples are Praseodymium for the 1300 nm band and Erbium for the 1550 nm band. Efficient doping with Er has been achieved in silica-based fibre /4/, while fluoride glasses /5/, of the so called ZBLAN family, have been investigated for Praseodymium doping. Optical amplifiers with Erbium doped fibres have become available commercially since 1991, while Praseodymium doped fibres still remain at the stage of a research product. Only very recently (at the Optical Fibre Communications Conference, February 1994) Hewlett-Packard has announced the first commercial amplifier for the 1300 nm optical band. In the following discussion only Erbium doped amplifiers will be considered.

Even for the relatively well known Erbium Doped Fibre Amplifier (EDFA), quite a work for optimisation of fibre material characteristics and structure is currently under way; the objectives of this work are the increase of the saturated power and saturated gain, a wider and flat spectral gain profile and a better pump efficiency. Methods to achieve these results may involve the use of co-dopants, like Al and Yb, to increase the spectral bandwidth and the pump energy transfer, an increase of the fibre Numerical Aperture and a reduction of the core diameter in order to increase the power density along the signal path. Process technology still needs definite improvements to control these effects (In particular co-doping), in order to satisfy design specifications and achieve a good level of reproducibility .

– WDM coupler

To couple into the active fibre the pump power, a wavelength sensitive coupler is required to achieve a minimum signal loss at λ_{sig} , and a maximum power transfer at the pump wavelength. In the most widely used configuration, the coupler is based on the directional coupler principle /6/; two fibres are fused together and pulled apart in order to bring in a close proximity the fibre cores for a well defined coupling length. A coupled mode propagation regime takes place, which causes a periodic power transfer back and forth between the fused fibres. As the transfer period (beat length) depends on the wavelength, it is usually possible to find a coupling length at which the required power transfer takes place with defined transfer ratio for two selected wavelengths.

Very good and reproducible results are usually obtained by a real time monitoring of the power transfer at the specific wavelengths during the fibre fusion process. The fused fibre Wavelength Division Multiplexer is a simple, reliable and inexpensive solution, fully adequate for 1550 nm EDFA amplifiers operating with 980 nm pump wavelength, with insertion loss of the order of 0,2 dB and extinction ratio better than 20 dB. Less satisfactory performance is available for operation with 1480 nm pump, rather close to the signal wavelength: in this case, to achieve the required extinction ratio a cascade of two or more identical WDMs may be necessary.

– optical isolator

Optical isolation is increasingly important in many fiber applications, as laser sources may show instabilities and intensity noise, if even a negligible fraction of the optical power is reflected back into the laser optical resonator. To avoid these parasitic effects, optical isolators are needed with an isolation ratio ranging from 30 to 60 dB.

The Faraday rotation (e. g. the non reciprocal rotation of the polarisation plane when the light propagates through certain crystals placed in a magnetic field, with the Poynting vector aligned to the field) is the effect on which most of optical isolators are based. The isolator basic structure includes at the input port a linear polariser, a Faraday rotator which rotates the polarisation plane by 45° and an output polariser aligned with this direction; any reflected light will be polarised at 90° with respect to the input polariser and not transmitted. The actual structure of an optical isolator is much more complex, in order to compensate for the dependence on temperature, wavelength and input light polarisation state. Other critical parameters are the extinction ratio of the polariser, the Verdet constant of the material for the Faraday rotator and finally the permanent magnet for the magnetic field. Therefore, a good isolator still remains quite an expensive component, and its cost account for a sizeable part of the full cost of the amplifier.

– pump sources

High power laser diodes are used as pump sources for optical amplifiers. Pump wavelengths can be chosen at 800, 980 and 1480 nm for the Er doped amplifier. Initially the 1480 pump wavelength was preferred because laser diode reliability was better assessed for the already developed InGaAsP/InP heterostructure system. Better performance may be achieved with pumping at 980 nm, as far as noise figure and efficiency are concerned /7/; moreover, 980 nm InGaAs/GaAs quantum well strained-lattice laser diodes with output power in excess of 250 mW are becoming available with increasing confidence about their reliability. Both 980 and 1480 nm pump wavelength are still used with increasing interest for the 980 nm operation.

At present, the choice of a specific pump wavelength imposes a number of compromises on other parameters of amplifier components (for instance, on the WDM coupler and on the fundamental mode cut-off of the active fibre and related bend losses), and a comprehensive evaluation of the best compromise is still under investigation.

2.2 Semiconductor optical amplifier

The Semiconductor Optical Amplifier (SOA, Fig. 2) is a basically different device with respect to the OFA, both in terms of its fabrication technology, and for its rather long term application potential.

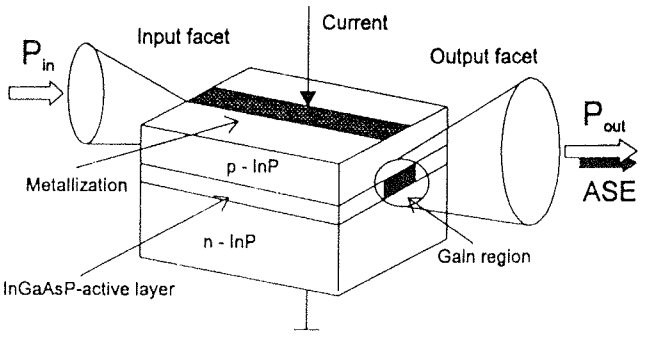

Fig. 2: Semiconductor optical amplifier: schematic block diagram

In practice, a semiconductor optical amplifier is basically built with the same technology required for a semiconductor laser, with one non trivial addendum: the need for a full suppression of the optical cavity feedback, which may be obtained by an efficient AR coating and by a tilting of the cavity axis with respect to the mirror facets. At present the SOA can not be considered as a practical alternative to the fibre amplifier, due to several disadvantages in its operation: among them the gain sensitivity to the polarisation of the input signal, the ripple in the spectral gain profile due to the residual reflectivity of the chip mirrors, which still can not be controlled to the required extent, and the high insertion losses due to the fibre pig-tailing, which negatively affects the amplifier noise figure. Moreover, the SOA may be affected by cross-talk effects from different wavelength channels and in the case of high speed modulation data transmission, due to the very short (1 ns) carrier lifetime. (In the case of the OFA, the equivalent parameter is of the order of several ms). A comparison between the two devices' characteristics is reported in the following table (Tab.1):

	SOA	EDFA	
GAIN	> 30 dB	> 40 dB	
PUMP EFFICIENCY	> 0,5 dB/mA	10 dB/mW	@ 980 nm
		5 dB/mW	@ 1480 nm
EXCITED STATE LIFETIME	1 ns	10 ms	
WAVELENGTH RANGE	700 - 1600 nm	1520 - 1580 nm	
INSERTION LOSS	5 - 6 dB	0,5 dB	
OPTICAL BANDWIDTH	> 40 nm	> 20 nm	
NOISE FIGURE	5 - 6 dB	3 dB	@ 980 nm
		6 dB	@ 1480 nm
SATURATION POWER	> 10 dBm	> 27 dBm	
POLARISATION SENSITIVITY	YES	NO	
CROSS-TALK SENSITIVITY	YES	NO	
OEIC CAPABILITY	YES	NO	

Tab. 1 - Performances of Semiconductor Optical Amplifier and Erbium Doped Fibre Amplifier

Perhaps, the most interesting potential feature of the SOA is its full integration compatibility with a monolithic Opto Electronic Integrated Circuit (OEIC); even if this potential could only be exploited in the long term, the possibility of optical signals amplification is a necessary condition for considering photonic circuits a feasible target. Other interesting intrinsic features of the SOA are the high speed direct current modulation capability (which may be used for optical signal processing), the wide band (0,5 GHz) photodetection capability, which may be used to sample the data of the optical carrier being amplified. By using a diffraction grating on the active region (like in a DFB laser structure) a narrow band active optical filter can be also implemented.

Feasibility of all these features has been already experimentally demonstrated and offers a wide range of interesting opportunities in the future development of advanced optoelectronic components and system, not only for telecommunication applications, but also for optical sensors and measurement's techniques. More details on SOAs can be found in /8/.

2.3 Operating characteristics and noise properties

One of the distinct advantages of optical amplifiers is their full transparency to the optical carrier modulation format, and the possibility to operate in a multiwavelength environment (Fig. 3). This flexibility is a key factor for understanding the impressive growth of commercial applications, in a very short time with respect to the R&D results. In fact, the EDFA is suitable for immediate upgrading of an existing optical communication link, and can easily accommodate future upgrading of the link as far as bit rate or data format are concerned. These are

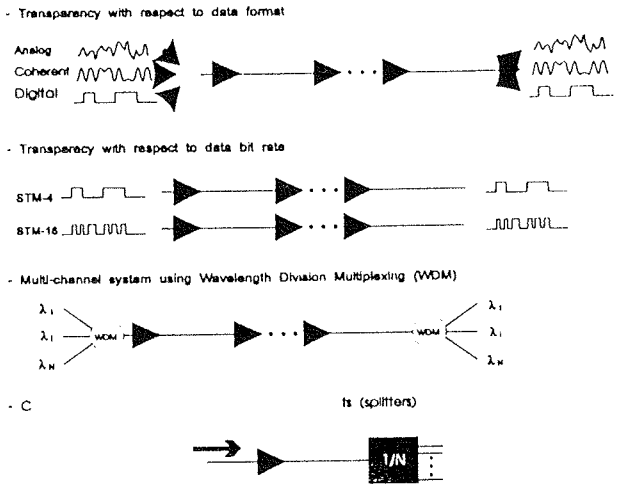

Fig. 3: Some peculiar characteristics of optical amplifier

valuable assets for Telecommunication Operators, that are always very conservative about any innovation that may cause a premature obsolescence of the huge investments already made in a network.

The EDFA can be designed for several specific functions in an optical link. It can be used as a booster on the transmitter side, to achieve high fibre input power, not available by standard semiconductor laser sources, as high gain preamplifier in front of a PIN photodetector on the receiver side, or as a line repeater. The noise figure is the relevant parameter that set a limit to the amplifier performance, at least as optical preamplifier or as line repeater.

Factors affecting the noise figure of an optical amplifier are due to the spontaneous emission, to the population inversion mechanism and to the signal losses (for coupling, residual reflectivity, absorption and scattering in the active medium). In particular, the amplified spontaneous emission (ASE), due to its wide spectral bandwidth, is causing a beat-noise in the optical detection process, due both to the signal-ASE beat and ASE- ASE beat, which set a fundamental limit of 3 dB for the noise figure of the amplifier /9/.

The noise figure (NF) is defined as the ratio between the amplifier input and output signal to noise (SNR) ratio, and is always greater than unity; in the limit of large amplified signals, NF can be written /10/ as

$$NF = \frac{2\,N(\nu_S) + |\eta_C \eta_D \eta_F(\nu_S)|^{-1}}{G(\nu_S)}$$

where η_C, η_D and η_F are the fibre-detector coupling efficiency, the detector quantum efficiency and the transmission (at ν_S) of an optical filter placed in front of the detector to limit the ASE spectral bandwidth; G is the EDFA gain and N the ASE noise, that can be written as a function of the spontaneous emission

$$N(\nu_S) = n_{sp}(\nu_S)\,(G(\nu_S) - 1)$$

where the spontaneous emission factor n_{sp} can have different expressions depending on the excitation mechanism, but it is unity when a full population inversion is achieved.

In ideal conditions for the detection process (η_C, η_D and $\eta_F = 1$), and in the high gain regime ($G >> 1$), from the above expressions results $NF \approx 2n_{sp}$; therefore, as much as full population inversion is achieved, as in the case of 980 nm pumping, the noise figure is near its limit of 3 dB. The simple concepts outlined here are very useful as practical amplifier's design rules for specific applications.

3. TECHNOLOGY AND DESIGN

A fiber optic amplifier can be designed with different criteria depending on the specific application. For digital communications saturated power is the main parameter for a booster amplifier, while small signal gain and noise figure are most important for a preamplifier and all these characteristics are relevant for a device used as line amplifier. Polarization sensitivity and polarization mode dispersion (PMD) shall also be considered, specially for analog applications, where distortion becomes the limiting factor. Gain equalization across the optical spectrum is evidently of primary importance for multiwavelength applications.

Some of these characteristics, as for example gain equalization, depend on the intrinsic properties of the active fiber. In aluminosilicate fibers for instance, due to homogeneous line broadening, the saturation spectrum is substantially broader and flatter than in other kinds of fibers /11/.

Amplifier's different architectures essentially reflect different pumping schemes (Fig. 4). Co-propagating pumping gives the best performances in terms of noise figure, as gain is higher in the first portion of the active medium, while counter-propagating and bidirectional pumping provide higher output power. With counter-propagating pumping moreover, especially in the case of 1480 nm pump wavelength, the residual pump power does not need to be filtered out from the signal line.

More sophisticated architectures can also be implemented: as an example, cascading of two stages with different gain and insertion of filters and optical isolators within the amplifying stages allow for shaping of the gain spectrum and provide improvement to the noise figure.

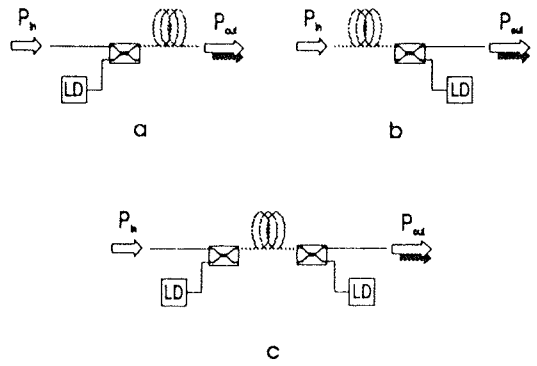

Fig. 4: Pumping schemes for EDFAs. a) co-propagating; b) counter-propagating; c) bidirectional

There are some technological limiting factors to the performances attainable from fiber optic amplifiers to date. For instance, even though it is possible in principle to increase the saturated power by cascading several amplifying stages, reliability assessments require to limit the number of pump sources, which are the most critical components from this point of view. With the most widely used pumping techniques, based on single mode laser diode sources which can provide about 150 mW from the chip at most, this sets a limit of 15-17 dBm to the power attainable from an amplifier. Losses in efficiency are caused essentially by the pigtailing of the laser with the fiber, with almost 50% coupling loss, by the intrinsic fiber efficiency (around 50% with the most recently developed active fibers) and by the insertion losses of passive components like couplers and isolators.

For high power amplifiers, a cladding pumping technique has been recently developed /12/. The radiation from the pump source is injected into a large diameter

(50 μm or more) guiding cladding sorrounding the active core. In this way high power (half watt or more) laser sources can be used.

To increase the absorption of pump radiation, Ytterbium-Erbium codoping has also been developed /13/. Ytterbium ions show a strong absorption band around 980 nm, more than 100 nm wide and excitation in this band is followed in phosphate glasses by efficient energy transfer to the resonant level of Erbium ions. The Erbium absorption cross section is therefore substituted by an effective cross section proportional to the ratio of Ytterbium to Erbium concentrations.

This mechanism is not effective in pure silica or aluminosilicate glasses, therefore a compromise between spectral characteristics and power shall be accepted. In addition the broad absorption spectrum allows for less stringent requirements on pump wavelength stability.

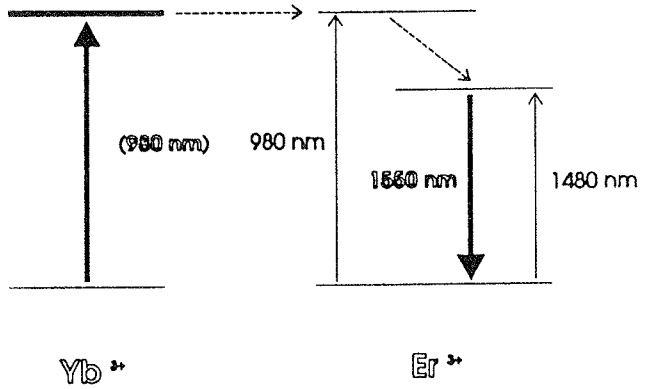

Fig. 5: Sensitization by Ytterbium-Erbium co-doping

4. APPLICATIONS AND TRENDS

4.1 Long haul

A few application schemes for long haul communication networks are illustrated in Fig. 6. Application of the EDFA to end functions (booster or optical preamplifier, Fig. 6b), in a point to point link, does not change the system design criteria. Only the use of the EDFA in a multi-repeater network application (Fig. 6d,f) affects the fundamental system characteristics and design rules. In a conventional (3R) electronic repeater technique, reshaping, retiming and regeneration functions are necessary which strictly depends on modulation formats and bit-rate. The 1R (Reshaping with available bandwidth up to 15 GHz) characteristics of the optical repeater make possible the direct handling of a full range of signals, with some care (optical band pass filters) to avoid the accumulation of ASE noise and saturation effects in a cascade of line repeater. In fact the noise figure optimisation may become the critical parameter for optical line repeater design, since for this application, both low noise and high output power capabilities are required. Other important system design aspects concern the position of the repeater along the link, which should be selected according to the best compromise between linear and saturation regime, in order to take the best advantage from the available NF of the amplifier. In the following table (Tab. 2) are reported results of a few experiments on long distance transmission with optical repeaters.

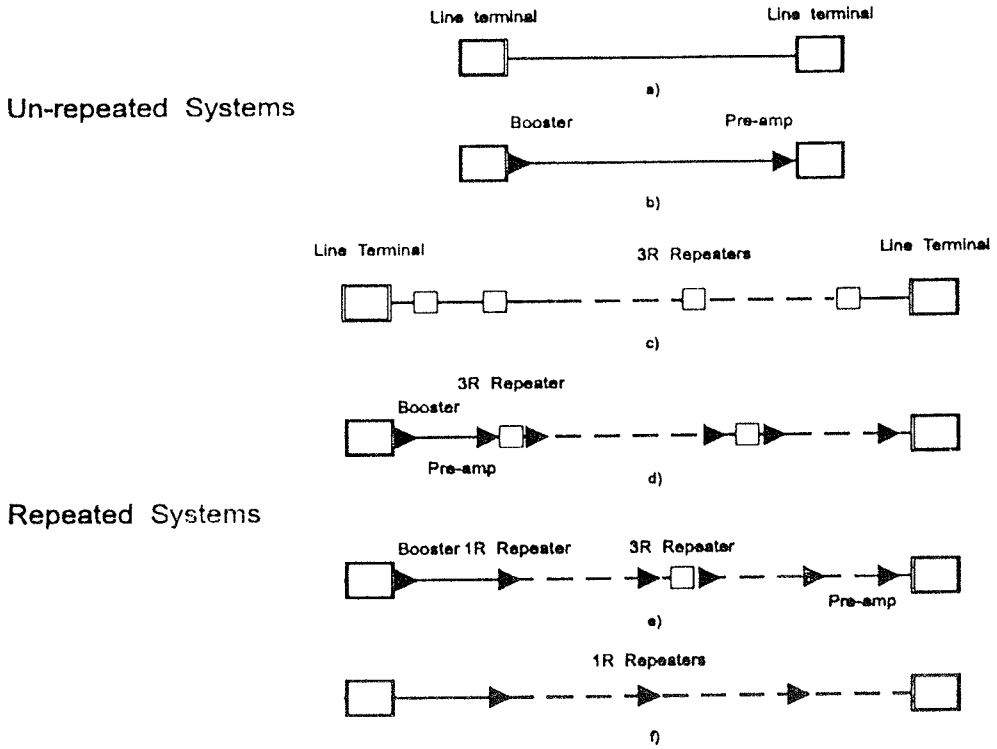

Fig. 6: Examples of application of OFAs in long haul links

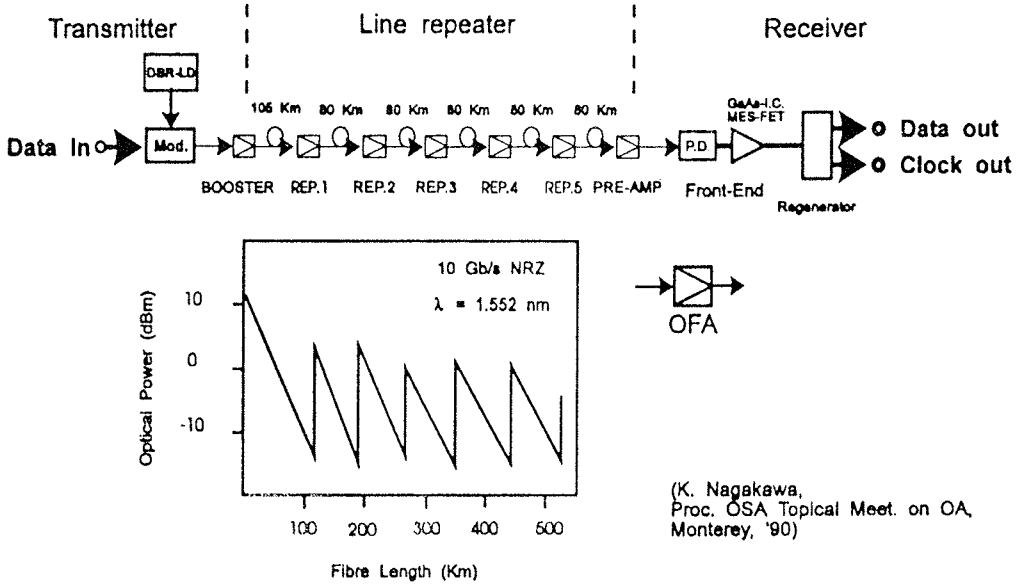

Fig. 7: Example of application of OFAs in a multi-repeater system operating at 10 GBit/s

Bit Rate (Gbit/s)	Link length (km)	N. Repeaters	Laboratory
2,5	1316	26	ALCATEL
2,5	2500	24	NTT
2,5	4500	48	NTT
5	14300	4*116 (loop)	AT & T
10	1500	22	KDD

Tab. 2- Transmission experiments with optical repeaters

A typical layout for a multi-repeater system is presented in Fig. 7, with total link span of 505 km and 5 intermediate repeaters 80 km spaced /14/. The most likely candidates for commercial applications of optical repeaters are the undersea communications: two sub-marine links equipped with EDFA both in the Atlantic (TAT-12) and Pacific (TPC-5CN) oceans, are already planned in 1995-96.

4.2 Distribution network

Characteristic topology of a distribution network is based on a point to multipoint architectures, which are schematically shown in Fig. 8. In many cases this implies that the signal power is splitted during transmission and distributed to each receiver. Therefore the available optical power is the factor which limits the maximum number of subscribers.

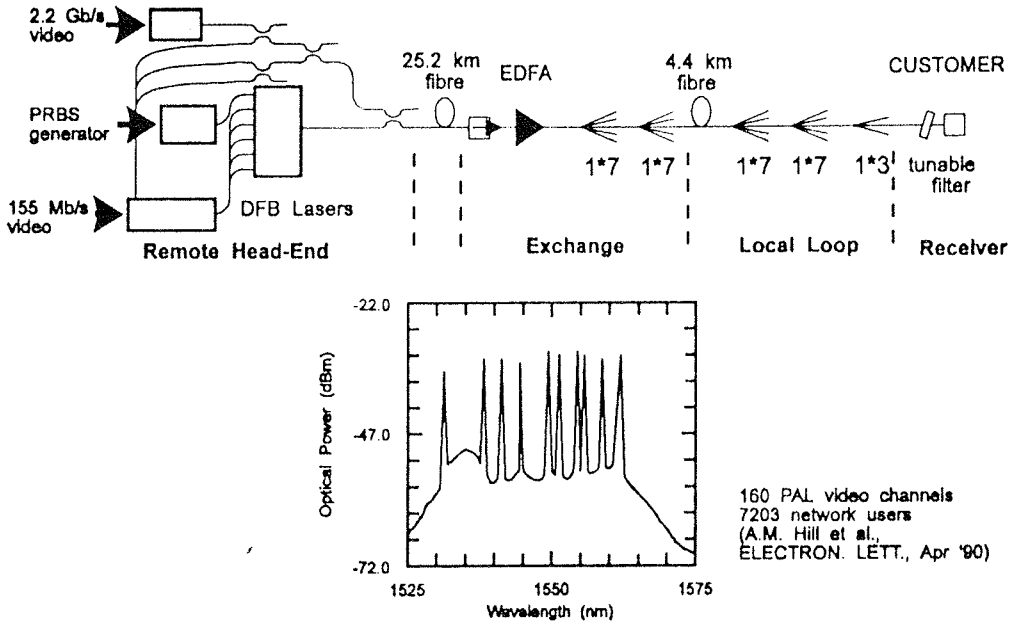

Fig. 8: Example of application of OFAs in a broadband distribution network

The high power EDFA is the natural solution to remove this limit; in principle, a 20 dB gain amplifier can increase the number of subscriber by a factor of 100, and it can be applied many times in the network when required. The low harmonic distortion and cross-modulation distortion characteristics of the EDFA are also very interesting for multiwavelength and multichannel transmission formats, which would be implemented in the future broadband distribution network. The combination of WDM techniques and multistage optical amplification has been already demonstrated /15/ potentially suitable for distributing more than 600 TV channels to more than 40 million users. Even if practical implementations of these applications still remain a quite long term target, a bright future is foreseen for the optical amplifier in the local loop.

5. CONCLUSIONS

A broad survey on optical amplifier characteristics and application features in telecom-munication networks has been presented. A wide range of very appealing opportunities for upgrading existing system performance have been already well demonstrated by field trials and laboratory experiments, but also are strongly supported by an increasing number of commercially available equipments.

While a basic understanding of optical amplifier operation has been achieved, many improvements in the fibre materials and guiding structure and in passive optical components are still actively under investigation, which may allow better performances, new design criteria and overall cost reduction. Cost is actually a limiting factor for a widespread use of optical amplifier in communication networks.

Still in the background, as far as practical applications are concerned for the time being, the semiconductor optical amplifier should not be neglected; in the medium term it may offer the right solutions for optical switching systems, where the monolithic integration of complex optical functions could be the only way for a practical system implementation.

REFERENCES

1. Review of rare earth doped fibre laser and amplifier, P. Urquhart, IEE Proc. J, 135, 1988 385.

2. Optical fibre laser and amplifier, Blackie and CRC Press, London 1991

3. Optical Processing of Information E. Snitzer, C. J. Koester, Spartan Books, Baltimore USA 1963

4. Solution doping technique for fabrication of rare-earth doped optical fibres, J. E. Townsend, S. B. Poole, D. N. Payne, Electron. Lett. 23 1987, 329

5. Rare Earth doped fluoride fibres for optical amplification, S.T. Davey et. al., Proc. SPIE 1581 1991, 144

6. Coupled mode theory for optical fibres, A. W. Snyder, J. Opt. Soc. Am. 11 1972, 1267

7. R. I. Laming, D. N. Payne, IEEE Photon. Technol. Lett. 2 1990, 418

8. Special Issue on Optical Amplifiers, IEEE J. of Ligthwave Tech., Feb. 1991

9. Semiconductor laser amplifier for single mode optical fibre communication, J. C. Simon, J. Opt. Commun., 4 1983, 51

10. Erbium doped fibre amplifiers: basic physics and characteristics, E. Desurvire, Chap 11 pag. 518, Rare Earth doped fibre lasers and amplifiers (Edited by M. Digonnet) M. Dekker NY 1993.

11. Optical and electronic properties of Rare Earth ions in glasses, W. J. Miniscalco, Chap 2 pag. 72, Rare Earth doped fibre lasers and amplifiers (Edited by M. Digonnet) M. Dekker NY 1993.

12. Nd^{3+} and Er^{3+} -doped silica fiber lasers, M. J. F. Digonnet and E. Snitzer, Chap 5 pag. 255, Rare Earth doped fibre lasers and amplifiers (Edited by M. Digonnet) M. Dekker NY 1993.

13. Nd^{3+} and Er^{3+} - doped silica fiber lasers, M. J. F. Digonnet and E. Snitzer, Chap 5 pag. 263, Rare Earth doped fibre lasers and amplifiers (Edited by M. Digonnet) M. Dekker NY 1993.

14. Optical amplifier for trunk and distribution network, K. Nakagawa, Proc. OSA Topical Meeting on optical amplifiers. (Monterey, CA) tuA1, 1990 96

15. High capacity broadcasting in the local loop with an EDFA power amplifier, A. M. Hill, D. B. Payne et al. Proc. 1st. IEEE Workshop on Passive Optical Networks, 8.2/1 London, May 1990

S. Cecchi, G. Randone and S. Rotolo
Italtel, Central Research Laboratories
Castelletto di Settimo Milanese,
Milano, Italy
tel. + 39 4388 7320
fax + 39 4388 7989

Prispelo (Arrived): 18.04.94 ***Sprejeto (Accepted): 24.05. 94***

UDK 621.3:(53+54+621+66), ISSN0352-9045 Informacije MIDEM 24(1994)2, Ljubljana

DEVICE MODELING AT LOW TEMPERATURES

Slavko Amon, Saša Sokolić, Danilo Vrtačnik
Laboratory for Electron Devices
Faculty of Electrical and Computer Engineering, University of Ljubljana

INVITED PAPER ON CAS-93, ROMANIA

Keywords: semiconductor devices, device modeling, semiconductor resistors, junction diodes, MOS capacitors, low temperatures, evaluation of results, calculation results, measurement results, testing results, comparison of results

Abstract: Device modeling at low temperatures is performed for several basic semiconductor devices (resistors, PN diodes, MOS capacitors). For the purpose of validation of calculated results, test structures were fabricated and characterized. The comparison of measured and calculated results indicates certain disagreement at low temperatures (< 30K).

Modeliranje elementov pri nizkih temperaturah

Ključne besede: naprave polprevodniške, modeliranje elementov, upori polprevodniški, diode junction, MOS kondenzatorji, temperature nizke, vrednotenje rezultatov, rezultati izračuna, rezultati meritev, rezultati preskušanja, primerjava rezultatov

Povzetek: V prispevku je predstavljeno modeliranje elementov pri nizkih temperaturah za nekatere osnovne polprevodniške strukture (upori, PN dioda, MOS kondenzatorji). Izračunani rezultati so bili preverjeni z meritvami na izdelanih testnih strukturah. Primerjava izmerjenih in izračunanih rezultatov kaže na določeno odstopanje v področju nizkih temperatur (< 30 K).

I. INTRODUCTION

Low temperature operation of semiconductor devices is gaining more and more attention in the semiconductor community. This is the consequence of several improved material properties at low temperatures that are crucial for the forthcoming solid state circuits with scaled-up complexity and performance.

At low temperatures, reduced carrier scattering results in higher carrier mobility and consequently in faster circuits. Better thermal conductivity allows greater power dissipation and therefore higher packing density and complexity. Degradation processes are scaled down many orders of magnitude leading to improved reliability and higher circuit complexity. Integration with superconducting structures is a challenge.

Excellent review papers were published recently /1,2/ giving insight into the important effects that determine device properties at low temperatures. Incomplete impurity ionization at low temperatures is still a demanding problem, especially in the case of high doping /3-8/. Carrier mobility variation with temperature is important effect for accurate modeling /9-12/. Several carrier generation-recombination effects, not very influent at room temperatures, should be taken into account at low temperatures to explain device behavior /13-16/. Internal barrier effects appearing at low temperatures are becoming important /17/. Selfheating effects can explain anomalies in electrical characteristics /18/.

In this work, the possibilities for device modeling at low temperatures were studied. For this purpose, basic test structures (resistors, junction diodes, MOS capacitors) were fabricated and measured from room temperatures to 20K. Device modeling was performed with device simulator MEDICI1.1 and process modeling with process simulator SUPREM3, both provided by TMA. Calculated results are compared with measurements and discussed.

II. RESISTORS

Resistors are interesting semiconductor devices for low temperature studies because they are relatively simple devices (Fig.1), revealing therefore clearly the important effects such as temperature dependence of mobility and impurity freeze-out.

Experimental. To study low temperature effects test resistors with three different doping levels were fabricated, measured and modeled: low-concentration (l_c) resistors, transition- concentration (t_c) resistors and high-concentration (h_c) resistors. Resistor impurity profiles are shown in Fig.2.

Resistors with *lc* and *hc* profiles were made on P-Si substrate, <100>, 16Ωcm Boron doped. Low concentration N-type resistors (*lc*) were made by ion implantation (Phosphorus, Energy 180keV, Dose 2.0e12cm-2), followed by drive-in (T = 1150°C, t=15h, ambient O2 dry).

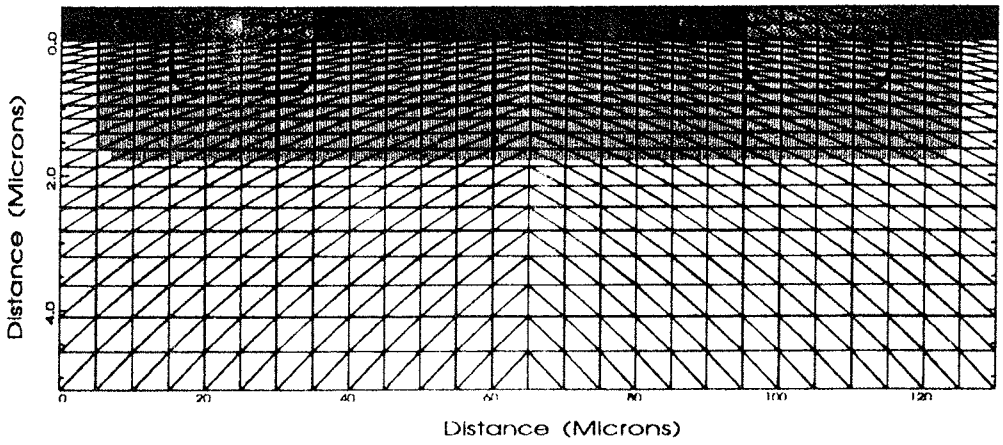

Fig. 1: Resistor structure and modeling grid

High concentration P-type resistors (h_c) were made into previously described l_c profile by an additional ion implantation (Boron, Energy 60keV, Dose 4.0e15cm-2), followed by drive-in (T = 975°C, t = 85min, ambient N2). Both profiles were measured by spreading resistance technique. The input profiles for device modeling, calculated and fitted by SUPREM3, are shown in Fig.2 as l_c and h_c profiles.

Transition-concentration P-type resistor (t_c) was made on N-type Si substrate, <100>, 10 Ωcm Phosphorus doped. Predeposition (BN975 solid diffusion source, T = 830°C, t=120min, ambient N2) was followed by drive-in (T = 1075°C, t = 120min, ambient O2 dry). The input profile for device modeling, obtained by SUPREM3 and fitted to the measurements (surface profile, sheet resistance), is shown on Fig.2 as t_c profile.

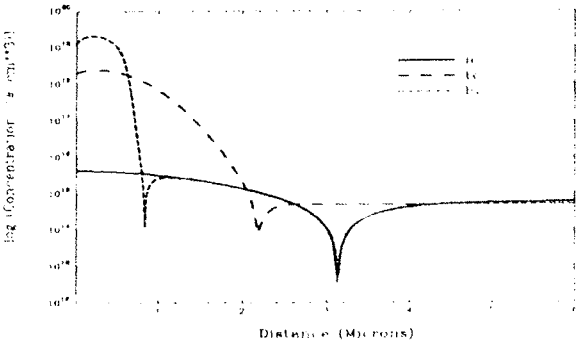

Fig. 2: Resistor impurity profiles

Mobility model. Resistance vs. temperature for different mobility models from room to low temperatures was calculated and compared with measured results (Fig.3). Different mobility models applied were /19/: concentration dependent mobility (CONMOB), analytical model introduced by Caughey and Thomas and improved by Selberherr (ANALYTIC), analytic model of Arora, et al. (ARORA), carrier- carrier scattering mobility model by Dorkel, et al. (CCSMOB), interface and bulk mobility model of Lombardi, et al. (LSMMOB), and Phu mobility model (PHUMOB).

The influence of different mobility models on the calculated resistance vs. temperature dependency can be observed from Fig.3. Variation of modeling results for different mobility models is considerable, illustrating the importance of good low temperature mobility model. It is concluded that the resistance variation with temperature (Fig.3) is best described with the model of Selberherr /20/, as shown separately in window on Fig.3a (scale unchanged). This mobility model will therefore be adopted for future calculations in this work.

Impurity freeze-out effect. The limitations of incomplete impurity ionization model is the next question of importance. Since the temperature dependency of incomplete ionization model directly influences the carrier freeze-out, it seems to be most important model for accurate device modeling at low temperatures. Therefore a brief description of possibilities for the incomplete impurity ionization modeling is given. Standard expressions for ionized impurity concentration ND^+, NA^- in the incomplete impurity ionization model are /19/

$$N_D^+ = \frac{N_D}{1 + GCB\exp\frac{E_{Fn} - E_D}{kT}} \quad (1)$$

$$N_A^- = \frac{N_D}{1 + GVB\exp\frac{E_A - E_{Fp}}{kT}} \quad (2)$$

where N_D, N_A are total donor and acceptor impurity concentrations, E_{Fn}, E_{Fp} Fermi electron and hole levels, E_D, E_A donor and acceptor energy levels, and GCB,GVB degeneracy factors for conduction and acceptor bands, respectively.

It is well known /3/ that (1) and (2) do not describe the deionization of impurities in the heavily doped regions correctly. Application of (1) in the heavily doped N^+

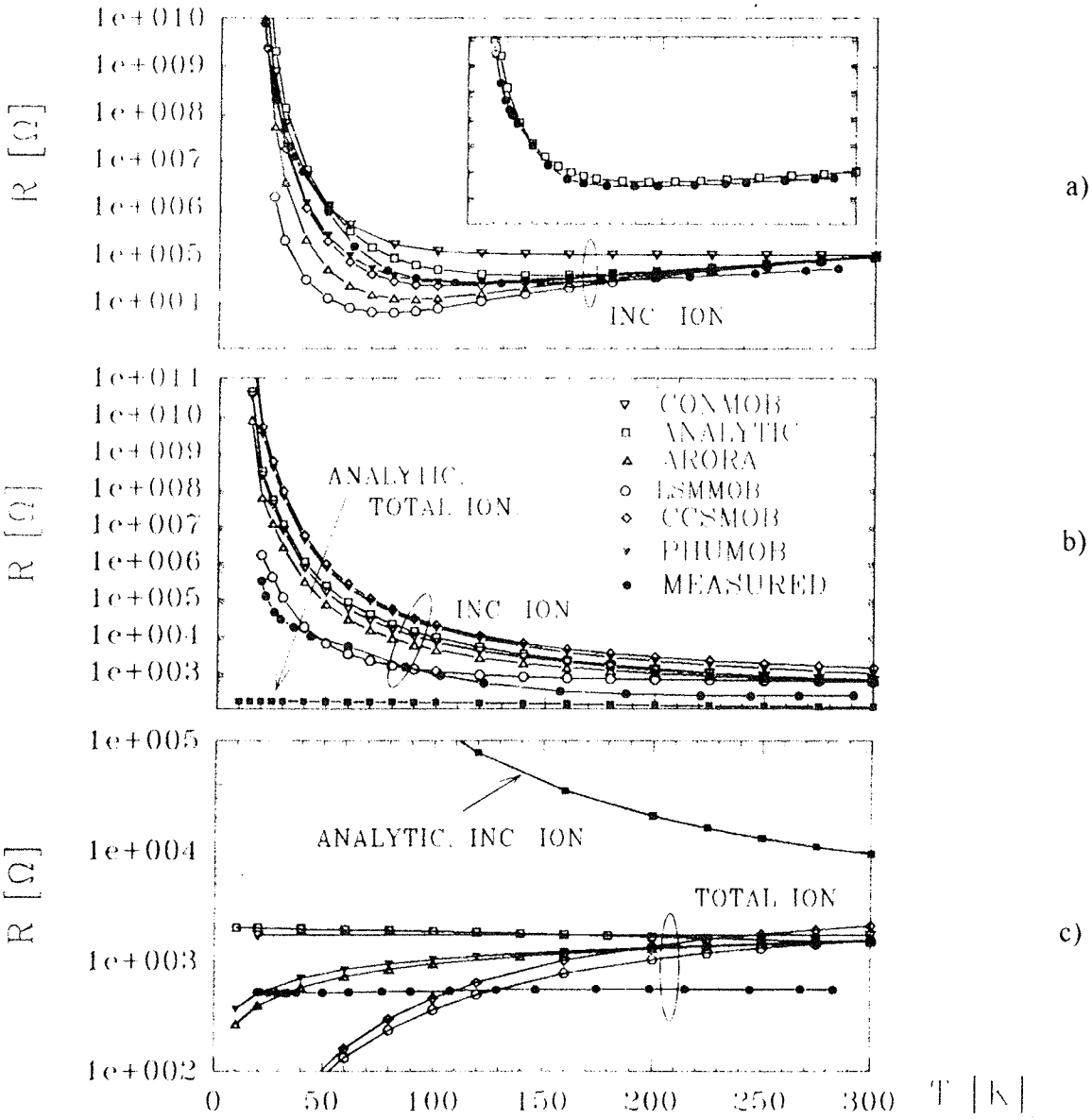

Fig. 3: Measured and calculated resistance vs. temperature for lc(a), tc(b) and hc(c) resistor

region modeling leads to significant discrepancies between actual N_{D+} and calculated ND+ /22/. Regions of lower doping concentration (< 1e18cm-3) can be described adequately with (1) and have therefore semiconductor nature of freeze-out. Regions of higher doping concentration (> 1e19cm-3) are metallic in nature, not revealing any impurity freeze-out even at low temperatures, and therefore are better described with the total ionization assumption /8,21/. Modeling in the transition region (1e18 - 1e19 cm-3) is not straightforward. Actual ND+ probably lies somewhere between ND+ as calculated by (1) and ND. By decreasing the temperature, the uncertainty of N_{D+} in the transition region even increases. Similar conclusions hold for P^+ regions. This model inadequacy results in inaccurate low temperature modeling of devices with dominant transition concentration region.

It can be seen from Fig.3 that for lower doping concentrations standard model for incomplete impurity ionization (1,2) performs well resulting in reasonable agreement between measured and modeled values (Fig.3a). For transition region of doping concentrations (1e18-1e19 cm-3), the model for incomplete impurity ionization (1,2) fails to give adequate results (Fig.3b). The model fails completely at high doping concentrations above 1e19cm-3 where the only possibility to get correspondence between measured and modeled results is to assume total impurity ionization (Fig.3c).

III. JUNCTION DIODES

Experimental. To study low temperature behavior of junction diodes, N^+P structures with impurity profile shown in Fig.4 were fabricated. Impurity predeposition step (BN975 solid diffusion source, T=930°C, t=40min, ambient N2) was followed by drive-in (T=850°C,

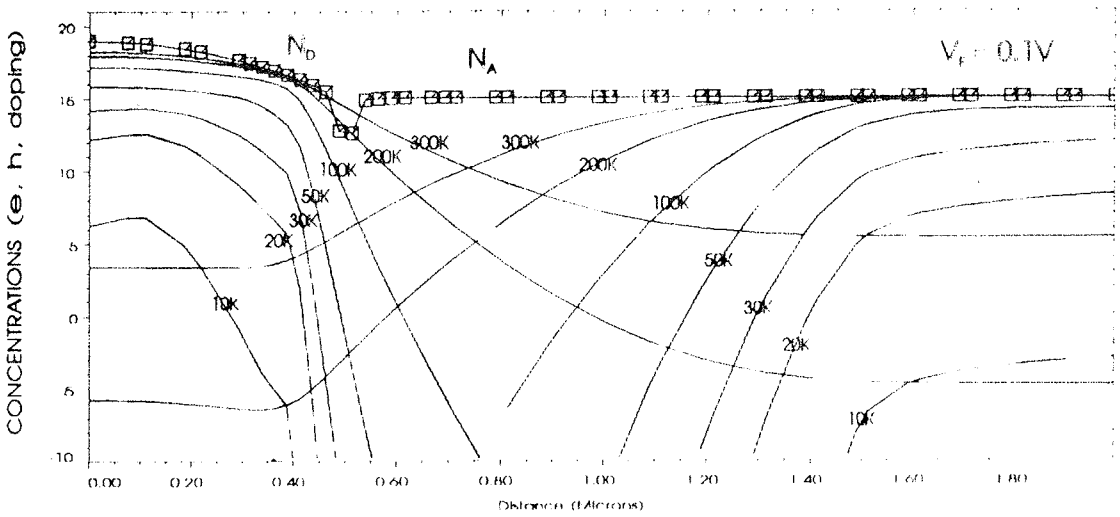

Fig. 4: Incomplete impurity ionization at low temperatures (freeze-out)

t=60min, ambient O2 dry). Input impurity profile for device modeling was obtained by SUPREM3 simulation fitted to measured values (junction depth, sheet resistivity, surface profile).

Modeling. Simulation of PN junction at low temperatures with standard ionization model (1) was performed. Calculated free carrier concentrations are shown on Fig.4. Strong carrier freeze- out effect calculated in highly doped region is unrealistic as described in ch.II. Therefore the device was divided into two regions: high concentration region (> 3.8e18cm-3) with total ionization assumption and low concentration region (< 3.8e18cm-3) where standard impurity ionization model (1) was preserved. Transition concentration between regions (3.8e18cm-3) suggested in /21/ was applied.

Resulting free carrier concentrations, based on regional impurity ionization approach, together with standard calculation result for comparison, are given in Fig.5. Regional approach gives more reasonable profiles and seems to be the best solution in absence of exact model for impurity ionization.

Forward I/V junction diode characteristics was measured and modeled from room to low temperatures (Fig.6). The correspondence is reasonable for higher temperature (> 50K) and lower current (< 1mA). The reason for disagreement at higher current, where ohmic drop due to the series resistance plays most important role, is probably in inaccurate modeling of series resistance. This is the consequence of simplifications related to the front contact topology of the device, influencing accurate modeling of series resistance significantly.

Disagreement at low temperatures (< 50K) seems to arise from the underestimated carrier concentration calculated by simulator. This leads to the necessity for the improvement of incomplete ionization model or for the addition of other carrier generation models at such low temperatures /16/.

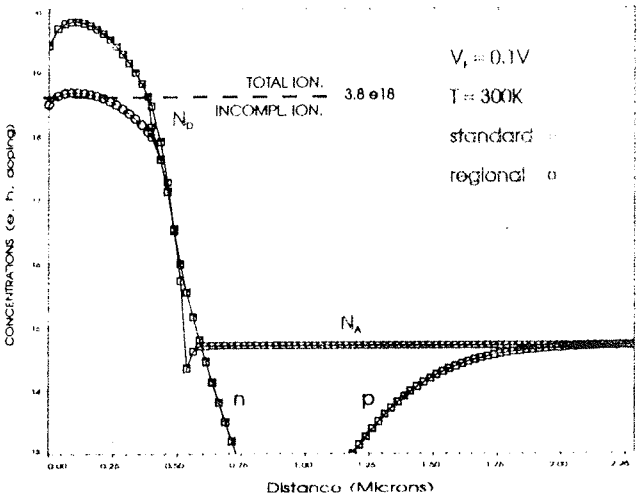

Fig. 5: Incomplete impurity ionization (regional approach)

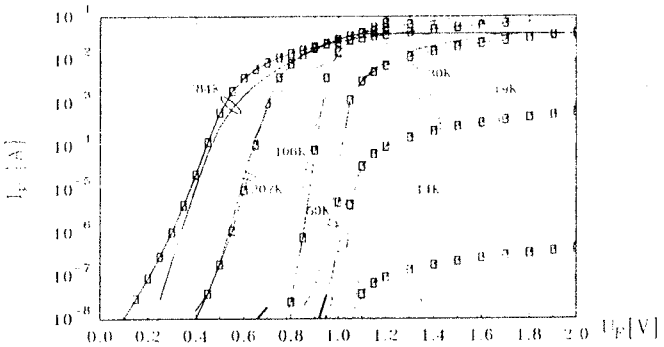

Fig. 6. PN diode forward IV characteristics (measured,modeled)

IV. MOS CAPACITORS

Experimental. Test MOS capacitors (tox=96nm) were fabricated on P-type 16Ωcm Si substrate. Necessity for front contacting of the bulk region led to high series resistance of the bulk even at room temperatures. High frequency (1MHz) CV plots were measured by HP 4280A C meter. Even at temperatures not much bellow 300K true high frequency CV curves could not be obtained due to the extremely slow formation of inversion layer under the gate. Therefore, deep depletion (DD) curves were measured even at slow sweep rate (< 0.1 V/s).

Modeling. Modeling DD CV plots with Medici is not possible since AC analysis cannot be performed in conjunction with transient analysis. Therefore direct comparison of whole calculated and measured curves is not possible as well. Measured and calculated capacitance and conductance in strong accumulation as a function of temperature are presented in Fig.7. Incomplete ionization model (2) and ANALYTIC mobility model /19/ were applied for the simulation. Since the temperature dependence of bulk series resistance is a dominant mechanism that affects capacitance and conductance of the sample /23/, reasonable agreement between calculated and measured curves is obtained.

Another comparison between experiment and simulation is related to the majority carrier freeze-out at the edge of depletion region. In order to determine the majority carrier concentration at the edge of depletion region, $1/C^2$ curves with slope directly proportional to the majority carrier concentration /24/ were plotted for different temperatures /23/. Even at temperatures bellow 70K, the same carrier concentration was obtained as at room temperature. This result, suggesting that no carrier freeze- out is present in the depletion region, has already been observed by other authors /25/. In contrast with experiment, lower (regularly frozen-out) majority carrier concentration was calculated at the edge of depletion region (Fig.8). Since this is an indirect comparison between experiment (capacitance) and simulation (majority carrier concentration) the question remains whether the extraction of majority carrier concentration from measured capacitance at low temperatures can be adequately described by conventional formulae /24/. If these formulae for doping profiling still hold at low temperatures, then the incomplete ionization model (1,2) seems not to be valid at the edge of depletion region, or some other carrier generation mechanisms are important. However, additional work on this subject is necessary for answering these questions.

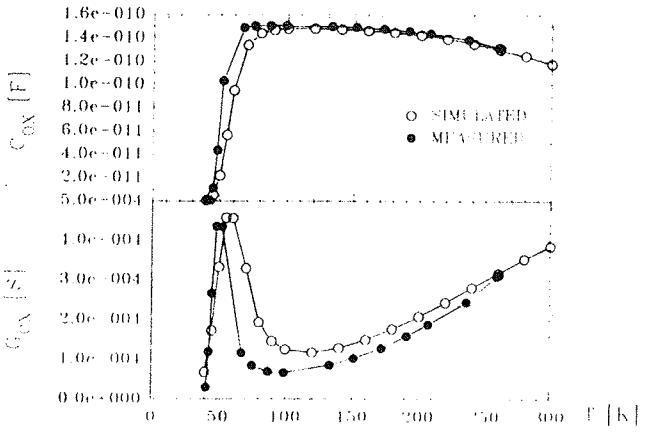

Fig. 7: Measured and calculated MOSC capacitance and conductance

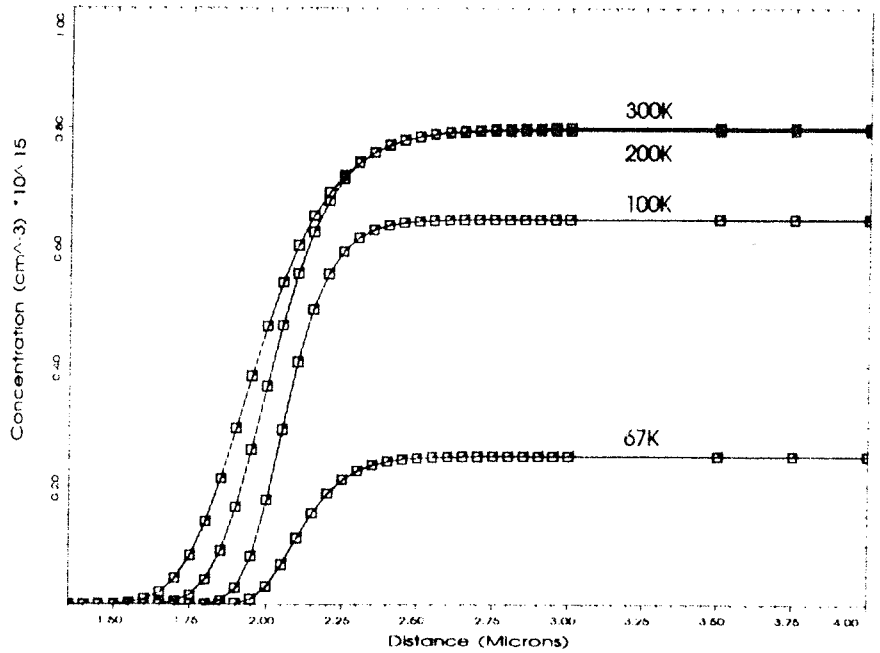

Fig. 8: Calculated freeze-out in the depletion region of MOS capacitor

V. CONCLUSION

Several basic semiconductor devices (resistors, PN junction diodes, MOS capacitors) were fabricated, measured and modeled.

For devices with sufficiently low doping concentrations (low concentration resistor) reasonable agreement was obtained down to 20K. Lack of a general model for incomplete impurity ionization, valid for all doping concentrations, causes several problems for low temperature modeling of devices with highly doped regions.

Modeling of PN junction diodes with properly selected models is in reasonable agreement for temperatures down to 50K. At lower temperatures calculated currents are lower then measured that is probably due to inadequate low temperature behavior of impurity ionization model and possibly to additional carrier generation mechanisms present in measured device.

In MOS capacitor, regularly frozen-out majority carrier concentration was calculated at the edge of the depletion region. Assuming the validity of expressions for doping profiling at low temperatures points to the inaccuracy of incomplete ionization model or presence of additional carrier generation mechanisms at the edge of depletion region.

Finally, due to ohmic drops in the frozen-out regions, increasing importance of actual device geometry for low temperature modeling was detected.

ACKNOWLEDGMENT

The authors wish to thank Prof. Giovanni Soncini /IRST/ for providing some of the test structures and spreading resistance measurements, and TMA for providing simulators MEDICI1.1 and SUPREM3.

REFERENCES

/1/ F.Balestra, G.Ghibaudo, "Overview of MOS Device Physics for Electronics," 15th Ann.Semicond.Conf. CAS'92, Romania, 1992.

/2/ M.J.Deen, "Low Temperature Microelectronics," Proc.ECS on Low-Temperature Device Operation, Washington, May 1991.

/3/ C.T.Sah, "Fundamentals of Solid-State Electronics," World Scientific Publising Co. Pte.Ltd, 1991.

/4/ S.M.Sze, "Physics of Semiconductor Devices," John Wiley&Sons, 1981.

/5/ C.Agrusti, G.U.Pignatel, R.Tangorra, "Modelling of Silicon JFETs at Low Temperatures," Proc.ECS Symp. on Low- Temperature Device Operation, Washington, May 1991.

/6/ D.P.Foty," Impurity Ionization in MOSFETs at Very Low Temperatures," Cryogenics, p.1056, vol.30, Dec 1990.

/7/ R.G.Pires, R.M.Dickstein, S.L.Titcomb,"Carrier Freeze-out in Silicon," Cryogenics, p.1064, vol.30, Dec 1990.

/8/ S.Selberherr, "MOS Device Modeling at 77 K," IEEE Trans.ED, p.1464, vol.36,no.8, Aug 1989.

/9/ A.Emrani, F.Balestra, G.Ghibaudo,"Generalized Mobility Law for Drain Current Modeling in Si MOS Transistors from Liquid Helium to Room Temperatures," IEEE Trans.ED, vol.40, no.3, March 1993.

/10/ D.B.M.Klaassen,"A Unified Mobility Model for Device Simulation-II," Solid-State Electronics, vol.35, no.7. p.961, 1992.

/11/ M.E.Weybright, J.D.Plummer,"Bipolar Transistor Modeling over Temperature," ECS Proc.Symp. on Low- Temperature Device Operation, Washington, May 1990.

/12/ G.Sh.Gildenblat, C.-L.Huang, N.D.Arora, "SplitC-V Measurements of Low Temperature MOSFET Inversion Layer Mobility," Cryogenics, vol.29, p.1163, Dec 1989.

/13/ S.H.Voldman, J.B.Johnson, T.D.Linton, S.L.Titcomb," Unified Generation Model With Donor and Acceptor-Type Trap States for Heavily Doped Silicon," IEDM Tech.Dig., p.349, 1990.

/14/ E.Simoen, B.Dierickx, M.-H.Gao, C.Claeys,"Transient Behaviour of Si MOS Transistors at Liquid Helium Temperatures," Proc.ECS on Low-Temperature Device Operation, Washington, May 1991

/15/ E.Simoen, B.Dierickx, L.Deferm, C.Claeys, "Analytical model for the current-voltage characteristics of a silicon resistor at liquid helium temperatures," Cryogenics, vol.30, p.1152, Dec 1990.

/16/ E.Simoen, B.Dierickx, L.Deferm , C.Claeys, G.Declerck, J.Appl.Phys., 68(8), p.4091,Oct 1990.

/17/ B.Dierickx, E.Simoen, L.Deferm, C.Claeys, "The hysteresis behaviour of silicon p-n diodes at liquid helium temperature," ESSDERC 90, Nottingham, Sept 1990.

/18/ E.A.GutierrezD., L.Deferm, G.Declerck,"Selfheating Effects in Silicon Resistors Operated at Cryogenic Ambient Temperatures," Solid-State Electronics, vol.36, no.1, p.41, 1993.

/19/ "Medici user's manual," TMA, Palo Alto, CA, 1992.

/20/ S.Selberherr, "Process and device modeling for VLSI," Microelectron.Reliab., vol.24, no.2, p.225, 1984.

/21/ M.Chrzanowska-Jeske, R.C.Jaeger, "BILOW-Simulation of Low-Temperature Bipolar Device Behaviour," IEEE Trans.ED, vol.36, no.8, Aug 1989.

/22/ S.Sokolić, S.Amon, F.Smole, D.Križaj, "Algorithm for Modelling Generally Described Semiconductors," COMPEL, vol.10, no.4, p.449, Dec 1991.

/23/ S.Sokolić, S.Amon, D.Vrtačnik, "Characterization of MOS Capacitors in the Wide Range of Low Temperatures," Proceedings of MIEL-SD'93 Conference, Bled, Slovenia

/24/ D.K.Schroder, "Semiconductor material and device characterization," John Wiley&Sons, 1990.

/25/ F.H.Gaensslen, V.L.Rideout, E.J.Walker, J.J.Walker, "Very Small MOSFET's for Low Temperature Operation, IEEE Trans.ED, vol 24, no.3, March 1977.

Prof.dr. Slavko Amon, dipl.ing.,
mag.Saša Sokolić, dipl.ing.Danilo Vrtačnik, dipl.ing.
Laboratory for Electron Devices
Faculty of Electrical and Computer Engineering,
University of Ljubljana
Tržaška 12, 61000 Ljubljana, Slovenia
tel. + 386 61 123 22 66
fax + 386 61 264 990

Prispelo (Arrived): 30.05. 94 *Sprejeto (Accepted): 10.06. 94*

UDK 621.3:(53+54+621+66), ISSN0352-9045 Informacije MIDEM 24(1994)2, Ljubljana

THE SUPERSTRUCTURES OF HIGH-Tc SUPERCONDUCTORS; AN ELECTRON MICROSCOPY STUDY

Ognjen Milat
Institute of Physics, University of Zagreb, Croatia

Keywords: high temperature superconductors, cuprates, crystal structures, superstructures, electron microscopy, electron diffraction, LABACUO superconductors, YBACUO superconductors

Abstract: The series of high-Tc superconducting layered cuprate compounds, related with YBCO and/or LABACUO, were investigated by electron microscopy and electron diffraction. These studies showed that the superstructural ordering usually took place mainly in the "CuO-chain" layers. Partial or complete replacements of Cu atoms by Ga, Al, ..., or S, C, ... atoms in the "chain"-layers induced commensurate superstructures or incommensurate modulated structures in the investigated cuprate compounds without profound modifications of their basic crystal structures.

Superstrukture visokotemperaturnih supravodiča; elektronsko mikroskopsko istraživanje

Ključne besede: superrprevodniki visokotemperaturni, kuprati, strukture kristalne, superstrukture, mikroskopija elektronska, difrakcija elektronska, LABACUO superprevodniki, YBACUO superprevodniki

Sažetak: Niz slojevitih kupratnih spojeva s visokim temperaturama supravodljivosti, poput YBCO ili LABACUO, istraživano je korištenjem elektronske mikroskopije i difrakcije. Istraživanja su pokazala da se superstrukturno uredjenje uobičajeno dogadja uglavnom u slojevima "CuO- lanaca". Djelomične ili potpune zamjene atoma Cu u ravninama "lanaca", atomima Ga, Al , , ili S, C, ... uzrokovale su sumjerljive nadstrukture ili nesumjerljivo modulirane strukture istraživanih kupratnih spojeva, bez značajnijih modifikacija njihovih osnovnih kristalnih struktura.

1. Introduction

The onset of the discovery of a series of cuprate compounds was given in 1981, with the synthesis of the $La_{2-x}Sr_xCuO_4$ (usually called LABACUO)[1], an isostructural variant of the compound La_2CuO_4, known since 1973[2]. After the discovery of a superconducting state with the relatively high transition temperature in these compounds ($T_c \approx 30K$[3]), the material $YBa_2Cu_3O_7$, usually termed YBACUO (or "1-2-3", or "Cu-1212"), was synthesized in 1987; it displayed the superconducting properties at $T_c \approx 93K$[4]. These materials are all layered compounds, based on the ordered stacking of a limited set of structural units, with the perovskite cube (general formula ABO_3) as the most dominant one. The basic crystal structure of all superconducting cuprates is characterized by the two-dimensional CuO_2-layer, which is generally believed to be crucial to superconductivity.

Since 1987., a large number of derivative cuprate compounds were synthesized by doping or by substitution of isovalent and oliovalent ions in the prototype LABACUO and YBACUO materials.

An overview of structural features induced by these element substitutions is presented here. The features were studied[5-10] by High-Resolution Electron Microscopy (HREM) and Electron Diffraction (ED) which provided powerful insight into the structural changes at the level of crystal lattice unit cell.

2. Basic crystal structures of superconducting cuprates

The properties of new cuprate phases can be investigated by inducing some structural modification in the well known phase and then, by correlating it with the effects on the properties of interest; in the present case, the properties related to the superconducting behaviour. Besides a more *physical way* of modifying a phase of material (by changing temperature, pressure, magnetic or electric field, ..), a rather *chemical way* to modify a compound is: the element substitution. This comprises complete or partial substitution of the particular element at the selected crystallographic sites, as well as co-substitutions by isovalent or oliovalent ions. It was found that oxygen atom can be substituted by vacancy, or F, or S; that Barium can be substituted by La or Sr; Yttrium by Ca or La-group of elements; while Copper can be replaced by transition metals, or Ga, Al, Hg, or even by the anion groups such as CO_3 or SO_4.

Figure 1. presents the HREM imaging of crystal structure of $(Nd_{.85}Ce_{.15})_2Sr_2GaCu_2O_9$ phase, an YBACUO derivative compound which reveals general feature of la-

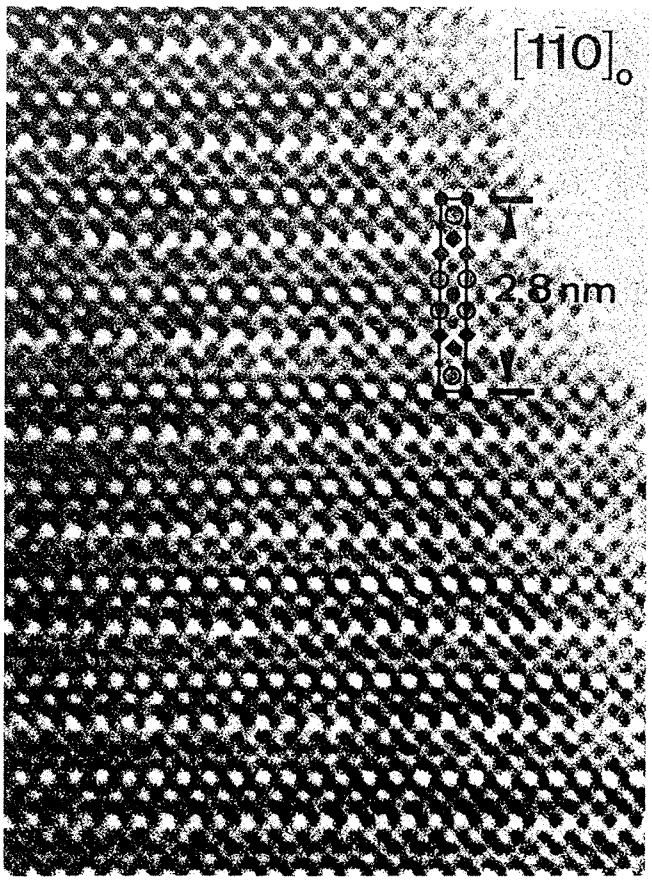

Fig. 1: *High resolution image of the Ga-2212 compound along the $a_p^{(1)}$ direction. The atom columns are imaged as dark dots. Unit cell is indicated by full lines; the open dots represent Sr, the squares represent rare- earth atoms in the fluorite-like lamella; the large and small dots represent Ga and Cu atoms, respectively; Oxygen atoms are not imaged.*

yered cuprates; each layer consists of one of the following basic structure-type units[11]:

(i) perovskite structure-type - units labeled "P1" to "P5" in fig.2; the single layer composition CuO_{2-x} depends on oxygen deficiency ($0 \leq x \leq 2$);

(ii) rock salt structure-type, labeled "RS" in fig.2; the single layer composition is BO (B= Ba, Sr, Tl, Nd,);

(iii) fluorite structure-type, labeled "F" in fig.2; the double layer composition is A-O_2-A (A= Y, Ca, rare-earth).

The combinations of stacking of these basic structure-types generate a number of derivative structures. All structure-types are related to the perovskite lattice by having a quasi-square mesh with the $a_{p(1)} \approx a_{p(2)}$ parameters within the layer; the third lattice parameter along the stacking direction depends on the number of layers constituting one unit slab $c_{p(n)} \approx na_{p(3)}$, as shown in fig.3.

The basic crystal structures of two prototype materials can thus be represented by the following stacking sequences:

- .... - (La/Ba)O - CuO_2 - (La/Ba)O - ..., for LABACUO, with the unit slab consisting of two basic structure-types: -RS-P1- (the slab thickness: $1/2c_p \approx 2a_p$) and,
- ... - $CuO_{1-\delta}$ - BaO - CuO_2 - Y - CuO_2 - BaO - ..., for YBACUO, with the unit slab consisting of four basic structure-types: -P4-RS-P1-P5-P1-RS- (the slab thickness: $c_p \approx 3a_p$), respectively.

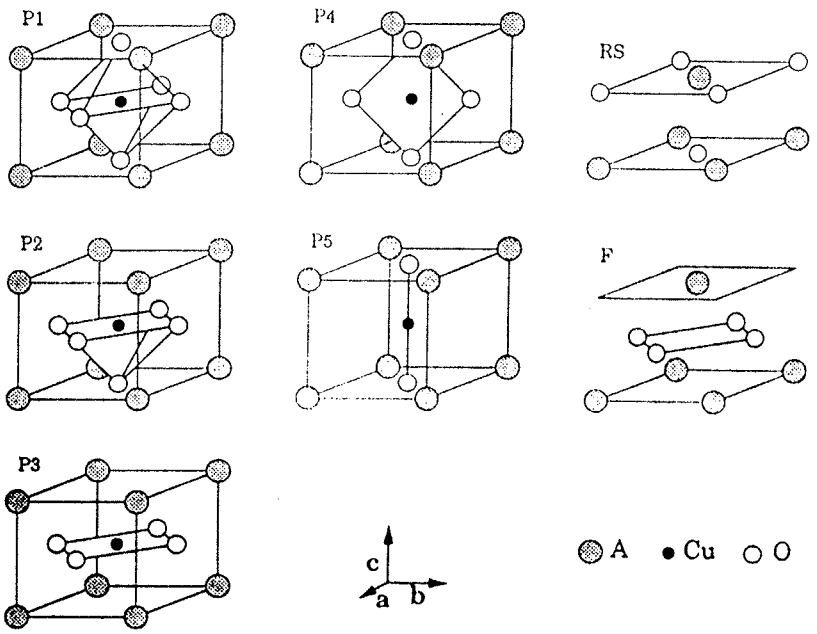

Fig. 2: *Basic structure-type units: perovskite - P1 to P5; rock salt - RS; fluorite - F. Each unit characterizes layer structure in the (axb) plane; layer stacking along the c direction.*

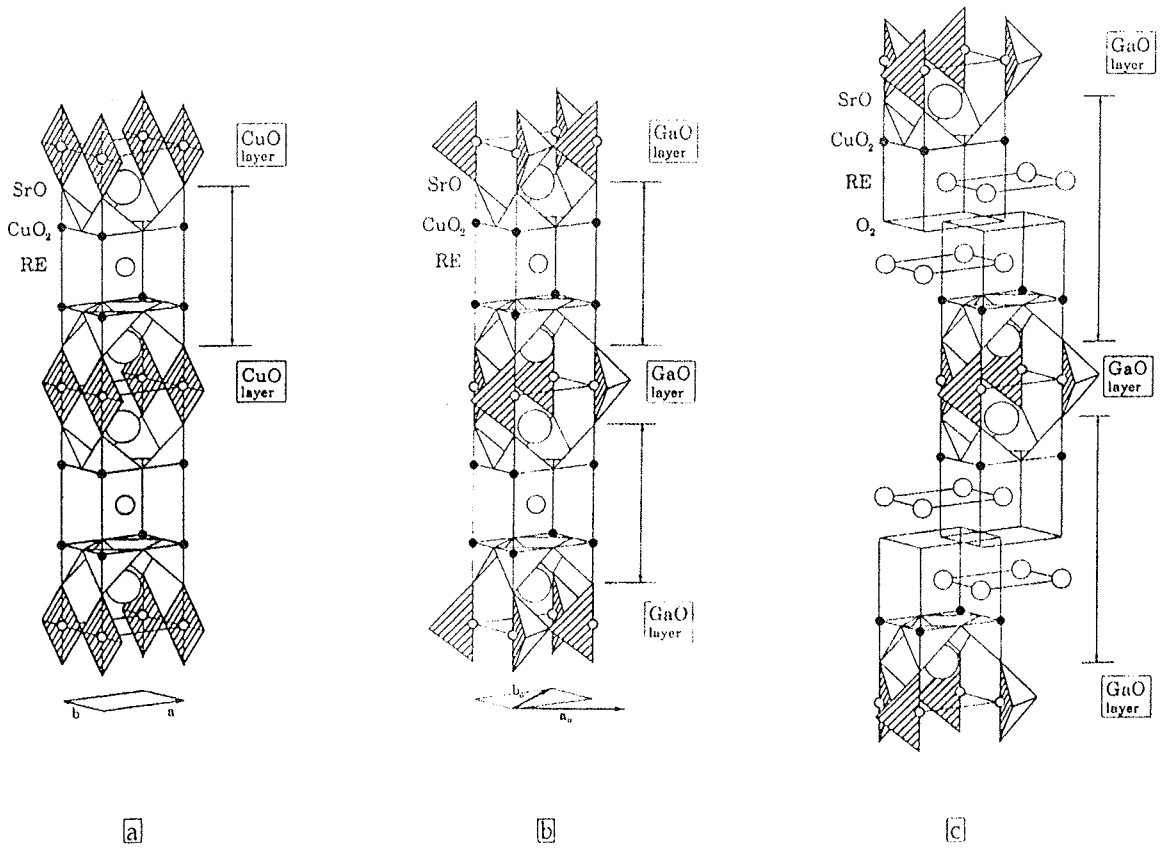

Fig. 3: *Schematic representation of basic structures of; (a) Cu-1212 ($YBa_2Cu_3O_7$) phase; (b) Ga-1212 ($RESr_2GaCu_2O_7$) phase; (c) Ga-2212 ($RE_2Sr_2GaCu_2O_9$) phase. The chains of CuO_4-squares run along the b_p direction, while he chains of GaO_4-tetrahedra run along the $b_o = a_p$-b_p direction;*

The basic structure of the derivative compound $(Nd_{.85}Ce_{.15})_2Sr_2GaCu_2O_9$, which is imaged in fig.1, can therefore be represented by the layer stacking sequence:

– ... - GaO - SrO - CuO_2 - RE-O_2-RE - CuO_2 - SrO - ...

3. Electron microscopy of basic structures and superstructures of superconducting cuprates

3.1. Superlattices of CuO-chains in "pure" YBACUO compounds

An important structural feature of the $YBa_2Cu_3O_{7-\delta}$ compounds, whose structure is schematically shown in fig.3(a), is its variable oxygen content. For $\delta = 0$ half of the oxygen sites in the $CuO_{1-\delta}$ layer are vacant (structure- type "P4" in fig.2), so that the "CuO-chains" of corner sharing "CuO_4-squares" in the BaO-CuO-BaO lamellae (fig.4(a)), run along the $|010| \equiv a_{p(2)}$ direction; the lattice is orthorhombic "ORTO I" (fig.3(a)); the $YBa_2Cu_3O_7$ phase exhibits superconductivity below $T_c \approx 93K$. For $\delta = 1$ all oxygen sites in the $CuO_{1-\delta}$ layer are vacant (structure-type "P5" in fig.2.), so that *no* "CuO-chains" are created in the BaO-Cu- BaO lamella; the lattice is tetragonal; the $YBa_2Cu_3O_6$ phase exhibits no superconductivity down to $T \approx 0K$. For $\delta = 0.5$ the "CuO-chains" are created at only half of the potential sites; each "chain" is succeeded by a row of vacancies so that the $YBa_2Cu_3O_{6.5}$ phase has the so-called "ORTO II" superlattice[12]: $a_{II}=2a_{p(1)}$, $b_{II}=a_{p(2)}$, $c_{II}=c_p$, which is schematically shown in fig.5(a).

A series of YBACUO phases were discovered by now[13]; the so called "1-2-3.5" and "1-2-4" phases with the corresponding compositions: $Y_2Ba_4Cu_7O_{15}$ and $Y_1Ba_2Cu_4O_8$, respectively. They were found to contain the "zig-zag" chains in a double $(CuO)_2$ layers[13] so that a slab of the "1-2-4" structure can be represented by the stacking sequence:

– ... - CuO-CuO - BaO - CuO_2 - Y - CuO_2 - BaO - ...

Besides incorporation of multiple (CuO)n "chain"-layers and oxygen deficiency in the single $CuO_{1-\delta}$ layer, the YBACUO compound is highly tolerant in accepting various substitutions which affect the superstructural ordering significantly[6-10], without profoundly modifying its basic structural features. A number of dopants: Ga, Co, Al, which are incorporated in the "chain"-layers, were found to induce superlattice formation, or incommensurate structure modulation.

3.2. The diagonal "GaO-chains" in the $(RE)_2Sr_2GaCu_2O_9$ compound

The title compound is the second member of a series of polysomatic phases:
$RESr_2GaCu_2O_7$,$(RE)_2Sr_2GaCu_2O_9$,$(RE)_3Sr_2GaCu_2O_{11}$, ...commonly called Ga-n212, fig.3.; they are related to the prototype YBACUO structure in the following way[7]:

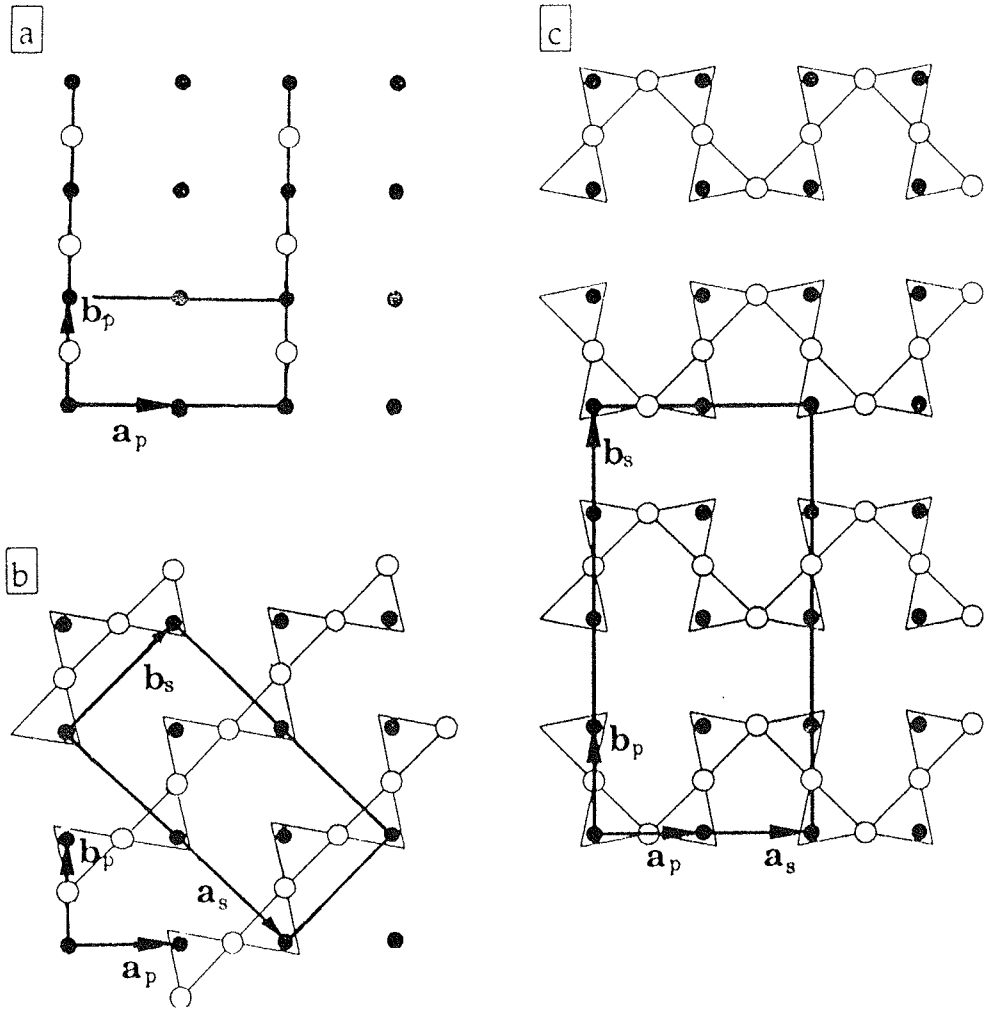

Fig. 4: Spatial view of coordination of oxygen atoms around a metallic atom M in the BO-MO-BO lamella: (a) the CuO_4 square planar coordination around a Cu atom; (b) the GaO_4 tetrahedral coordination around a Ga atom.

(*) the Ga atoms substitute the Cu atoms in the "CuO-chain" layer, while Sr substitutes for Ba in the adjacent "RS" layers. Due to the strong tendency of Ga atoms to be tetrahedrally coordinated by oxygen, the basic structure type "P4" (fig.2), is modified as shown in fig.4(b). A configuration of corner sharing GaO_4-tetrahedra[6,7] in the SrO-GaO-SrO lamellae, forms the "GaO-chains" which run along the diagonal perovskite directions (fig.5(b));

(*) the Y layer is substituted by the single RE, or double RE-O_2-RE, or triple RE-O_2-RE-O_2-RE lamellae having the fluorite-like structure "F" (fig.2); RE stays for the solid solution RE= $Nd_{.85}Ce_{.15}$.

The basic structures of the Ga-n212 compounds can thus be represented by the layer stacking sequences:

– ... - GaO - SrO - CuO_2 - RE-$(O_2$-RE$)_{n-1}$ - CuO_2 - SrO - ...

The basic lattices are related to the perovskite unit cell with variable c-parameter: a_p = 0.38 nm, b_p =0.38 nm, $c^{(n)}_p$ (= 1.14, 1.41, 1.68 nm for n= 1,2,3, respectively);

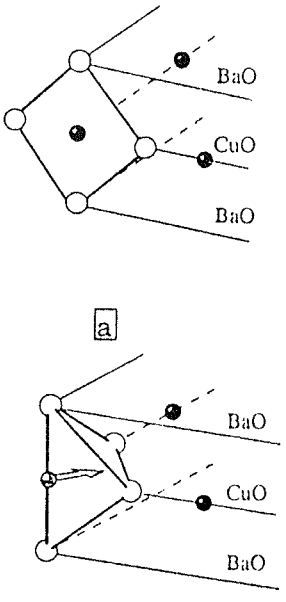

Fig. 5: Plane arrangements of chains in the BO-MO-BO lamella: (a) plain CuO-chains on the $(2a_p^{(1)} x a_p^{(2)})$ ORTO II cell of $YBa_2Cu_3O_{6.5}$ phase (b) diagonal GaO-chains on the $(2\sqrt{2}\, a_p x \sqrt{2}\, a_p)$ cell of $(RESr_2GaCu_2O_7)$ phase; (c) meandering AlO-chains on the $(4a_p^{(1)} x 2a_p^{(2)})$ cell of $RE_2Sr_2AlCu_2O_9$ phase;

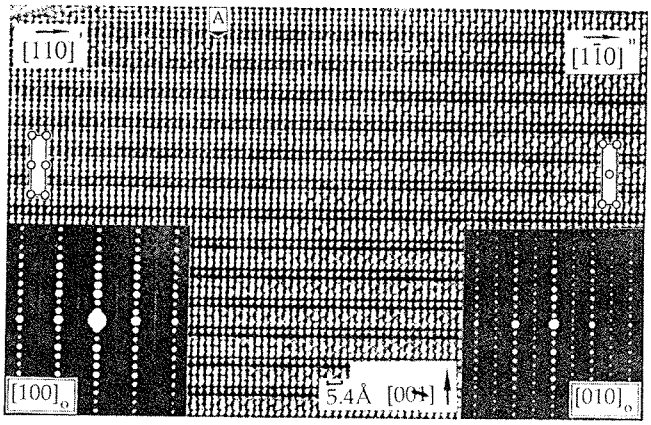

Fig. 6: *High resolution image of an area of Ga-1212 crystal containing two orientations of diagonal chains; in the right part - the pairs of dark dots forming horizontal bars represent the GaO_4-chains viewed along their length; in the left part - the GaO_4-chains, which run perpendicular to the viewing direction, can not be resolved out of the basic structure. The changing of chains' orientation by 90° in a single SrO-GaO-SrO lamella is marked by A.*

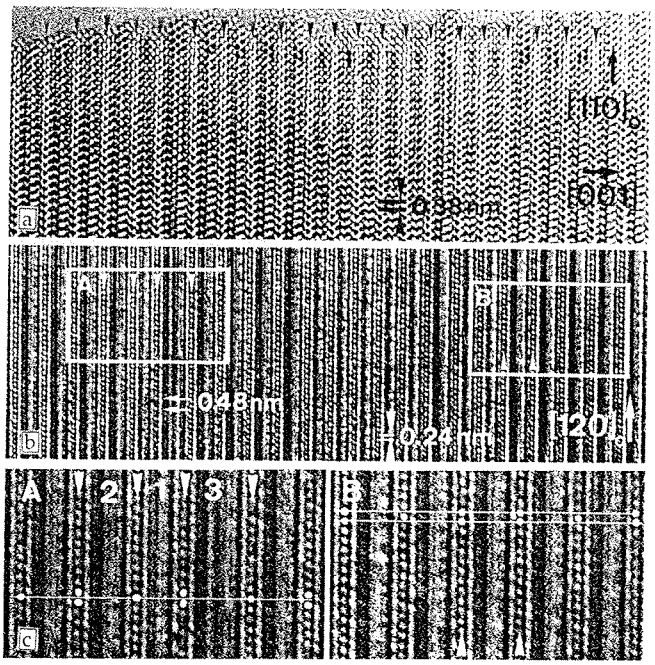

Fig. 7: *High resolution images of an area of coherently intergrown slabs of three Ga-n212 phases (n=1, 2, and 3).*
(a) the dark dot arrays reveal atomic positions of the basic layered structures; the GaO planes which separate unit slabs are marked by the arrowheads on top margin;
(b) vertical rows of bright dots separated by 0.24 nm represent GaO layers of the SrO-GaO-SrO lamellae; the dot separation of 0.48 nm (marked by the pair of horizontal arrows) reveals the alternating GaO_4-chain directions' arrangement schematized in fig.5(b); the frames A and B are enlarged in (c)
(c) the positions of Ga atoms in the GaO_4-chains are resolved as bright dots; the chain-layers are marked by arrowheads; the digits on the top display the numbers of RE layers in the intergrown slabs.

the superlattice cell has parameters[6]: $a_s = 2a_p\sqrt{2}$, $b_s = a_p\sqrt{2}$, $c_s = c^{(n)}_p$, as shown in fig.5(b).

The HREM imaging of the $RESr_2GaCu_2O_7$ structure in fig.6. discloses "GaO-chains" running along two perpendicular orientations in the basic perovskite lattice. The pattern of bright dots in the right part of fig.6 reveals the basic structure where the "chains" are oriented edge-on along the imaging direction, while the pattern in the left part of fig.6. represents the same basic structure where the "chains" are oriented perpendicular to the viewing direction. Orientation of the "chains" may change by 90° within a single SrO-GaO-SrO lamella, marked by **A** in fig.6. For a single orientation of the "GaO-chains" two opposite chain directions: L-left, and R-right (fig.5(b)), may alternate regularly causing the doubling of the superperiod; this two time larger periodicity is locally imaged by bright dots with the spacing of 0.48 nm, marked by the pair of arrows in fig.7(b). The HREM imaging of fig.7. shows also a sequence of coherently intergrown slabs of the Ga-n212 phases with n= 1, 2, and 3 (indicated by the digits: 1, 2, and 3 in fig.7(c)). The positions of Gallium atoms in the SrO-GaO-SrO lamellae of these slabs, are visible as bright dots with the spacing of 0.24 nm in the vertical rows of well resolved dots in fig.7(b&c). The superstructure arrangements of the GaO_4-chains within the SrO-GaO-SrO lamellae was found to be the same for all Ga-n212 phases regardless the number of RE layers in their unit slabs[7].

3.3. The meandering "AlO-chains" in the $RE_2Sr_2AlCu_2O_7$ compound

The $(Y_{.75}Ce_{.25})_2Sr_2AlCu_2O_7$ compound, termed here Al-2212, has the same basic structure as the Ga-2212 phase since the Al ions favour a tetrahedral coordination by oxygen, like the Ga atoms. The corner sharing AlO_4 tetrahedra (fig.4(b)), exhibit different superstructural ordering termed "meandering chains" arrangement[10], however. This superstructure is based on a $4a_{p(1)} \times 2ap(2)$ xcp superlattice, fig.5(c).

The HREM imaging of an Al-2212 crystal along the principal zone direction |010| in fig.8, discloses all relevant features of the basic structure (fig.8(a)), as well as of the superstructure (fig.8(b)&(c)). The bright dot pattern in fig.8(a) represents the channels between the atomic columns, while the dark dots point to the projections of metal atoms. The horizontal rows of black dots correspond with the layers indicated in the inset legend of fig.8(a). The superstructure of the AlO_4 tetrahedra, which correspond with the formation of meandering chains in the SrO-AlO-SrO lamellae, can be revealed under slightly different imaging conditions in fig.8(b). The bright dots here point to the positions of the AlO_4 tetrahedra. The spacing between the bright dots in some rows which represent the AlO-layers reveals the period doubling in accordance with the separation between the meandering "chains", shown in fig.5(c). The imaging of fig.8(c) shows that the superstructural ordering is not restricted to the AlO-layers only, but also modulates the

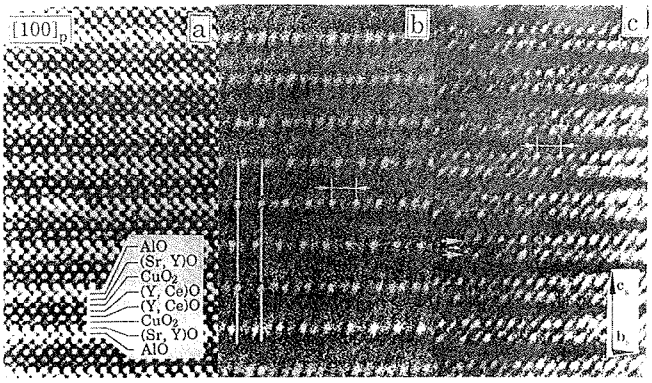

Fig. 8: *High resolution imagings of a wedge-shaped Al-2212 crystal under different thickness and defocus conditions;*
(a) thin area, Scherzer defocus - dark dot pattern reveals basic structure so that each layer can be easily identified (legend in the inset);
(b) thicker area, low underfocus - horizontal rows of bright dots represent the AlO layers; two levels of dot brightness and the indicated double periodicity confirm the meandering AlO-chain arrangement as it is schematized in fig.5(c);
(c) thicker area, high underfocus - two levels of dot brightness in the double hoorizontal rows show that the meandering AlO-chain arrangement modulates also the adjacent SrO layers in the SrO-AlO-SrO lamellae.

adjacent SrO-layers in the SrO- AlO-SrO triplet lamellae marked by the arrows.

3.4. The modulated structure due to the "SO-chain" in the $RESr_2(Cu_{.78}S_{.22})Cu_2O_{7-\delta}$ compound

It was reported recently[8] that Sulphur atoms in the form of SO_4-groups could partially substitute for copper in the $CuO_{1-\delta}$ planes of the Cu-1212 phase, thus creating the S- 1212 phase. The basic structure of this S-1212 phase is represented by the layer stacking sequence:

– .. - $(Cu_{.78}S_{.22})O$ - SrO - CuO_2 - RE - CuO_2 - SrO - .., where RE stays for solid solution: $Y_{.74}Ca_{.16}Sr_{.10}$.

The electron microscopy investigations[8] revealed the aggregation of the SO_4-tetrahedra in the "chains" along $b_p \equiv a_{p(2)}$ direction. The higher brightness of clusters of dots in fig.9, was attributed to the positions of these "SO_4-chains". Due to the ordering of "chains" in a way that along $a_{p(1)}$ the sequences of two to three "CuO_4-chains" are succeeded by single "SO_4-chain", fig.9, the average separation between the "SO_4-chains" is close to the harmonic mean of $4a_p$ and $3a_p$ i.e, $a_m \approx 3.43\ a_p$. The interpretation of the observed incommensurate modulated structure in terms of concentration "SO_4-chain" waves[9], is emphasized in fig 9(b) by two families of parallel lines which cross close to the highest "SO_4-chain" concentration.

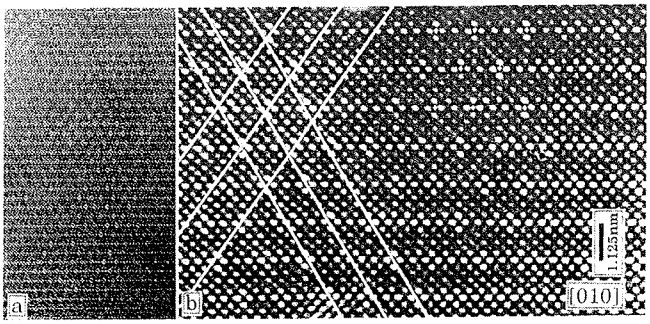

Fig. 9: *High resolution images of S-1212 phase:*
(a) horizontal rows of dots reveal layered basic structure while the modulation is marked by two sets of heavy lines in (b). Clusters of four brighter dots centered in the (Cu/S)O layers correspond with the positions of SO_4-chains viewed edge-on;
(b) high magnification image - the maxima of modulating wave, can be easily seen under grazing angles. The separation between the clusters of brighter dots (the SO_4-chains) in each (Cu/S)O layer is either $3a_p$ or $4a_p$.

3.5. The CO_3-"loops" in the $Sr_2CuO_2(CO)_3$ compound

The HREM imaging of the $Sr_2CuO_2(CO_3)$ compound, shown in fig.10, reveals three levels of its crystal structure: the basic structure (which is based on the LABACUO lattice: a_p =0.38 nm, $c_p \approx 2a_p$); the modulated -Sr-CuO_2-Sr- block-layer structure; and the superstructure due to long range ordering of CO_3 units in the planes ensandwiched by the block- layers[9], fig.10. This basic structure is related with the prototype LABACUO structure in a way that one out of the two CuO_2 layers is replaced by the CO layer[9] so that the corresponding stacking sequence is:

– ... - CuO_2 - SrO -CO- SrO - ...

In fig 10(a), which images the very thin area of the crystal, the bright dot pattern represents the projected basic structure; the rows corresponding to the basic structure-type layers are marked by horizontal arrows on the left margin. The features of the superstructure are only weakly discernible by two levels of dot brightness and two times larger periodicity, indicated by the arrowheads around the vertical line in fig.10(a). Fig.10(b) shows the same crystal under the slightly different imaging conditions, where the bright dot pattern only reveals two times larger spacing of 0.34 nm, due to the superlattice ordering of the CO_3 units. They are ordered on a "closed loop" arrangement[9] within each triple-layer SrO-CO-SrO lamella.

Two modes of the "CO_3-loops" ordering correspond with two types of Bravais superlattices[9]. The computer simulation of HREM imaging of these two types of superlattice unit cell are shown in fig.10(c)&(d) (with three times larger magnification than the experimental imaging in fig.10(b)). By comparing the computed images

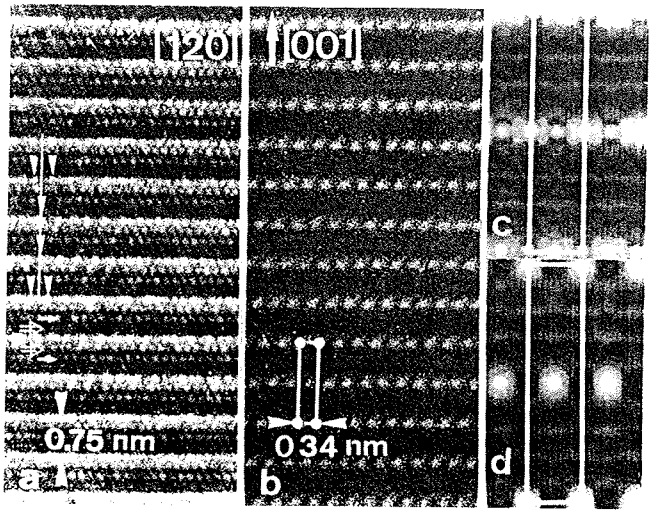

Fig. 10: *High resolution images of a wedge-shaped $Sr_2CuO_2(CO_3)$ crystal: (a) thin area where the bright dot array corresponds to the projected basic structure (legend on the left margin: a triangle, two open arrows and two small arrows indicate the CO_3, Sr, and CuO_2 layers. Brightness modulation, representing the superstructural ordering in the CO_3 layers, is marked by the arrowheads around vertical line; (b) thicker area of the same crystal where only the positions representing the superlattice nodes due to the "CO_3-loops" arrangement are imaged as bright dots; (c)&(d) computer calculated images of the superlattice cells for two types of "CO_3-loops" ordering (magnification is three times larger than in (b).*

versus the observed one, we can conclude that the model of the "CO_3-loops" arrangement which corresponds with the calculated image in fig.10(d) is more likely to represent the superstructure than the model-arrangement corresponding to the calculated image in fig.10(c).

3.6. The CuO_2-"ribbons" in nonsuperconducting $Ca_{.85}CuO_2$ compound

The structure of non-stoichiometric $Ca_{.85}CuO_2$ is remarkable because of two reasons:

(i) the way in which the complicated non-stoichiometry was found to be accommodated in a rather simple crystal structure[14,15];

(ii) the way in which this structure is related to the so-called "parent structure"[16] of $Ca_{.85}Sr_{.15}CuO_2$, fig.11(b). The basic structure can be represented by the layer stacking sequence:

– ... - CuO_2 - Ca - ...

The HREM imaging in fig.12(a) reveals the position of Ca and Cu atoms in the projected structure of $Ca_{.85}CuO_2$; such imaging provided an interpretation of this structure in terms of two constituent sublattices[15]: the "CuO_2-ribbons" based on the face-centred orthorhombic cell[14], and the interstitial array of calcium atoms: the "Ca-chains" with the oblique monoclinic cell[14] indicated in fig.11(a), respectively. The framework of this "CuO_2-ribbons" in the structure of $Ca_{.85}CuO_2$ phase, is different when compared either to the arran-

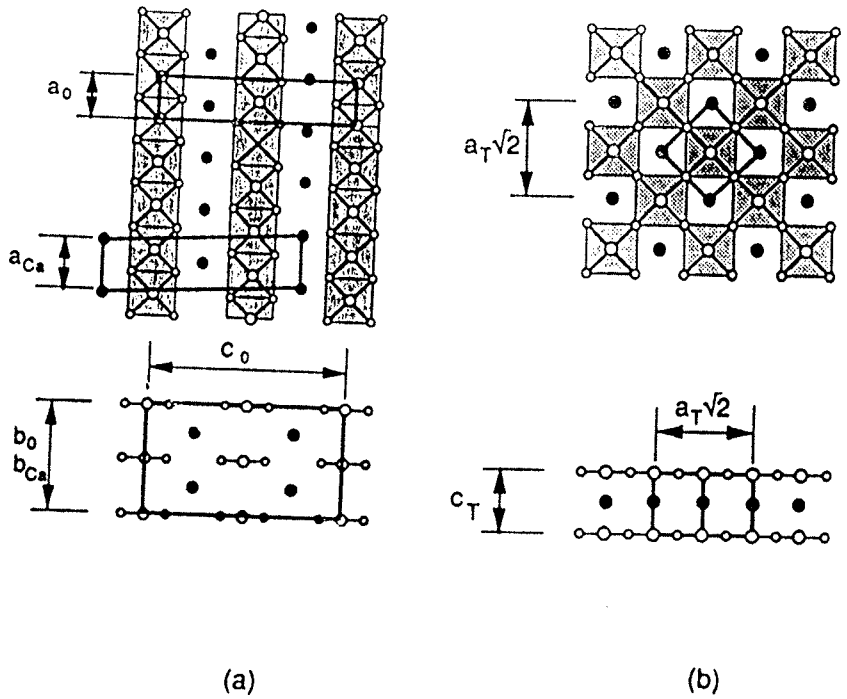

Fig. 11: *Schematic projections of two calcium cuprate structures: (a) the non-stoichiometric $Ca_{.85}CuO_2$ monoclinic phase a long two directions: |010| (top) and |100| (bottom); (b) the "parent" ($Ca_{.85}Sr_{.15}$)CuO_2 tetragonal phase along two directions: |001| (top) and |110| (bottom); Larger and smaller open dots represent Cu and O atoms, while full dots represent Ca or Sr atoms. CuO_4 squares are shaded; the unit cells are indicated by full lines.*

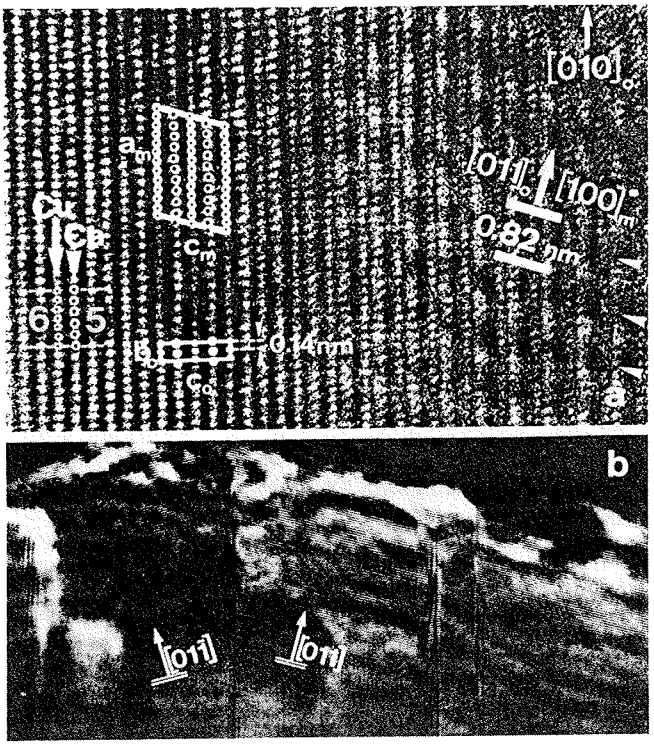

Fig. 12: *(a) High magnification high resolution image of $Ca_{.85}CuO_2$ phase revealing well resolved positions of Cu atoms (marked by smaller dots) and Ca atoms (marked by larger dots). Note that six Cu-Cu separations correspond with five Ca-Ca separations as in the top drawing of fig.11(a). Unit cells of the basic structure and the modulated superstructure are indicated; the modulation is emphasized by arrowheads on the right margin;*
(b) Low magnification image revealing superlattice modulation fringes in twinned domains.

gement of the "CuO-chains" in the prototype structure of YBACUO phase, or to the arrangement of the superconducting "CuO_2-sheets" of the corner sharing CuO_4 squares, in the "parent structure"[16] of $(Ca_{.85}Sr_{.15})CuO_2$ phase, fig.11(b).

Due to non-stoichiometry (Ca/Cu = x = 0.85 ≈ 5/6), the actual structure in fig.11(a) is a modulated array with the average Ca-Ca spacing 20% larger than the Cu-Cu spacing along the "ribbon" direction so that $5a_{Ca}$ nearly coincides with $6a_{Cu} \equiv 6a_o$, as it is indicated in the left part of fig.12(a). The modulated structure with the period of 0.82 nm is revealed as the modulation of dot brightness, indicated by the arrowheads on the right margin of fig.12(a). The modulation was found along two equivalent basic lattice directions[17], with the sharp boundaries between the twin domains, fig.12(b).

4. Conclusions

The presented high resolution electron microscopy studies provided structural features of a number of cuprate phases on the scale of crystal lattice unit cell.

The superstructure of high-Tc superconducting cuprates can be tailored at the atomic level by the aliovalent ion substitutions and/or the suitable oxygen stoichiometry control in the basic multiple-layer perovskite structures. The prototype YBACUO and LABACUO compounds are highly tolerant in accepting various substitutions without profoundly modifying their basic structures. The superconducting properties, as well as the superstructural features are drastically affected, however. A number of metallic and metalloid dopants: Ga, Al, and C, S, ... which are preferentially incorporated in the "chain"-layers when Ba is sumultaneously replaced by Sr, were found to induce superstructures or incommensurate modulated structures. This points to the conclusion that the Sr atoms in the adjacent rock-salt type layers are more adoptable to the varieties of arrangements in the SrO-MO-SrO lamella of high-T_c superconducting cuprates.

5. Acknowledgements

I gratefully acknowledge the Commission of EC for the Grant No: DG XII-SCI1*913167 and the fruitful collaboration with G. Van Tendeloo, J. Van Landuyt and S. Amelinckx at EMAT - University of Antwerp (RUCA), Belgium, as well as with C. Greaves at School of Chemistry, University of Birmingham, UK.

References:

(1) N. Nguyen, J. Chiosnet, M. Hervieu, B. Raveau; J. Sol. Stat. Chem., 39, (1981), 120

(2) J.M. Longo, P.M. Raccah; J. Sol. Stat. Chem., 6, (1973), 526

(3) J.G. Bednorz and K.A. Müller; Z. Phys. B 64, (1986), 189

(4) M.K. Wu, R.J. Ashburn, C.J. Torng, P.H. Hor, R.L. Meng, L. Gao, Z.J. Huang, J.Q. Wang, C.W. Chu; Phys. Rew. Lett., 58, (1987), 908

(5) G. Van Tendeloo, T. Krekels, O. Milat, S. Amelinckx; Journal of Alloys and Compounds, 195, (1993), 307

(6) T. Krekels, O. Milat, G. Van Tendeloo, S. Amelinckx, T.G.N. Babu, A.J. Wright and C. Greaves; J. Sol. State Chem., 105, (1993), 313

(7) O. Milat, T. Krekels, G. Van Tendeloo, S. Amelinckx; Journal de Physique I France, 3 (1993), 1219

(8) T. Krekels, O. Milat, G. Van Tendeloo, J. Van Landuyt, S. Amelinckx, P.R. Slater, C. Greaves; Physica C 210, (1993), 439

(9) O. Milat, G. Van Tendeloo, S. Amelinckx, T.G.N. Babu, C. Greaves; Journal Solid State Chem., 109, (1994), 5

(10) O. Milat, T. Krekels, S. Amelinckx, T.G.N. Babu, C. Greaves; Physica C 217, (1993), 444

(11) G. Van Tendeloo, S. Amelinckx; J. El. Mic. Technique, 8, (1988), 285

(12) S. Adachi, O. Inoue, S. Kawashima, H. Adachi, Y. Ichikawa, K. Setsune, K. Wasa; Physica C168, (1990), 1

(13) H.W. Zandbergen, R. Gronsky, K. Wang, G. Thomas; Nature, 331, (1988), 596

(14) O. Milat, G. Van Tendeloo, S. Amelinckx, T.G.N. Babu, C. Greaves; Solid State Commun. 79, (1991), 1059,

(15) O. Milat, G. Van Tendeloo, S. Amelinckx, T.G.N. Babu, C. Greaves; Journal Solid State Chem., 101, (1992), 92

(16) T. Siegrist, S.M. Zuhark, D.W. Murphy and R.S. Roth; Nature, 334, (1988), 231

(17) O. Milat, G. Van Tendeloo, S. Amelinckx, T.G.N. Babu, C. Greaves; Journal Solid State Chem., 97, (1992), 405

dr. Ognjen Milat , dipl.ing.
Institute of Physics, University of Zagreb
Bijenička 46; POBox 304, HR-41001 Zagreb, CROATIA
tel + 386 41 271 544
fax. + 385 41 421 156

Prispelo (Arrived): 25.04.94 ***Sprejeto (Accepted): 24.05.94***

IMPEDANČNA SPEKTROSKOPIJA

Damir Metelko, Stane Pejovnik
Kemijski inštitut, Ljubljana

Ključne besede: lastnosti materialov, lastnosti električne, področja frekvenčna, območja široka, spektroskopija impendančna, plasti tanke, elektrokemija, površine mejne, prevajanje električno, sistemi večfazni, transport elektronov, prehod elektronov, delci nabiti

Povzetek: Impedančna spektroskopija je postala ena od pomembnejših metod za preiskovanje strukture faznih mej (interfaces) in proučevanje elektrokemijskih reakcij na mejnih površinah. V tem prispevku so predstavljene osnove, potrebne za tiste inženirje, ki metode ne poznajo. Tehnika omogoča tudi proučevanje elementarnih procesov električnega prevajanja v večfaznih sistemih. Sistem vzbudimo z električnim signalom (tokovnim ali napetostnim) in opazujemo odziv. V odzivu so zajeti vsi mikroskopski procesi, ki potekajo v merjencu po vzbuditvi. To je lahko: transport elektronov; prehod elektronov na fazni meji na nabite in nevtralne atome, ki izvirajo iz preiskovanca ali okolice (oksidacije, redukcija); tok nabitih delcev v elektrolitu in podobni procesi. Posamezne procese lahko identificiramo s fenomenološkim pristopom ali z uporabo osnovnih fizikalnih in kemijskih principov.

Impedance Spectroscopy

Keywords: material properties, electrical properties, frequency domains, broad ranges, impendance spectroscopy, thin films, electrochemistry, interfaces, electrical conduction, polyphase systems, electron transport, electron transfer, charged particles

Abstract: The impedance spectroscopy has become an important method for investigation of interfacial electrical structures and electrochemical reactions. Additionally, the impedance technique is frequently used for studying fundamental processes of electrical conduction in polyphase systems. In this contribution the basics for those not acquainted with the method are given. The system under investigation is excited by a current or a voltage signal and the corresponding response is measured. The response includes all microscopic processes taking place in the system after the excitation, e.g. electron transport in bulk, electron transport across an interface - including the electrochemical charge transfer (oxidation, reduction), ion transport in electrolytes, and other related processes. Individual processes may be identified by using a phenomenological description or by applying basic physical and chemical principles.

1. Teoretične osnove

Osnovna pogoja, da lahko nek sistem preiskujemo z impedančno spektroskopijo sta, da sistem zadovoljuje principa linearnosti (odziv sistema na vsoto posameznih vzbujanj je enak vsoti odzivov na posamezna vzbujanja) in časovne nespremenljivosti (odziv sistema na poljuben vzbujalni signal se s časom ne spreminja).

Če preiskovanec vzbudimo z delta funkcijo, se na to vzbujanje odzove z značilnim odzivom, ki ga imenujemo odzivna funkcija h(t) (Slika 1a).

Ker lahko poljubno vzbujanje vedno predstavimo z vsoto posameznih delta funkcij različnih amplitud ob različnih časih, je (po principu linearnosti) tudi odziv preiskovanca vsota odzivov na posamezna vzbujanja z delta funkcijo skozi ves čas vzbujanja (sl. 1b)

Vsoto odzivov predstavimo s konvolucijskim integralom /1/, ki povezuje odziv i(t) in vzbujanje u(t) prek odzivne funkcije (1). Ob poznavanju odzivne funkcije lahko torej vedno enolično določimo odziv sistema na poljubni vzbujalni signal. Odzivna funkcija popolnoma določa preiskovani sistem, zato jo ob karakterizaciji tega sistema poizkušamo določiti.

$$u(t) = \int_0^\infty i(t-\tau)\cdot h(t)\, d\tau \qquad (1)$$

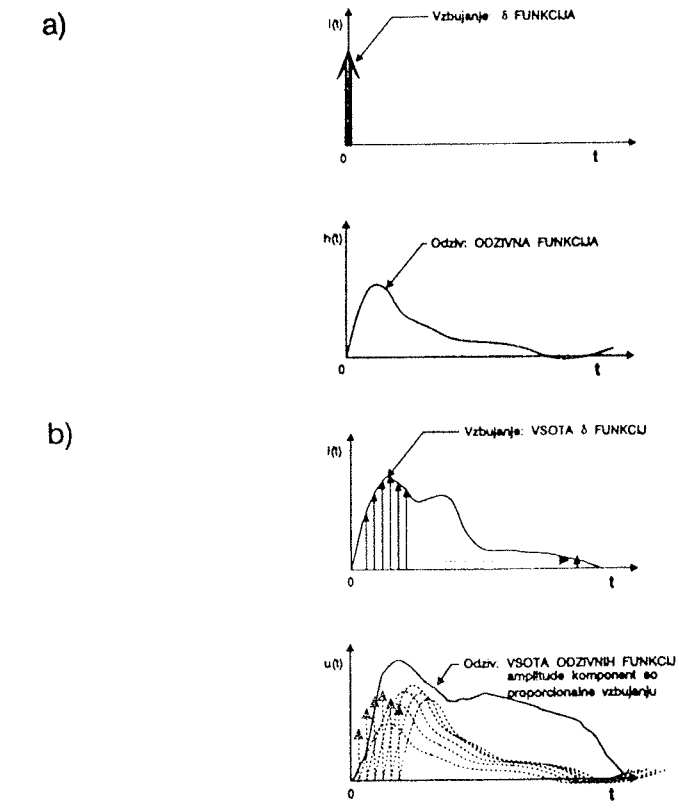

Slika 1: a) Vzbujanje z delta funkcijo in pripadajoča odzivna funkcija, b) Vzbujanje z vsoto delta funkcij in pripadajoči odziv kot vsota odzivnih funkcij

Enolična karakteristika sistema - odzivna funkcija - je torej rešitev integralske enačbe - konvolucijskega integrala. Integralske enačbe so v splošnem težko rešljive. Pri iskanju rešitve integralskih enačb konvolucijskega tipa si pomagamo z zelo učinkovito metodo reševanja: na konvolucijskem integralu izvršimo Fourierjevo transformacijo /2a/.

$$X(\omega) = \int_0^\infty x(t)\, e^{-j\omega t} dt \qquad (2a)$$

$$x(t) = \frac{1}{2\pi} \int_0^\infty X(\omega)\, e^{j\omega t} d\omega \qquad / \qquad (2b)$$

Fourierjeva transformacija /2a/ preslika neodvisno spremenljivko čas (t) v frekvenco (ω) - iz časovnega nas prestavi v frekvenčni prostor. Odziv sistema u(t) preide v U(ω), vzbujanje i(t) pa v I(ω). Fourierjevo transformiranko odzivne funkcije h(t) imenujemo frekvenčni odziv sistema - Z(ω). Seveda so sedaj spremenljivke I(ω), U(ω) in Z(ω) kompleksne (tipa a + jb), medtem, ko je frekvenca ω realna (1). Po Fourierjevi transformaciji preide konvolucijski integral /1/ v produkt frekvenčnega odziva in vzbujanja /3/.

$$U(\omega) = Z(\omega) \cdot I(\omega) \qquad (3)$$

Glede na to, da v časovnem prostoru sistem enolično definira odzivna funkcija, analogno tudi v frekvenčnem prostoru njena transformiranka - frekvenčni odziv - popolnoma karakterizira preiskovani sistem.

2. Določanje frekvenčnega odziva

Z(ω) je razmerje med odzivom in vzbujanjem v frekvenčnem prostoru. Eksperimentalna določitev frekvenčnega odziva je enostavnejša kot vzbujanje merjenca z delta funkcijo in snemanje odzivne funkcije.

Frekvenčni odziv ponavadi določimo tako, da merjenec vzbujamo z monokromatskim sinusnim napetostnim signalom ter opazujemo amplitudo in fazo tokovnega odziva. Kvocient med vzbujalno napetostjo in odzivnim tokom, podan pri točno določeni frekvenci, imenujemo impedanca. Če merimo impedanco prek določenega frekvenčnega območja, dobimo frekvenčni odziv sistema na tem območju.

Frekvenčni odziv je kompleksna veličina. Ponavadi ga grafično predstavimo v kompleksni ravnini - v t. im. Nyquistovem diagramu. Na realno os nanašamo realni del, na imaginarno os pa imaginarni del impedance. Vrh vektorja, ki povezuje koordinatno izhodišče z impedančno točko, opiše prek določenega frekvenčnega območja krivuljo, ki ji pravimo frekvenčni odziv.

Seveda določitev frekvenčnega odziva kljub temu ni tako enostavna. Realni sistemi (baterije, akumulatorji, tanki filmi ...) imajo v splošnem zelo omejeno območje linearnosti. Ponavadi je treba vzbujati realni sistem z napetostmi, ki imajo amplitudo od nekaj do nekaj deset milivoltov. Če ima merjenec poleg vsega še napetost odprtih sponk (OCV), je treba tako vzbujalnemu signalu prišteti še OCV.

Pri nizkih amplitudah napetostnega vzbujanja so ustrezno nizke tudi amplitude tokovnih odzivov. V takih primerih sta tako tokovni kot napetostni signal v veliki meri prekrita z motnjami in šumom. Ko merjenec vzbujamo s periodičnim signalom /4/, ki ima amplitudo U_0, ima odziv v splošnem obliko /5/

$$u(t) = U_0 \cdot \sin(\omega t) \qquad (4)$$

$$i(t) = I_0 \cdot \sin(\omega \cdot t - \varphi(\omega)) + \sum_n K_n \sin(n \cdot \omega - \varphi_n) + S(t) \qquad (5)$$

Prvi člen v /5/ predstavlja harmonični tokovni odziv z amplitudo I_0 in faznim premikom $\phi(\omega)$, v drugem je vsebovanih n višjih harmonikov osnovnega tokovnega odziva, ki imajo amplitude K_n in fazne premike ϕ_n, tretji člen (S(t)) pa predstavlja šum.

Za dovolj natančno določitev impedance pri dani frekvenci moramo iz odzivnega signala izsejati motnje - drugi in tretji člen zgornje enačbe. Merilni postopek je prikazan na sliki 2. Dejansko gre za razvoj odzivnega signala v Fourierjevo vrsto pri vzbujalni frekvenci.

Na opisanem principu zgrajeni instrumenti pokrivajo frekvenčno območje meritve od 0.1mHz pa do nekaj MHz z natančnostjo meritve pod 0.5%.

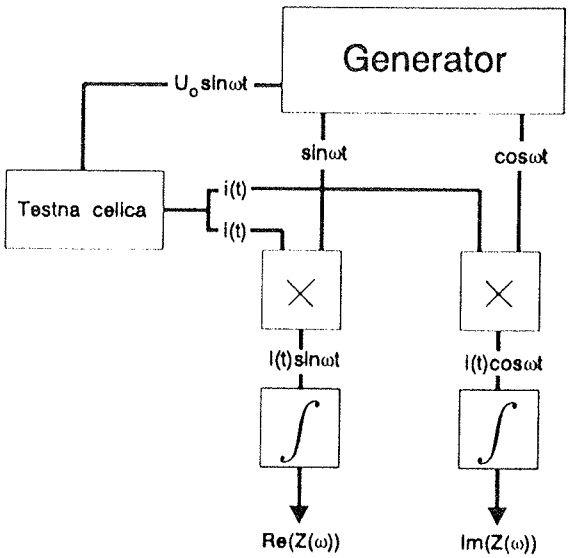

Fig. 2 *Blokovna shema instrumenta za merjenje impedance: odzivni signal i(t) množimo prvič z normirano vrednostjo vzbujalnega signala (u(t)/Uo) s faznim premikom 0 (sin ωt) in drugič s faznim premikom normiranega signala za π/2 (cos ωt). Dobljena produkta integriramo preko periode vzbujalnega signala, pri čemer odpadejo višje harmonske komponente, ostane samo osnovni harmonik, ki je popačen s šumom. Če integriramo preko več period vzbujalnega signala, se proporcionalno številu integracijskih period zmanjša tudi šum.*

Dobra stran opisane merilne metode je velika neobčutljivost na motnje, sama meritev pa je dolgotrajna, saj merimo frekvenčni odziv po posameznih frekvencah. Meritev lahko skrajšamo tako, da vzbujamo merjenec z vsoto monokromatskih sinusnih signalov, vendar postane v tem primeru izločanje motenj težje.

Merjenec lahko vzbujamo tudi s poljubnim aperiodičnim signalom in merimo njegov odziv. Na vzbujalnem in na odzivnem signalu nato izvedemo Fourierjevo transformacijo ter tako dobimo frekvenčna spektra obeh signalov. Komponente frekvenčnega spektra obeh signalov, ki pripadajo enakim frekvencam, med seboj podelimo (izračunamo impedanco) in na ta način določimo frekvenčni odziv. Postopek imenujemo dekonvolucija, vse osnovne meritve pa izvedemo v časovnem prostoru.

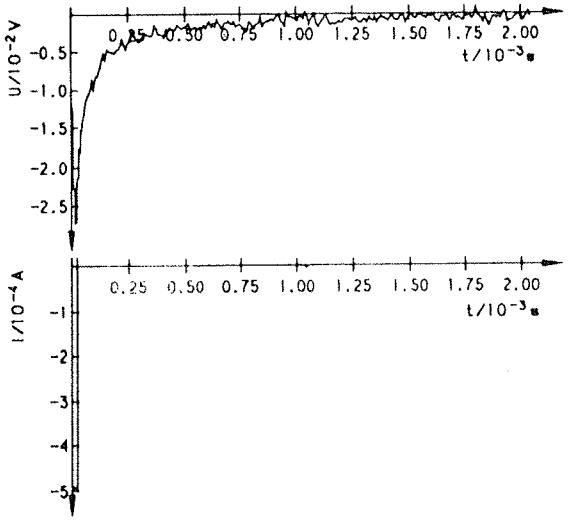

Fig. 3 *Vzbujanje s tokovnim pulzom (I) in pripadajoči odziv (U)*

Ponavadi vzbujamo merjenec s kratkim tokovnim pulzom in merimo napetostni odziv (slika 3) /2/.

Težav pri takem načinu določanja frekvenčnega odziva je več.

Vzbujalni in odzivni signal imata zaradi zagotavljanja linearnosti nizke amplitude in sta zato zelo občutljiva na motnje. Motnje lahko učinkovito zmanjšamo z večkratnim vzbujanjem in snemanjem odziva, kar pa podaljša čas meritve.

Če vzbujamo merjenec s pravokotnim pulzom, postane določanje frekvenčnega odziva v poljubnih frekvencah nemogoče. Frekvenčni spekter pravokotnega pulza ima namreč obliko sin (x) / x, kar pomeni, da nekatere komponete v frekvenčnem spektru niso zastopane, nekatere pa imajo zelo nizko amplitudo. Težavo lahko rešimo tako, da spreminjamo dolžino pulza, s katerim vzbujamo merjenec.

Z opisanim načinom določanja frekvenčnega odziva dosežemo natančnosti znotraj 10%, kar je dovolj za rutinska merjenja (3).

3. Identifikacija frekvenčnega odziva

Elektrotehnika obravnava tri osnovne elemente: upor, kondenzator in tuljavo. Tok in napetost na teh elementih povezujejo enačbe /6/ (upor R), /7/ (kondenzator C) in /8/ (tuljava L).

$$U(t) = R \cdot i(t) \tag{6}$$

$$u(t) = \frac{1}{C}\int_0^t i(\tau)\, d\tau \tag{7}$$

$$U(t) = L \cdot \frac{di(t)}{dt} \tag{8}$$

Enačbe /6/, /7/ in /8/ preslikamo v frekvenčni prostor (na njih naredimo Fourierjevo transformacijo) in dobimo njihove transformiranke /9/, /10/ in /11/

$$U(\omega) = R \cdot I(\omega) \tag{9}$$

$$U(\omega) = \frac{1}{j\omega C} \cdot I(\omega) \tag{10}$$

$$U(\omega) = j\omega L \cdot I(\omega) \tag{11}$$

Frekvenčni odziv teh treh elementov (razmerje U(ω) / I(ω)) za osnovne tri elemente podajajo enačbe /12/, /13/ in /14/:

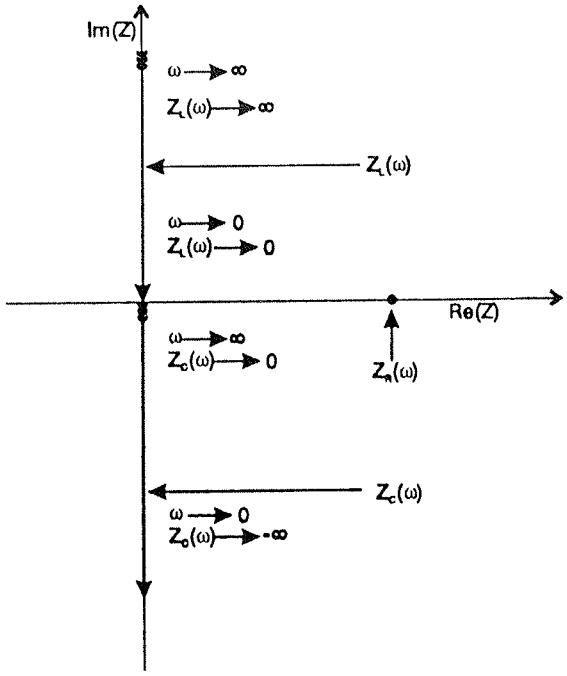

Fig. 4 *Frekvenčni odzivi upora ($Z_R(\omega)$), kondenzatorja ($Z_C(\omega)$) in tuljave ($Z_L(\omega)$). Impedanca upora je neodvisna od frekvence in je tako točka na realni osi. Impedanca kondenzatorja je pri nizkih frekvencah visoka (skozi kondenzator enosmerna napetost ne poganja toka), z rastočo frekvenco pa pada. Kondenzator suče fazo za konstantnih -π/2. Tuljava ima pri nizkih frekvencah nizko impedanco (pri enosmernih razmerah je idealna tuljava kratki stik), ki s frekvenco narašča. Fazni zasuk tuljave je konstantnih π/2*

$$Z_R(\omega) = Z_R = R \quad (12)$$

$$Z_C(\omega) = \frac{1}{j\omega C} \quad (13)$$

$$Z_L(\omega) = j\omega L \quad (14)$$

Frekvenčni odzivi posameznih elementov, narisani v Nyquistovem diagramu, so podani na sliki 4.

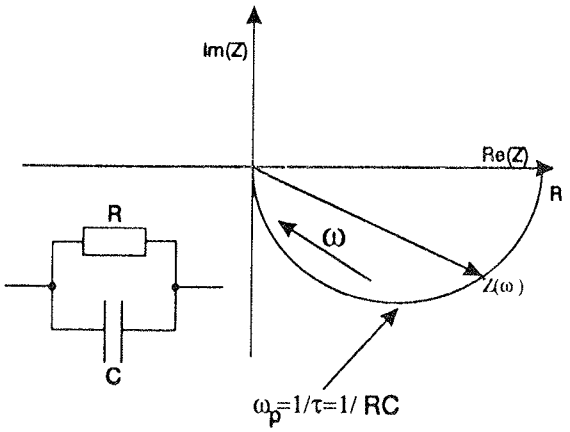

Fig. 5 *Vzporedna vezava upora in kondenzatorja in pripadajoči frekvenčni odziv.*

Z različnimi vezavami opisanih treh elementov je mogoče ponazoriti poljuben frekvenči odziv. Če je imaginarni del izmerjenega frekvenčnega odziv pretežno pozitiven, pravimo, da ima merjenec induktivni karakter, če pa je v večini negativen, pravimo, da je karakter merjenca kapacitiven.

V kemiji imajo realni merjenci ponavadi kapacitivni karakter, kar kaže na to, da v neki obliki akumulirajo naboj.

4. Primer identifikacije: vzporedna vezava upora in kondenzatorja

Če sestavljamo posamezne elemente z znanimi frekvenčnimi odzivi (npr. Z_1 in Z_2), izračunamo skupni frekvenčni odziv po enačbi /15/ za zaporedno in enačbi /16/ za vzporedno vezavo dveh elementov.

$$Z_1(\omega) \; zap. \; Z_2(\omega) = Z_1(\omega) + Z_2(\omega) \quad (15)$$

$$Z_1(\omega) \; vzp. \; Z_2(\omega) = \frac{Z_1(\omega) \cdot Z_2(\omega)}{Z_1(\omega) + Z_2(\omega)} \quad (16)$$

V primeru vzporedne vezave R in C dobimo frekvenčni odziv /17/

$$Z(\omega) = \frac{R}{1+j\omega\tau}; \quad \tau = RC \quad (17)$$

Frekvenčni odziv vzporedne vezave upora in kondenzatorja, predstavljen v Nyquistovem diagramu, vidimo na sliki 5.

Rezultat je polkrog v kompleksni ravnini. Če imamo več zaporedno vezanih paralelnih RC elementov, dobimo v kompleksni ravnini več polkrogov - ločili smo posamezne elemente vezja.

Če poznamo ali predpostavljamo posamezne procese, ki akumulirajo naboj v realnem merjencu, lahko pripišemo izmerjenemu frekvenčnemu odzivu določeno električno vezje - nadomestno shemo - in z impedančno spektroskopijo določimo elemente nadomestne sheme. Na ta način smo določili in ločili tudi fizikalne (kemijske) procese, ki smo jih predvideli v nadomestni shemi.

5. Zaključek

Impedančna spektroskopija je edina metoda, ki pokaže električne lastnosti materialov v širokem frekvenčnem območju. Komercialni merilni sistemi pokrivajo frekvence med mHz in nekaj MHz, so pa relativo dragi. Če se zadovoljimo z nižjo točnostjo, lahko s pomočjo spominskega osciloskopa in PC računalnika, ocenimo frekvenčni odziv merjenca na nekaj % natančno ob bistveno nižji vrednosti aparaturne opreme.

Posebna težava impedančne spektroskopije je interpretacija meritve. Procese v merjencu moramo dobro poznati, da lahko s pomočjo impedančne spektroskopije pridobimo o njem dodatne informacije. Opisana metoda je zato predvsem dopolnilna metoda pri določanju električnih lastnosti materialov, ki pa lahko ob pravilni uporabi in skrbni interpretaciji veliko pove o procesih, ki se dogajajo v materialu.

Literatura:

1. W. McC. Siebert, Circuits, Signals and Systems, MIT Press, Cambridge, 1986.

2. D. Metelko, Magistrsko delo, Fakulteta za elektrotehniko in računalništvo, Ljubljana, 1990.

3. D. Metelko, J. Jamnik, S. Pejovnik, J. Appl. Electrochem. 22 (1992) 638-643.

mag. Damir Metelko, dipl. ing. el.
prof. dr. Stane Pejovnik, dipl. ing. kem.
Kemijski inštitut, Ljubljana, Hajdrihova 19
tel. + 386 61 123 20 61
fax. + 386 61 125 70 69

Prispelo (Arrived): 10.06. 94 ***Sprejeto (Accepted): 15.06.94***

TIME PROPERTIES OF THE NEURAL NETWORK CELLS

Igor Belič
VŠNZ, Ljubljana

Keywords: neuronics, neural networks, neural cells, time properties, neural cell models, neural systems, system responses, time constants, input signals, time functions

Abstract: The article describes the basic neural cell model. The time properties of the single neural cells are introduced and the influence of the various time constants of the neural cells on the neural system response is studied. The different time constants of the neural cells lead to the completely different time responses of the system. It is clear that the neglecting of the cell time constants can lead to the completely unpredictable results when the analogue neural cell models are used.

Časovne lastnosti nevronskih celic

Ključne besede: neuronika, omrežja nevronska, celice nevronske, lastnosti časovne, modeli celic nevronskih, sistemi nevronski, odzivi sistema, konstante časovne, signali vhodni, funkcije časovne

Povzetek: Prispevek opisuje osnovni model nevronske celice. Študiran je vpliv različnih časovnih konstant nevronskih celic, s katerimi se le te odzivajo na vhodne signale. Če upoštevamo različne časovne konstante celic v nevronskih sistemih, potem se sistem pri spreminjanju časovnih konstant, povsem drugače odziva na enake vhodne signale. Zanemaritev različnosti časovnih konstant nevronskih celic lahko vodi pri analognih nevronskih sistemih do nepredvidljivih posledic. Pri digitalnih simulacijah ta zanemaritev ni tako pomembna.

NEURAL CELL MODEL

So far it is not completely understood how biological neurones functionate. Only the complete knowledge of neural cells functionality makes it possible to develop the adequate artificial model of the neural cell.

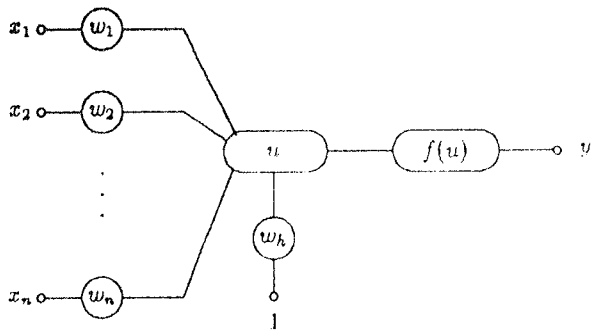

Fig. 1: Model of the neural cell

It is also very important that the neural cells are understood as the elements that functions only in the interaction among the vast number of neurones. One neurone alone has no sense.

The artificial neurone is the element with following properties:

1. It receives the set of input signals denoted by x_i; (i = 1,2, ..,n). It is an n input element. Input signals can come from the external or internal (within the neural system) source.

2. Neurone summates the input signals. Prior to summation, input signals are multiplied by the adequate weight constants w_i. Therefore neurone performs the cumulative weighted sum of the input signals.

3. Neurone has only one output. The output value is calculated with the so called activation function f(u). It performs the mapping of the cumulative sum into the output cell value.

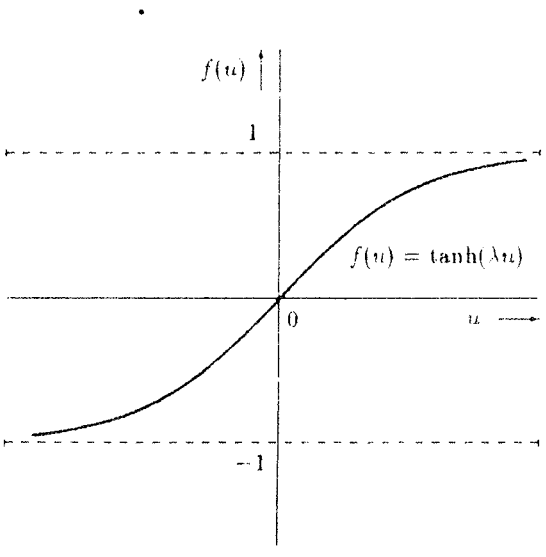

Fig. 2: Cell activation function

$$u = \sum_{i=1}^{n} w_i x_i - h \qquad (1)$$

x_i - signal on the i - th cell input

w_i - weight on the i - th cell input

h - cell activation threshold

The function f(u) is typically some continuous non-linear function. In most cases the following function is used:

$$f(u) = \tanh(\lambda u) \qquad (2)$$

lambda - the activation function slope parameter

Time Properties of The Cell Cumulative Sum Formation

The input signals cumulative sum development can be described with the differential equation

$$\tau \frac{du(t)}{dt} = -u(t) + \sum_{i=1}^{n} \left(w_i x_i - h \right) \qquad (3)$$

τ - Cell time constant.

The solution of this differential equation is the group of parametric functions of the type

$$u(t) = Ce^{-\frac{t}{\tau}} + K \qquad (4)$$

where

$$K = \sum_{i=1}^{n} \left(W_i x_i - h \right) \qquad (5)$$

The solution of the differential equation tells that the neural cell responds to the input signals with a time delay proportional to the cell time constant τ.

In the literature authors usually make some simplifications of the neural cell models in order to make the computations simpler and faster. One of the commonly accepted simplification sets the value of τ to 0. The first consequence is that artificial neural cells summate the input signals without the time delay. This simplification neglects the fact that the time properties of the neural cells can be different. The difference in cell time constants introduces the time dependant response in the neural networks and the adaptation of the cell time constants can be denoted as the learning of the time response.

Following is the example of the time response for the small neural network system where the cells have the different time constants.

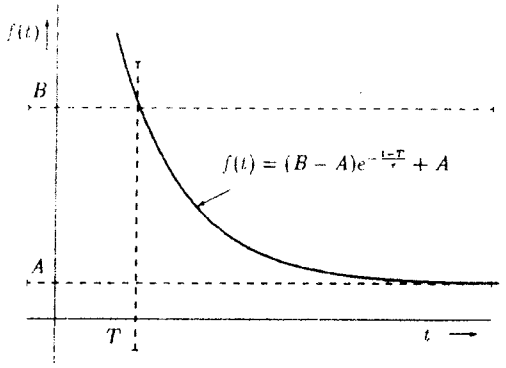

Fig. 3: Transition of the cell output state from the value A to B

The cell output state transition is represented by the function plotted on the fig. 3.

Changing the cell time constants together with the cell input weights adaption is the process of learning. The effect of the cell time constants becomes far more important in a very large neural networks with feedback loops.

Examples

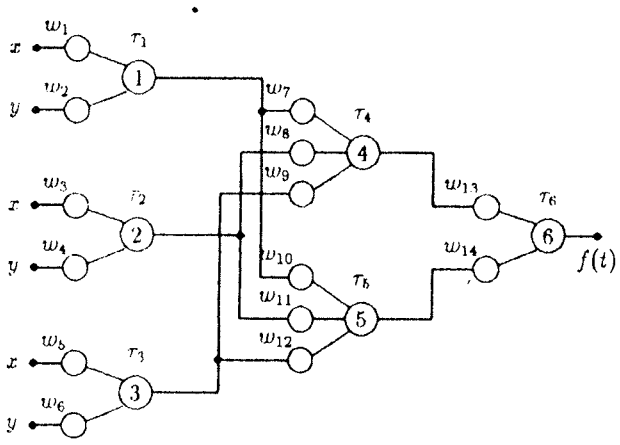

Fig. 4: Test neural network system

The strict proof of the stated effect can only be done with the mathematical tools. Let us make only a short example where the small neural network system is observed.

The test neural network system consists of three input cells, two hidden cells and one output cell. The output time function was observed for the various input signals, for the different weight and time constant sets.

Case 1: Inputs signals z and y are sinusoidal functions.

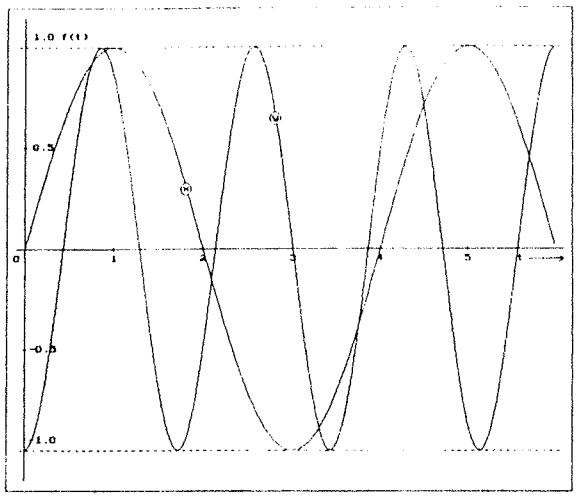

Fig. 5: Input signals

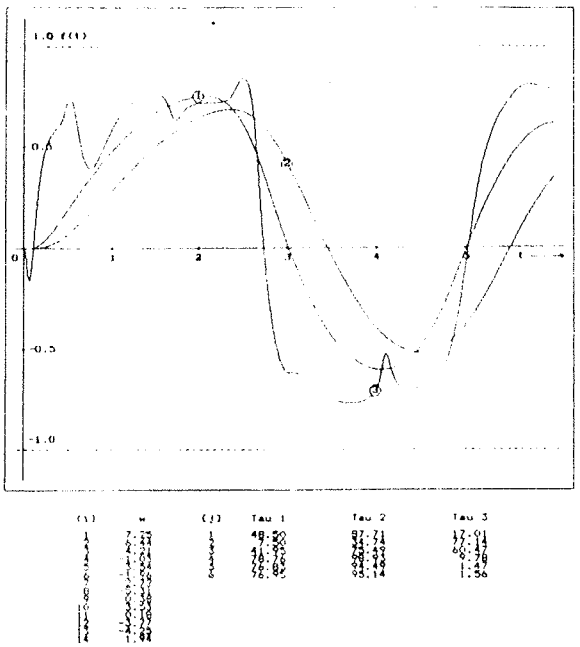

Fig. 7: Output time function for randomly chosen time constants with weight set 2.

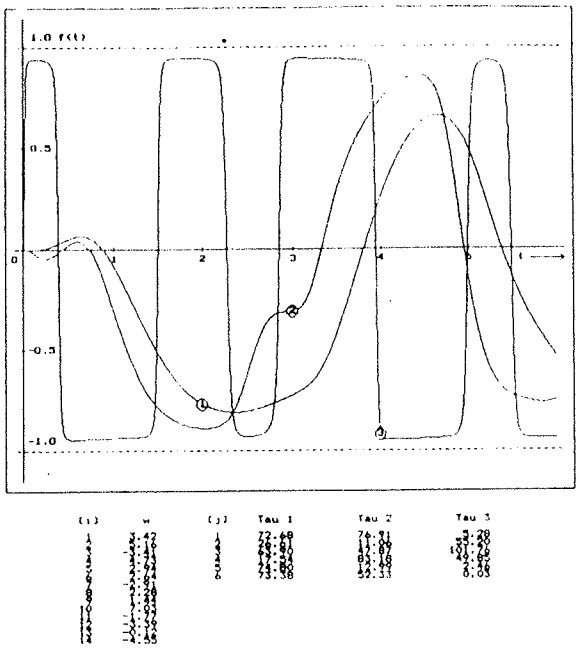

Fig. 6: Output time function for randomly chosen time constants with weight set 1.

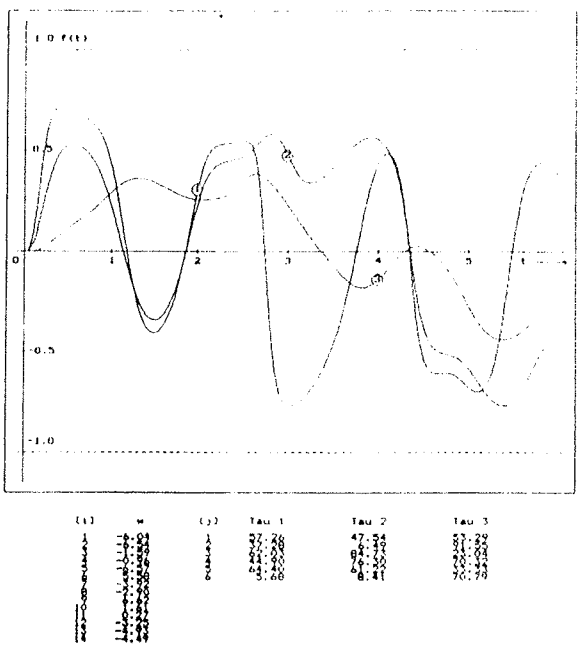

Fig. 8: Output time function for randomly chosen time constants with weight set 3.

Case 2: Input signals z and y are impulses.

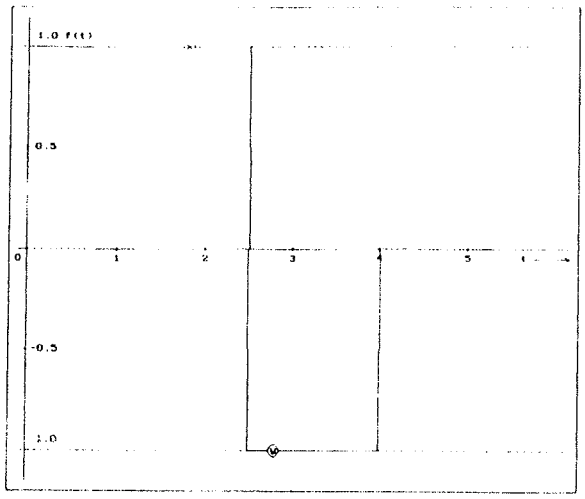

Fig. 9: Input signals

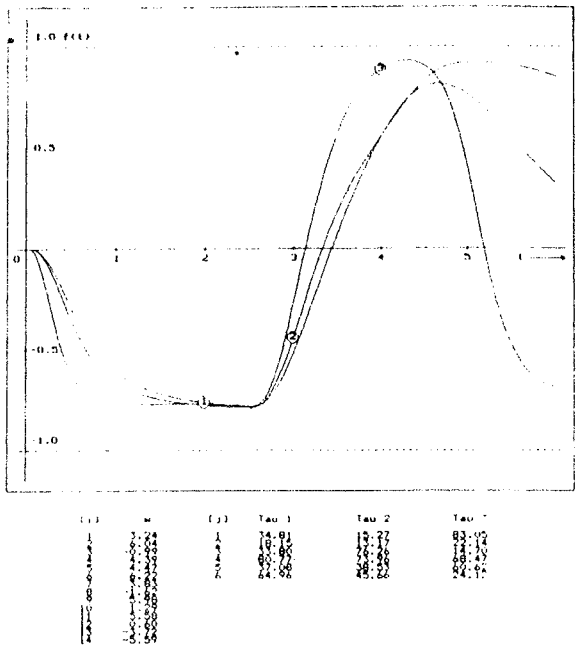

Fig. 11: Output time function for randomly chosen time constants with weight set 5.

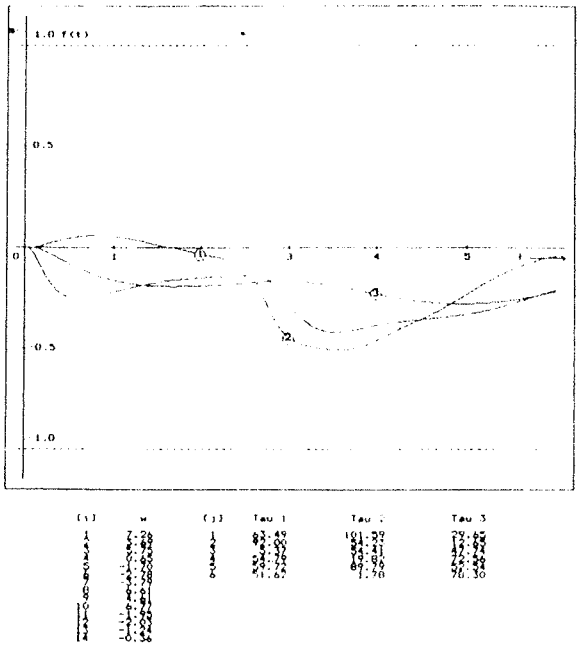

Fig. 10: Output time function for randomly chosen time constants with weight set 4.

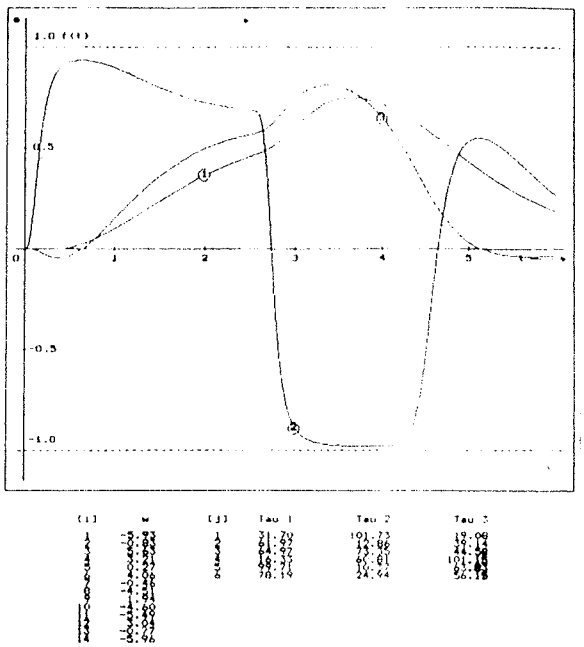

Fig. 12: Output time function for randomly chosen time constants with weight set 6.

From the examples it is perfectly clear that the neural cell time constants can contribute to the different system time responses. At this point the architecture of the neural networks can be proposed in the way described on the following figure.

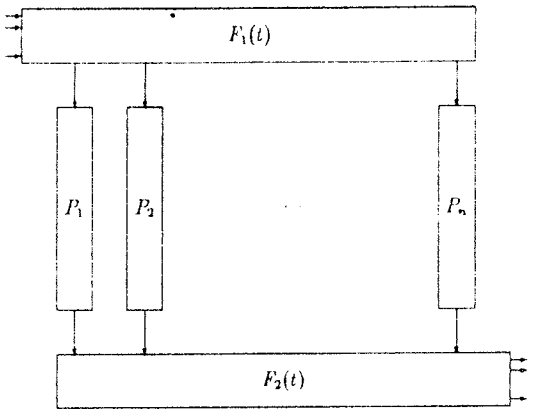

P_1, P_2,... P_n - Time independent neural network subsystems

Fig. 13: The structure of the neural network system with the time dependant and time independant subsystems.

CONCLUSION

Authors usually neglect the influence of the various neural cell time constants. The impact on the behaviour of the neural network is strong when the large, analogue systems with feedback connections are used. In such systems the neglecting of the fact that cells have different time constants can lead to unpredictable system time responses. Furthermore when different cell time constants are used, the learning process consists of two steps. The first step is the adaption of the cell weights and the second is the adaption of cell time constants. The examples showed that the influence of the various time constants can not be neglected.

BIBLIOGRAPHY

/1/ D.O.Hebb, Organisation of Behaviour, New York., John Wiley & Sons, 1948.

/2/ T.Kohonen, Self Organisation and Associative Memory, Berlin, Springer Verlag, 1985.

/3/ G.Matsumoto, Neurocomputing - Neurones as Microcomputers, Future Generations Computer Systems, Elsevier Sci.Publ. vol.4,(39 - 51), 1988.,

/4/ B.Kosko, Neural Networks and Fuzzy Systems, Englewood Cliffs, Prentice Hall International Inc., 1992.

/5/ I.Belič, Self Controlling Neural Network PROCEEDINGS MIPRO 93 - MIS, RISC, Rijeka, 1993.

mag. Igor Belič, dipl.ing.
VŠNZ,
Kotnikova 8, Ljubljana

Prispelo (Arrived): 28.03.94 ***Sprejeto (Accepted): 24.05.94***

UDK 621.3:(53+54+621+66), ISSN0352-9045 Informacije MIDEM 24(1994)2, Ljubljana

RAZVOJ SMPS ELKO S POUDARKOM NA IZBIRI NJEGOVIH SESTAVNIH DELOV

Josipina Černetič
ISKRA Elektroliti, Mokronog, Slovenija

Ključne besede: kondenzatorji elektronski, priključki radialni, SMPS napajalniki komutacijski, ESR upornost serijska ekvivalentna, elektroliti kemijski, vrelišče visoko, napetost enosmerna, tok izmenični, temperature visoke, frekvence visoke, obremenitve visoke, doba trajanja

Povzetek: Nove napajalnike izdelujejo v stikalni tehniki (SMPS), temu morajo biti prilagojeni tudi elektronski sestavni deli.
Cilj našega dela je razviti elektrolitske kondenzatorje (ELKO), ki ustrezajo uporabi v stikalnih napajalnikih (SMPS ELKO) in jih v Iskri, tovarni Elektroliti tudi proizvajati. Dodatne zahteve za SMPS ELKO so predvsem dovoljena visoka obremenitev z enosmerni napetosti superponiranim izmeničnim tokom (Ief) in možnost delovanja pri frekvencah do prek 500KHz. V članku so opisani vplivi delovnega elektrolita in anodne folije na višino ESR in na segrevanje ELKO zaradi priključitve določenega Ief. Za ugotovitev intenzivnosti segrevanja ELKO smo merili temperaturo na ohišju ELKO. Prikazana je odvisnost med ESR in višino Ief, ki segreje ohišje ELKO za 1°C. Omenili smo problem ESR elektrolitov, ki vsebujejo gama-butirolakton.

SMPS Elektrolytic Capacitors Developments Aim to Select Their Constituent Parts

Key words: electrolytic capacitors, radial connections, SMPS, switch mode power supply, ESR, equivalent series resistance, chemical electrolyts, high boiling point, dc voltage, AC current, high temperatures, high frequencies, high loading, lifetime

Abstract: New series of power supplies are produced as switch mode power supplies (SMPS), therefore all contained electronic parts must suit to new requirements.
The aim of our work is to develop and to produce SMPS electrolytic capacitors in ISKRA ELEKTROLITI factory. Extra requirement for SMPS capacitors is mainly allowed high load with ripple current and ability to operate by frequencies above 500KHz. In present article are described influences of working electrolytes and anode foil on ESR height and heating of capacitors caused by load with Ief. We had been measuring temperature on surface (case) of capacitors to find out temperature changes. Chart is showing dependence between ESR and Ief which heats the surface of capacitors for 1°C to 3°C. We have mentioned the problem of resistance of electrolytes which contain gamma-butyrolacton.

1. UVOD

V letu 1990 je bila na Japonskem celotna produkcija kondenzatorjev 119 bilijonov kosov, od tega 26 bilijonov kosov aluminijevih elektrolitskih kondenzatorjev (v nadaljevanju ELKO). Poleg tega je opazen trend povečevanja porabe teh elektronskih sestavnih delov, kajti njihova uporaba se širi na nova področja: v procesno kontrolo, avtomatizacijo obratov, avtomatizacijo uradov, informacijsko tehniko, zabavno elektroniko itd. /1/

Kritična enota, ki dobavlja moč celi napravi, je napajalnik. Čedalje več proizvajajo napajalnike, ki uporabljajo stikalni sistem. Ti napajalniki se imenujejo (switch-mode power supply, v nadaljevanju SMPS). Ti napajalniki so mnogo učinkovitejši od prejšnjih. Ugotovili pa so, da je napajalnik lahko precej manjši in s tem cenejši, če deluje na visoki frekvenci. V bližnji prihodnosti zanimive frekvence so v območju od 200 KHz do prek 500 KHz. Ker je eden od sestavnih delov SMPS tudi ELKO, velja zanj enaka zahteva in sicer da mora biti sposoben dobro delovati v območju visokih frekvenc s precejšnjimi enosmerni napetosti superponiranimi izmeničnimi tokovi. /2/

Običajnim ELKO začneta pri visokih frekvencah ekvivalentna serijska upornost (v nadaljevanju ESR) in impedanca naraščati, kar onemogoča dobro delovanje SMPS. Zato razvijamo tudi v tovarni Elektroliti nove ELKO, ki bodo izpolnjevali velike zahteve za delovanje v stikalnih napajalnikih. To nalogo sofinancira tudi MZT, prvi rezultati tega dela so opisani v tem prispevku.

2. IMPEDANCA, ESR IN SUPERPONIRAN IZMENIČNI TOK

Dodatne zahteve za ELKO, ki je primeren za vgradnjo v SMPS, so naslednje:

1. nizka ESR in impedanca
2. visoko vrelišče elektrolita
3. dolga življenska doba pri visoki temperaturi
4. dopustma visoka obremenitev s superponiranim izmeničnim tokom pri visokih frekvencah

Impendanco sestavljajo kapacitivni, ohmski in induktivni upor:

$$Z = \sqrt{ESR^2 + \left(\omega \cdot L - \frac{1}{\omega \cdot C}\right)^2}$$

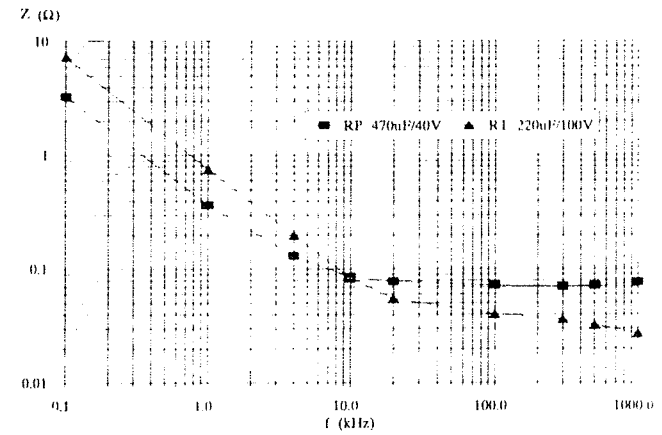

Slika 1: Frekvenčna odvisnost impedance

kar je predstavljeno na sliki 1.

Pri nizkih frekvencah (cca 100Hz) je močno prevladujoča kapacitivna upornost:

$$Z \approx Z_1 = \frac{1}{\omega \cdot C}$$

Pri srednjih frekvencah (cca 10^4Hz) je prevladujoča ohmska upornost:

$Z \approx Z_2 = ESR$

Pri visokih frekvencah (> $1 \cdot 10^6$ Hz) je prevladujoča induktivna upornost:

$Z \approx Z_3 = \omega \cdot L$

Iz povedanega sledi, da je v za nas zanimivem frekvenčnem območju prevladujoča ohmska upornost. Vplivi na ohmsko upornost so razvidni iz naslednje enačbe (3):

$ESR = r \cdot R_E \cdot d/2F$

r - upornostni faktor

R_E - upornost delovnega elektrolita

d - debelina papirja

F - površina anodne folije

Ohmsko upornost torej lahko zmanjšamo z zmanjšanjem upornosti elektrolita, s tanjšim in manj gostim papirjem in z uporabo manj jedkane folije.

Nizek ESR ELKO in visoko vrelišče delovnega elektrolita sta potrebna zato, da ELKO lahko obremenimo z visokim enosmerni napetosti superponiranim izmeničnim tokom (v nadaljevanju Ief). Za prikaz parametrov, ki vplivajo na višino dovoljenega Ief, navajamo enačbo iz standarda DIN 41240:

$I_{ef} = \sqrt{K \cdot S/ESR}$

I_{ef} - maksimalno dovoljen izmenični tok pri 100Hz, 40°C (A)

K - faktor, odvisen od površine ELKO

S - površina ELKO (cm^2)

ESR - ekvivalentna serijska upornost (Ω)

Ta izračun velja za temperaturo ELKO 40°C. Če želimo priključiti ELKO na višjo temperaturo, ustrezno zmanjšamo I_{ef}, glede na to, za koliko °C dopustimo segrevanje ELKO zaradi priključitve I_{ef} pri določeni temperaturi okolice. Torej, na višino maksimalno dovoljenega I_{ef} vplivajo ESR, velikost ELKO in dovoljeno segrevanje ELKO zaradi priključitve I_{ef}.

3. EKPERIMENTALNI DEL

Glede na velik vpliv delovnega elektrolita na parametre ELKO smo največ časa posvetili prav razvoju in izbiri le-tega. Kot impregnante smo uporabili 5 eletrolitov, ki imajo naslednje osnovne komponente in parametre:

Oznaka	Setava	R_{30} (Ωcm)	T_{vrel} (°C)
1	TMAP, γ-butirolakton	100	> 150
2	maleinat, m. formamid	130	>150
3	adipat, et.glikol (1)	135	122
4	zmes soli, et.glikol	240	135
5	adipat, et.glikol(2)	95	115

R_{30} - specifična upornost delovnega elektrolita

T_{vrel} - vrelišče delovnega elektrolita

Kot je razvidno iz sestave, imajo elektroliti različna topila in prevodne soli. Iz literature nam je znano dejastvo, da topilo bistveno vpilva na permeabilnost papirja in s tem na prevodnostne karakteristike ELKO. V te elektrolite smo impregnirali radialne ELKO različnih vrednosti in dimenzij. Za ELKO enakih vrednosti smo uporabili različno predformirane ali različno jedkane folije. Glede papirja nismo eksperimentirali ampak smo uporabili naše izkušnje in vse vzorce navili z nam dostopnim najboljšim papirjem.

Vzorci ELKO:

ELKO	U_{pf}(V)	dxl ELKO
150μF/10V	16	8x11
150μF/10V	22	8x11
100μF/40V	70	10x15
100μF/40V	49	10x15

U_{pf} - predformirana napetost uporabljene anodne folije

dxl - dimenzije ELKO v mm

Začetne meritve ESR so razvidne iz slik 2 in 3.

Za ugotavljanje obremenljivosti naših ELKO z I_{ef} smo merili segrevanje ELKO zaradi priključitve I_{ef}. Preizkus smo izvršili v komori, termostatirani na + 105°C ± 0,1°C.

Segrevanje kondenzatorja smo merili s pomočjo posebnega merilnega sistema, na ohišje ELKO smo pritrdili merilno sondo. Registrirali smo tokove, ki so segreli površino ELKO za 1°C in 3°C.

4. REZULTATI

Odvisnost ESR od vrste elektrolita in predformirne napetosti anodne folije je prikazana na slikah 3 in 4.

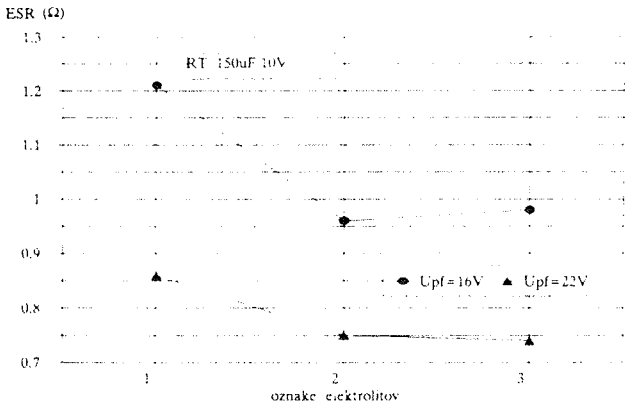

Slika 2: ESR v odvisnosti od vrste elektrolita in višine

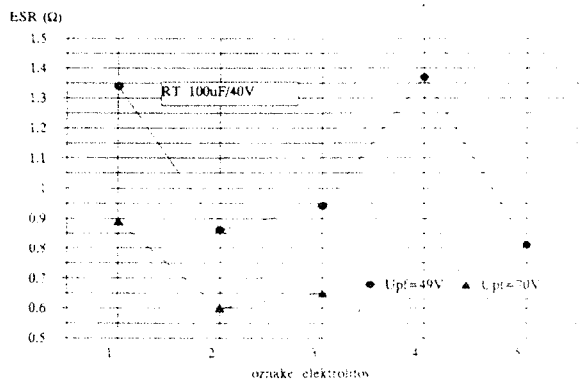

Slika 3: ESR v odvisnosti od vrste elektrolita in višine predformirne napetosti anodne folije

Če primerjamo upornosti elektrolitov z ESR ustreznih ELKO vidimo, da dobimo glede na R_{30} nesorazmerno visok ESR pri elektrolitu 1, ki vsebuje kot topilo gama-butirolakton. Japonci ta problem rešujejo s posebno vrsto papirja.

V naslednjih diagramih prikazujemo segrevanje ELKO v odvisnosti od višine priključenega $I_{ef.}$,

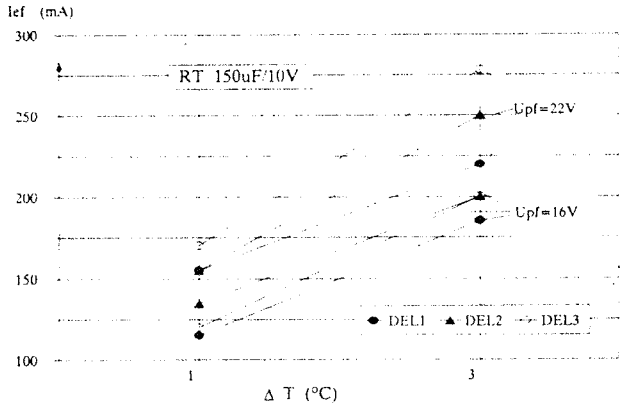

Slika 4: Segretje površine ELKO v odvisnosti od priključenega Ief

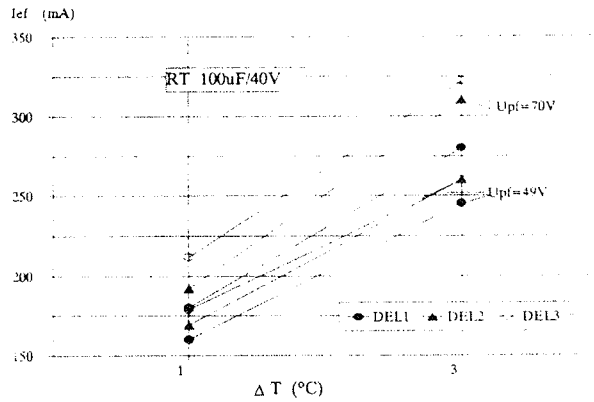

Slika 5: Segretje površine ELKO v odvisnosti od priključenega Ief

Temperatura komore = +150°C ± 0,1°C

Merilna frekvenca = 50Hz

S slik 4 in 5 je razviden velik vpilv elektrolita in uporabljene folije na intenzivnost segrevanja kondenzatorja ob priključitvi na I_{ef}. Višina dovoljenega I_{ef}, ki segreje površino ELKO za 1°C ali 3°C, je v obratnem sorazmerju z ESR ELKO. Zanimivo pa je, da ELKO z elektrolitom 3 dovoljuje višjo obremenitev z I_{ef} za enako segretje površine kot ELKO z elektrolitom 2. Elektrolit 3 je klasični glikol-adipatni elektrolit, elektrolit 2 pa brezvodni elektrolit, topilo je metilformamid.

5. POVZETEK IN ZAKLJUČEK

Naši rezultati kažejo na to, da so sestavni deli ELKO, kot sta folija in papir, prikrojena klasičnim glikol-adipatnim ali glikol-boratnim elektrolitom. Pri brezvodnih elektrolitih nastopi problem specifični upornosti elektrolita nesorazmerno visok ESR ELKO. Rešitev tega problema je v novih materialih, predvsem v tem elektrolitom prilagojenem papirju. Klasični glikolni elektroliti imajo tudi to veliko pomanjkljivost, da imajo prenizko vrelišče za doseganje velikih I_{ef} pri temperaturi +105°C ali več. Brezvodni elektroliti imajo visoka vrelišča, zato lahko dopustimo višje segrevanje ELKO. Poleg tega so pri teh

temperaturah časovno zelo stabilni in mnogo manj korozivni kot glikolni elektroliti. Naši preliminarni preizkusi življenske dobe ELKO z elektrolitom 1 so te dobre lastnosti potrdili.

Literatura:

/1/ Shodo Noda, List of Techniques Expands for Small, Sturdy capacitors, Jee, sept 1991, str, 94-97

/2/ Takumi Nakata, Long-Life, Low-Impedance Aluminum Electrolytic Capacitors Overcome Many Problems, JEE, April 1989, swtr. 46-49

/3/ K.H.Thiesbürger, Der Elektrolyt-Kondensator, 1982

mag. Josipina Černetič, dipl.ing.
ISKRA ELEKTROLITI
Mokronog
Razvojni oddelek
Tržaška 2
61000 LJUBLJANA
tel. + 386 61 213 716

Prispelo (Arrived): 25.04.94 ***Sprejeto (Accepted): 24.05.94***

KARAKTERIZACIJA V VAKUUMU NAPARJENIH TANKIH PLASTI ALUMINIJA NA SILICIJEVE REZINE.

B. Praček, S. Muštra
Institut za elektroniko in vakuumsko tehniko, Ljubljana, Slovenija

Ključne besede: mikroelektronika, tehnologija polprevodniška, plasti tanke, rezine silicijeve, naparevanje vakuumsko, nanašanje aluminija, oksidacija termična, AES Auger spektroskopija elektronska, C-V metoda kapacitivno napetostna, interferometrija

Povzetek: Že dolgo časa predstavlja nanašanje tankih plasti aluminija na silicijeve rezine pomemben del polprevodniške tehnologije. V članku so prikazani rezultati karakterizacije teh plasti s spektroskopijo Augerjevih elektronov, C-V metodo in interferometrijo. Prikazani rezultati so dobljeni s preiskavo šestih karakterističnih vzorcev. Na tri vzorce so bile tanke plasti aluminija nanešene s pomočjo elektronskega topa, na preostale tri vzorce pa z indirektnim uporovnim ogrevanjem na volframski špirali. Na po enem vzorcu od obeh skupin je bila, pred nanosom aluminija, na silicijevih rezinah s termično oksidacijo izdelana samo tanka plast silicijevega dioksida, oba vzorca pa sta bila n-tip. Na drugih dveh je z difuzijo bora izdelan np spoj ter na preostalih dveh z difuzijo fosforja pn spoj. Debelina, kemična sestava in elektronske lastnosti tako naparjenih plasti aluminija se razlikujejo: največje razlike so v plasteh, ki so nanešene na silicijev dioksid, zaradi znane redukcije tega z aluminijem. Prav tako smo opazili, da so plasti nanešene z elektronskim topom veliko boljše glede na gibljive in negibljive naboje, katere vnašajo v oksid.

Characterization of Thin Aluminium Films Vacuum Evaporated on Silicon Substrates

Key words: microelectronics, semiconductor technology, thin films, silicon wafers, vacuum evaporation, aluminium deposition, thermally grown silicon oxide, AES, Auger electron spectroscopy, capacitance-voltage method, interferometry

Abstract: For a long time vacuum evaporation of thin aluminium films has been a constitutive part of semiconductor technology. This article presents some results on characterization of these films by Auger electron spectroscopy, capacitance-voltage and interferometric methods. The results presented have been obtained by examining six characteristic samples. On three of them aluminium has been evaporated by electron beam technique; other tree were coated with aluminium by evaporation from tungsten spiral. In each group of samples one of samples has been previously covered by thermally grown silicon oxide; second sample has been doped by boron and third by phosphorus. Thickness, chemical composition and electronic properties of these films are different; films deposited on the silicon dioxide show the most prominent differences because of the well known reduction of silicon dioxide by aluminium. Also, it has been confirmed that electron beam evaporated samples show better characteristics concerning the contents of fixed and mobile charges in the underlining oxide.

1. Uvod

Vakuumsko naparjene plasti aluminija so že dolgo nepogrešljiv sestavni del polprevodniške tehnologije. Dobro nanašanje in legiranje, dobra električna prevodnost, možnost fotolitografskega postopka in nizka cena so zelo zaželene lastnosti v proizvodnji polprevodnikov. Aluminij se uporablja tako za vmesne plasti kot tudi za kontaktiranje silicija z ohišji (ožičenje). Uporabne lastnosti nanešenih plasti aluminija bodo odvisne od njihove končne kemične sestave in strukture. V članku podajamo rezultate karakterizacije tankih plasti aluminija, ki so nanešene v vakuumu z dvema različnima metodama: naparevanjem iz volframske špirale in nanašanjem s pomočjo elektronskega topa.

2. Izdelava vzorcev

Vsi vzorci so izdelani na podlagah iz silicijevih rezin z orientacijo <111> in premera 2". Vzorca št.1 in št.4 sta termično oksidirana do debeline silicijevega dioksida okoli 0.4 μm in sta bila n tipa z upornostjo 3-5 ohm cm.

Plast aluminija je na vzorec št.1 naparjena iz volframske špirale na vzorec št.4 pa nanešena s pomočjo elektronskega topa. Vzorca št.2 in št.5 sta imela za podlago silicijevi rezini p-tipa, upornost je znašala 3-5 ohm cm in

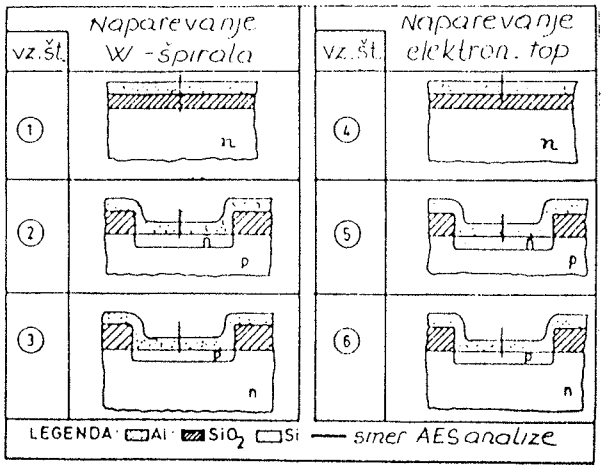

Slika 1: Shematski prikaz prereza vzorcev

sta bili oksidirani do debeline SiO_2 okoli 1 μm. S fotolitografskim postopkom sta bili pri obeh vzorcih v oksidu narejeni odprtini, sledil je postopek dopiranja s fosforjem in nato nanašanje aluminija. Plast aluminija je na vzorec št.2 naparjena iz volframske špirale na vzorcec št.5 pa nanešena s pomočjo elektronskega topa. Vzorca št.3 in št.6 sta imela za podlago silicijevi rezini n-tip oksidirani in pripravljeni na enak način kot vzorca št.2 in št.5 sta pa po odpiranju odprtin dopirana z borom pred nanašanjem aluminija. Plast aluminija je na vzorec št.3 naparjena iz volframske špirale na vzorec št.6 pa je nanešena s pomočjo elektronskega topa. Shematski prikaz preseka na opisani način izdelanih vzorcev z označeno smerjo ionskega jedkanja pri AES profilni analizi kaže slika 1.

3. Interferenčna in optična karakterizacija

Interferometrične meritve so pokazale, da je pri vseh šestih vzorcih debelina nanešenih plasti aluminija dokaj enaka in da znaša okoli 0.4 μm. Prav tako je optična interferometrija pokazala, da je debelina termično izdelanega silicijevega dioksida na podlagah vzorcev št.1 in št.4 pred nanašanjem aluminija, znašala okoli 0.38 μm. Preiskave z optičnim mikroskopom pri 500 kratni povečavi niso pokazale bistvenih razlik v izgledu in strukturi plasti.

4. AES karakterizacija

Vzorce smo pritrdili na nosilec vzorcev z nagibom 60 stopinj in vgradili v spektrometer Augerjevih elektronov (Phisical Electronics Ind. SAM 545 A). Vakuumski sistem je nato evakuiran do tlaka pod $2.5x10^{-7}$ Pa. Za analizo je uporabljen statični curek primarnih elektronov energije 3 keV in tok elektronov 0.5 μA. Vpadni kot curka primarnih elektronov glede na normalo na površino je znašal 30 kotnih stopinj. Vzorci so jedkani z dvema sovpadajočima curkoma ionov argona z energijo 1 keV, ki sta rastrirala na površini 5mm x 5mm pri vpadnem kotu 47 kotnih stopinj. Hitrost jedkanja Cr/Ni standarda je bila okoli 3 nm/min. Podatki dobljeni iz spektrov Augerjevih elektronov posnetih med profilno analizo so uporabljeni za izdelavo profilnih diagramov prikazanih na slikah 2-7. Na ordinati diagramov so nanešene intenzitete Augerjevih vrhov in na abscisi čas ionskega jedkanja. V legendi zraven diagrama je za vse detektirane elemente označeno pri kateri energiji se v spektru Augerjevih elektronov nahaja njihov vrh.

4.1 Rezultati AES profilne analize

Profilni diagram vzorca št.1 (slika 2.), plast aluminija debeline 0.4 μm naparjena iz volframske špirale na 0.38 μm debelo plast silicijevega dioksida, kaže na površini prisotnost tanke oksidne plasti. Vrh aluminija pri energiji 54 eV pripada aluminiju vezanemu v Al_2O_3. Na površini in deloma tudi v tanki oksidni plasti zaznamo manjšo koncentracijo ogljika kot kontaminanta. Tanka površinska oksidna plast, debeline okoli 10 nm izgine že po štirih minutah ionskega jedkanja. Vse do 130-te minute jedkanja se nahaja plast čistega aluminija, ko se pojavijo vrhovi: Si(78eV), ki pripada siliciju vezanemu v SiO_2, vrh Si(92eV) pripada elementarnemu siliciju in vrh kisika O(510eV). Mejo med Al in SiO_2 dosežemo po 150-tih minutah jedkanja (debelina okoli 0.45 μm).

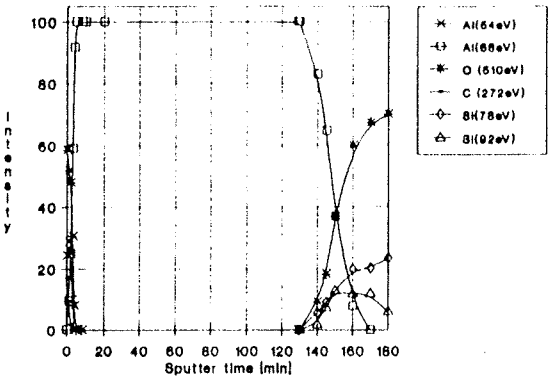

Slika 2: Profilni diagram vzorca št. 1

Profilni diagram vzorca št.2 (slika 3.), plast aluminija debeline 0.4 μm naparjena iz volframske špirale na silicijevo rezino dopirano z fosforjem kaže, da je na površini tega vzorca skoraj dvakrat debelejša plast Al_2O_3 kot na vzorcu št.1, kontaminacija površine in oksidne plasti z ogljikom pa je temu zelo podobna. Po 140-tih minutah ionskega jedkanja se pojavi vrh elementarnega Si(92eV). Mejo med čisto plastjo Al in Si dosežemo po 155-tih minutah jedkanja (okoli 0.46μm). Fosforja kot dopanda nismo zaznali, ker je v koncentracijah pod mejo občutljivosti AES metode.

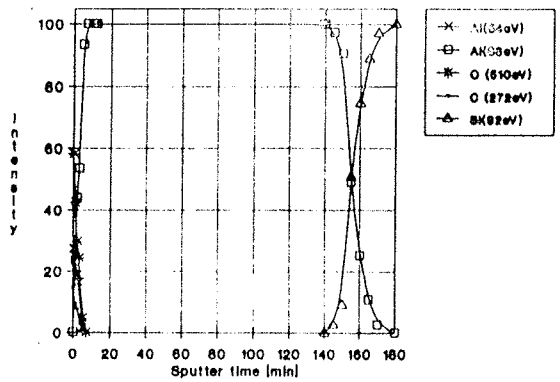

Slika 3: Profilni diagram vzorca št. 2

Profilni diagram vzorca št.3 (slika 4.), aluminij naparjen iz volframske špirale na silicijevo rezino, ki je bila dopirana z borom. Na površini vzorca št.3 je oksidna plast aluminija za malenkost tanjša kot pri vzorcu št.2 in tudi kontaminacija z ogljikom je nekoliko manjša. Čas ionskega jedkanja, ko zaznamo pojav elementarnega Si(92eV) in čas, ki je potreben, da dosežemo mejo Al/Si pa je polnoma enak. Bora prav tako ne zaznamo zaradi koncentracije, ki je pod mejo detekcije.

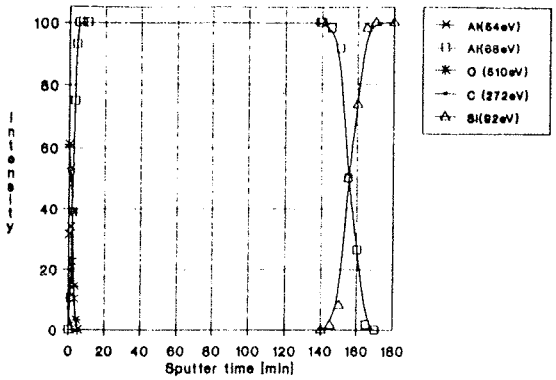

Slika 4: Profilni diagram vzorca št. 3

Profilni diagram vzorca št.4 (slika 5.), plast aluminija debela 0.4 μm nanešena na 0.38 μm debelo plast silicijevega dioksida s pomočjo elektronskega topa kaže, da je na površini tega vzorca plast Al_2O_3 skoraj trikrat debelejša, koncentracija ogljika pa dvakrat večja kot pri vzorcih št. 1, 2 in 3. Po 165 minutah jedkanja zaznamo vrhove Si(78eV), Si(92eV) in O(510eV). Mejo med Al in SiO2 dosežemo po 185 minutah jedkanju (okoli 0.56 μm).

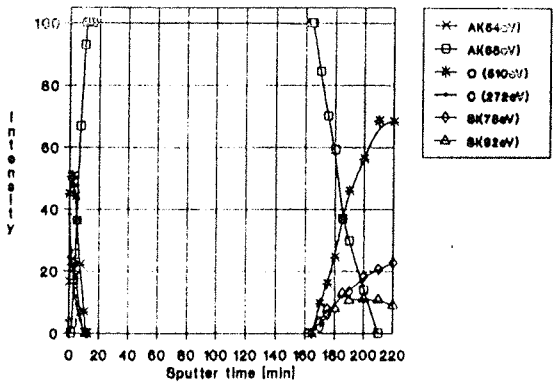

Slika 5: Profilni diagram vzorca št. 4

Profilni diagram vzorca št.5 (slika 6.), plast aluminija debela 0.4 μm nanešena na silicijevo rezino dopirano z fosforjem ima na površini tanko plast aluminijevega oksida, ki izgine že po 10-minutnem jedkanju (okoli 30 nm). Tudi tanka plast Al_2O_3 tega vzorca je kontaminirana z ogljikom vendar dosti manj kot plast na vzorcu št.4 in nekoliko manj, kot na vzorcih št.1, 2 in 3. Vrh elementarnega kisika se pojavi po 160 minutah jedkanja, mejo med Al in Si pa dosežemo po 185 minutah jedkanja (okoli 0.54 μm).

Profilni diagram vzorca št.6 (slika 7.), plast aluminija debela 0.4 μm nanešena na silicijevo rezino dopirano z borom s pomočjo elektronskega topa je zelo podoben diagramu vzorca št.5 (slika 6.) razen, da je približno enako debela tanka plast Al_2O_3 dosti bolj kontaminirana z ogljikom.

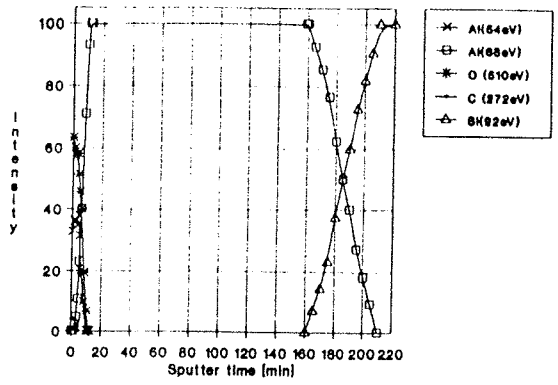

Slika 6: Profilni diagram vzorca št. 5

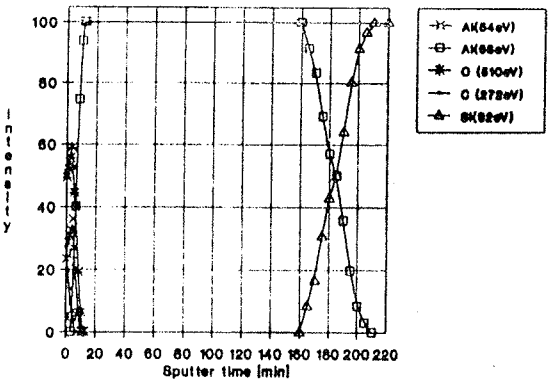

Slika 7: Profilni diagram vzorca št. 6

5. CV karakterizacija

Vzorca št.1 in št.4 smo uporabili tudi za meritve količine gibljivih in negibljivih nabitih delcev s pomočjo TBS metode /1/. Vzorec št.1 na katerega je bila 0.4 μm debela plast aluminija naparjena iz volframske špirale na 0.38 μm debelo plast SiO_2 je v oksidu vseboval Q = 3.41 x $10E^{11}$ q/cm^2 negibljivih in Q = 5.37 x $10E^{11}$ q/cm^2 gibljivih nabitih delcev.

Vzorec št.4 na katerega je bila 0.4 μm debela plast aluminija nanešena s pomočjo elektronskega topa na 0.38 μm debelo plast SiO_2, pa je v oksidu vseboval Q = 2.05 x $10E^{11}$ q/cm negibljivih in Q = 1.83 x$10E^{11}$ q/cm^2 gibljivih nabitih delcev.

5. Diskusija

Znano je, da se na površini aluminija takoj po nanašanju v vakuumu, tvori tanka plast Al_2O_3 /2/. Proces oksidacije površine poteka v dveh fazah: prva je kemisorbcija kisika in za to kemična reakcija, ki tvori oksid. Vsi z AES metodo analizirani vzorci so imeli na površini tanko oksidno plast aluminija na in v kateri smo zasledili različno vsebnost ogljika. Medsebojne razlike v debelini tanke oksidne plasti aluminija na površini, pri vzorcih na katere je naparevan aluminij iz volframske špirale in tistimi na katere je nanašan s pomočjo elektronskega topa so posledica več vzrokov: različni tlak (vakuum) pri

PRIKAZI DOGODKOV, DEJAVNOSTI ČLANOV MIDEM IN DRUGIH INSTITUCIJ

Priznanje "AMBASADOR REPUBLIKE SLOVENIJE V ZNANOSTI"

Priznanje "AMBASADOR REPUBLIKE SLOVENIJE V ZNANOSTI" sta letos prejela dva člana društva MIDEM, eminentna znanstvenika in pedagoga prof. dr. Zvonko Fazarinc in prof. dr. Stane Pejovnik. Uredniški odbor društva se pridružuje čestitkam.

PRIZNANJE "AMBASADOR REPUBLIKE SLOVENIJE V ZNANOSTI"SO DO SEDAJ PREJELI:

1991:

akademik prof.dr. Robert Blinc - fizika trdne snovi

prof.dr. Ivan Bratko - umetna inteligenca

prof.dr. Vinko Dolenc - nevrokirurgija

prof.dr. Aleksandra Kornhauser - kemijsko izobraževanje in informatika

prof.dr. Dušan Mlinšek - gozdarstvo

prof.dr. Slavoj Žižek - filozofija

1992:

prof.dr. Lidija Andolšek - ginekologija

prof.dr. Janez Peklenik - proizvodni sistemi

prof.dr. Gabrijel Kernel - fizika delcev

prof.dr. Vladimir Klemenčič - socialna in politična geografija

1993:

akademik prof dr. Vinko Kambič - otorinolaringologija

akademik prof.dr. Anton Trstenjak - teologija in psihologija

prof.dr. Vid Pečjak - psihologija

prof.dr. Vito Turk - biokemija

1994:

akademik prof.dr. France Bernik - slavistika

prof.dr. Zvonko Fazarinc - elektrotehnika

prof.dr. Dušan Keber - medicina

prof.dr. Stane Pejovnik - kemija

prof.dr. Slavko Splichal - komunikologija

Priznanje AMBASADOR REPUBLIKE SLOVENIJE V ZNANOSTI je prejel za raziskovalne dosežke v zadnjih letih prof.dr. STANE PEJOVNIK

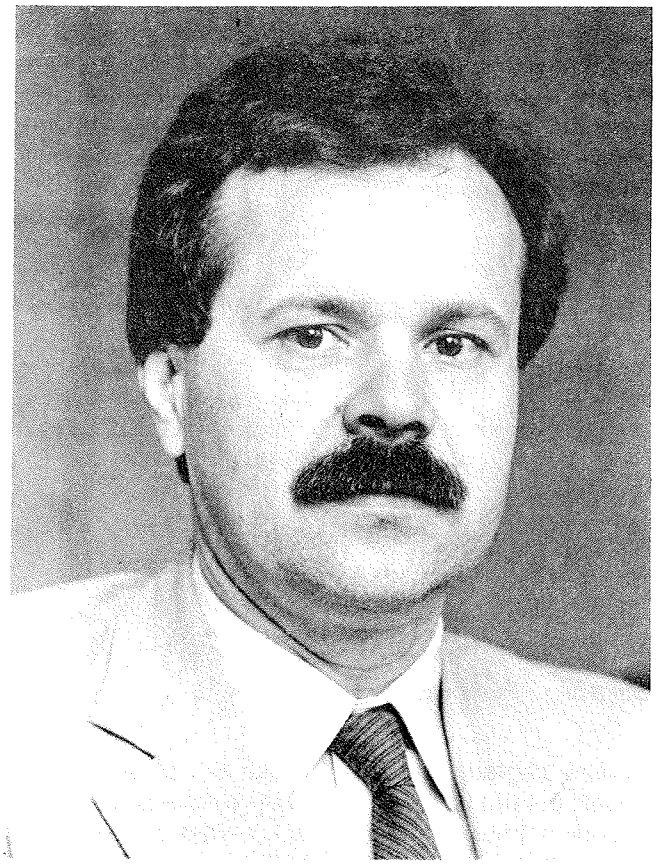

prof.dr. STANE PEJOVNIK

Diplomiral je s področja kemije, doktoriral v Ljubljani, redni profesor na Oddelku za kemijo in kemijsko tehnologijo Fakultete za naravoslovje in tehnologijo Univerze v Ljubljani, direktor Kemijskega inštituta v Ljubljani.

Profesor dr. Stane Pejovnik je uveljavljen raziskovalec na področju znanosti o materialih. O raziskavah procesa sintranja, materialih za moderne kemijske izvore električne energije, o razvoju in uporabi impedančne spektroskopije v raziskavah ionskih kristalov in fazne meje med kovinami in ionskimi prevodniki je objavil skupaj s sodelavci več kot 100 znanstvenih in strokovnih del in sodeloval na številnih mednarodnih strokovnih srečanjih. Za uspešno delo kot sekretar svetovnega kongresa o sintranju je že leta 1981 prejel posebno priznanje,

poleg tega pa je stalno sodeloval v programskih odborih mednarodnih konferenc s področja sintranja in s področja vede o materialih. Je sourednik dveh knjig, s prispevki s konferenc o sintranju in zeolitih, ki sta bili izdani pri Elsevierju. Vrsto let je urednik mednarodnega strokovnega časopisa Acta Stereologica - uradne revije Mednarodne stereološke družbe. Kot vabljeni gost je predaval na univerzah in drugih raziskovalnih institucijah po Evropi, S. Ameriki in Japonski. Na North Carolina State University je leta 1987 predaval predmet Uvod v vedo o materialih in leta 1992 na tehnični univerzi v Gradcu kot gostujoči profesor predmet Moderna keramika.

Profesor Pejovnik je član uglednih mednarodnih združenj, kot so American Chemical Society, International Society of Electrochemistry, International Institute for Science of Sintering in International Society for Stereology, kjer je bil tudi predsednik Komiteja za instrumentacijo. V letu 1990 je dvakrat deloval kot ekspert UNIDO za keramiko v Turčiji.

Pomemben del dejavnosti profesor Pejovnika poteka na področju znanstvene politike. Njegov prispevek na tem področju ni cenjen samo v slovenskem prostoru, zato je aktivno sodeloval na različnih mednarodnih srečanjih s področij znanstvene politike in prenosa znanstvenih in tehnoloških dosežkov. Od leta 1990 je član tehničnega komiteja za kemijo Programa COST Evropske unije in od leta 1993 predsednik Komiteja za področje "Kemija na površinah in faznih mejah" Programa COST za kemijo, kar je veliko priznanje. Od leta 1993 je član Slovensko nemškega komiteja za znanstveno sodelovanje in član slovenske UNESCO komisije ter od 1994 predsednik slovenskega UNESCO odbora za naravoslovne vede.

Kot direktor Kemijskega inštituta je pomembno prispeval k temu, da je inštitut postal doma in v svetu cenjena raziskovalna ustanova. Mednarodne povezave, ki so nastale na njegovo pobudo, poučevanje na uglednih tujih univerzah, poznavanje problemov raziskovalne politike v različnih državah in vodenje enega od projektov COST Evropske unije so nedvomno močno prispevali k uveljavljanju Slovenije v svetu.

Priznanje AMBASADOR REPUBLIKE SLOVENIJE V ZNANOSTI je prejel za dolgoletne raziskovalne dosežke prof.dr. ZVONKO FAZARINC

Diplomiral je s področja elektrotehnike, doktoriral v ZDA, kjer je z disertacijo o sintezi radioastronomskih merjenj leta 1965 doktoriral na Stanford University. Istega leta se je zaposlil v laboratorijih firme Hewlett-Packard v Palo Altu, Kalifornija. Firma je ena izmed najuglednejših družb za elektronsko in procesno merilno tehniko v svetovnem merilu.

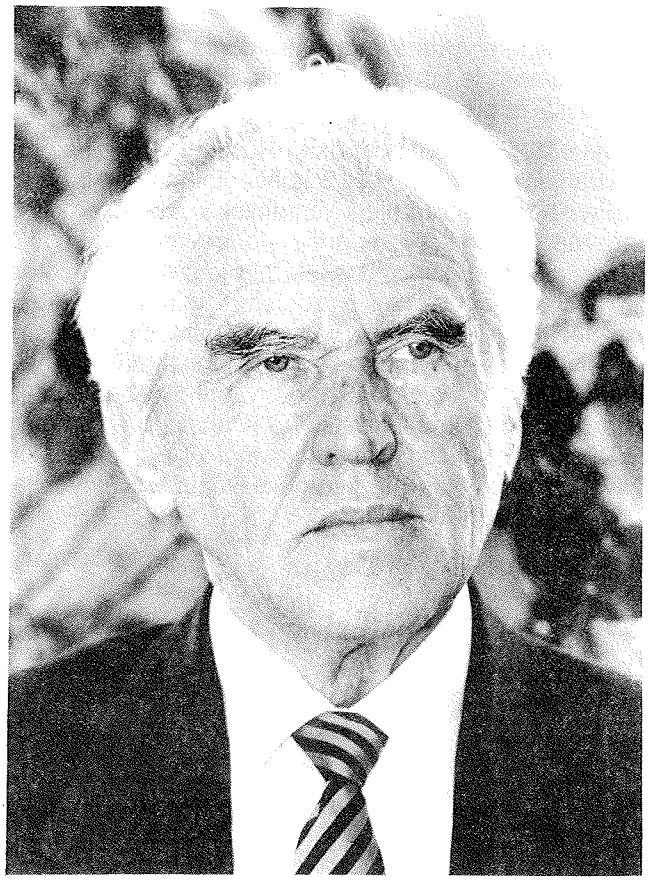

prof.dr. ZVONKO FAZARINC

Profesor Fazarinc je že leta 1966 izdelal računalniški program, ki je simuliral nelinearna elektronska vezja. Ken Van Bree, sodelavec iz laboratorijev Hewlett-Packarda, se spominja, da je bil takrat profesor Fazarinc edini na svetu, ki je to znal in zmogel. Njegovo delo je bilo temelj programa SPICE, ki so ga kasneje na Kalifornijski univerzi v Berkeleyu povzdignili na raven industrijskega standarda.

V letu 1978 je profesor Fazarinc postal direktor novoustanovljenega laboratorija za obsežno področje elektronskih instrumentov, integriranih vezij, ultra-hitrih analogno/digitalnih pretvornikov, procesiranja signalov, distribuiranih sistemov, načrtovanja programske opreme in orodij ter komunikacijskih protokolov. Vsi, ki se ukvarjajo s temi področji vedo, da so instrumenti in protokoli, ki so nastali v laboratorijih Hewlett-Packarda, svetovni standard. V tistem času je vpeljal sistem elektronske pošte, ki je povezal vse laboratorije v okviru Hewlett-Packarda, načrtoval je optične komunikacijske povezave. S svojim vizionarskim talentom, tehnološkim znanjem in znanstveno suverenostjo, je bil profesor Fazarinc vedno nekoliko pred svojim časom. Njegove zamisli in načrti se uresničujejo šele v zadnjih letih.

Pomemben je prispevek profesorja Fazarinca na področju sistemov za globalno določanje lokacije z visoko ločljivostjo. Leta 1980 je bil član sveta direktorjev firme Trimble Navigation, ki uspešno trži dvanajst izdelkov za globalno pozicioniranje. V letu 1980 je bil vodja projekta, s katerim so v Hewlett-Packardu naredili prvi osciloskop,

hibridni sistem vrhunskega instrumenta in računalnika. Ta instrument je istega leta revija Electronic Products proglasila za produkt leta.

Od leta 1987 dalje se profesor Fazarinc ukvarja s promoviranjem izvirne zamisli o konceptnem učenju naravoslovnih ved. Jedro njegove zamisli je, da je temeljne naravne zakonitosti mogoče poučevati s pomočjo računalniških simulacij. Uspelo mu je izdelati nazorne simulacije najzahtevnejših problemov iz teorije elektromagnetike in relativnosti. V ta projekt se je doslej vključilo dvanajst evropskih univerz, na katerih je profesor Fazarinc vedno zaželen predavatelj. Za sodelovanje v projektu, ki se imenuje COLOS (Conceptual Learning of Science), se sedaj poteguje tudi enajst ameriških univerz. V projekt je vključena tudi Republika Slovenija, za kar ima največje zasluge prav profesor Zvonko Fazarinc.

V vseh letih plodnega raziskovanja je profesor Fazarinc promoviral svojo domovino, jo predstavljal v svetu in prispeval k temu, da je firma Hewlett-Packard sponzorsko opremila številne laboratorije na Univerzi v Ljubljani z vrhunsko raziskovalno opremo.

Profesor Zvonko Fazarinc je objavil vrsto znanstvenih in strokovnih člankov v uglednih revijah in je solastnik patenta digitalne kontrole analognih vezij, podeljenega v ZDA.

Je ustanovni član uredniškega odbora strokovne in znanstvene revije Computer Application in Engineering Education, ki je bila v letu 1993 proglašena za najboljšo revijo na področju znanosti, tehnologije in medicine v ZDA.

22nd INTERNATIONAL CONFERENCE ON MICROELECTRONICS, MIEL'94
30th SYMPOSIUM ON DEVICES AND MATERIALS, SD'94
MIEL-SD 94
ADVANCE PROGRAM
September 28. - September 30. 1994
TERME ZREČE - ROGLA, SLOVENIA

ORGANIZER

MIDEM - Society for Microelectronics, Electronic Components and Materials

Dunajska 10, 61000 Ljubljana, SLOVENIA

SPONSOR

Ministry of Science and Technology of Republic Slovenia

PROGRAM COMMITTEE

Borut Lavrenčič, Slovenia
Iztok Šorli, Slovenia
Slavko Amon, Slovenia
Giovanni Soncini, Italy
Radomir Kužel, Czech Republic
Marko Hrovat, Slovenia
Janez Trontelj, Slovenia
Marija Kosec, Slovenia
Spomenka Beseničar, Slovenia
Bojan Jenko, Slovenia
Monika Jenko, Slovenia

ORGANIZING COMMITTEE

Franc Jan, Slovenia
Darko Belavič, Slovenia
Meta Limpel, Slovenia
Miloš Komac, Slovenia
Brane Kren, Slovenia
Rudi Ročak, Slovenia

GENERAL INFORMATION

The 22nd conference on microelectronics MIEL 94 continues the tradition of the annual international conferences organized by MIDEM, Society for Microelectronics, Electronic Components and Materials, Ljubljana, Slovenia. For the third time, the conference is organized jointly with the 30th Symposium on Devices and Materials, SD 94, another annual meeting of the same Society.

Both Conferences are well known through the distinguished guest speakers. As well, several hundred scientists from all over the world took part in these conferences in the past. The goal of connection and building of the friendship between the scientists and their companies remains the keystone of the organizer.

This year, special session devoted to presentation of microelectronics laboratories and enterprises will be held. The aim of the presentation is being acquainted with the work and possibilities of different research groups, companies and their projects.

The conference will be held in **TERME ZREČE - ROGLA**, Slovenia, a picturesque tourist resort, **SEPTEMBER 28th - 30th.**

PREPARATION OF THE PAPERS

The papers have to be prepared on maximum **6 pages A4 format**, ready for reproduction in the Proceedings.

RECEIPT DEADLINE

Deadline for the manuscript of the paper is **September 1st.**

CONFERENCE PROCEEDINGS

Invited papers and accepted papers will be published in the conference proceedings distributed at the conference registration.

LANGUAGE AND PRESENTATION

Official conference language is English.

Each author will have 10 minutes to orally present his paper. 5 minutes are reserved for discussion.

REGISTRATION

The registration fee is US$ 300. MIDEM Society, as well as Conference sponsor members have 20% discount while MIDEM members have 30% discount. The fee includes free access to all conference events, including welcome cocktail party and the conference dinner on September 29th.

An information and registration desk will be opened from Wednesday, September 28., to Friday, September 30., from 8:00 to 19:00 and also Tuesday, September 27., from 17:00 to 20:00.

CONFERENCE VENUE

The Conference will be held from September 28th to September 30th, at Hotel Planja, Rogla, Slovenia.

TRAVEL AND ACCOMMODATION

You can arrive to Rogla, Slovenia, first by plane to the airport of Ljubljana or Maribor.

By car, take exit from the main road between Celje and Maribor, following signs for Zreče and Rogla. You need about half an hour of slow drive to reach Hotel Planja on Rogla from Zreče town.

We strongly recommend accommodation in Hotel Planja, where Conference takes place.

The room reservation has to be made directly to :

TURIZEM UNIOR ZREČE
Hotel PLANJA, MR.SANDI PLAUSTEINER
Cesta na Roglo 15, 63214 Zreče, Slovenia
TEL. +386 - (0)63 - 762 451
FAX. +386 - (0)63 - 762 446

SOCIAL EVENTS

The cocktail party will be organized on Wednesday, September 28th and the Conference dinner on Thursday, September 29th.

Program and organizing committee :

MIDEM
Dunajska 10
61000 Ljubljana, SLOVENIA
TEL.+386 - (0)61 - 312 898,
FAX.+386 - (0)61 - 319170

Secretary of the conference:
Mrs.Meta Limpel

CONFERENCE PROGRAM

WEDNESDAY, SEPTEMBER 28

9:00 WELCOME AND OPENING CEREMONY

9:30 INVITED PAPER

J.TRONTELJ : Trends in Mixed Signal Asic Design

10:30 COFFEE BREAK

10:45 MIEL SESSION ON INTEGRATED CIRCUITS

D.STRLE : On the Low Voltage, Low Power Analog CMOS Circuit Design

S.OŽBOLT, J.TRONTELJ, L.TRONTELJ : High Voltage Transistors in Integrated Analog Stages

A.PLETERŠEK, J.TRONTELJ : Low Noise Design Using Compatible Lateral Bipolar Transistors in CMOS Technology

S.STARAŠINIČ, J.TRONTELJ : Two Channel ASIC for Implanted System

V.KUNC, J.TRONTELJ, L.TRONTELJ : A Study of Resolution Limitation for Integrated Picoampere Measuring System

M.JENKO : Stochastic Phenomena in the Design of High Speed VLSI Circuits - The Dumand Chip

K.LUTHER,T.KRISTOFFERSSON, H.SCHLEIFER, W.RECZEK : Design Concept for a 5V/3.3V DRAM in a 5V Technology

12:30 LUNCH

14:30 INVITED PAPER

H.VIEFHAUS : Surface, Interface and Thin Film Analysis in Material Science

15:30 MIEL SESSION ON INTEGRATED CIRCUITS

W.KAUSEL, H.KREMSER : 4-Channel CMOS Subscriber Line Interface Kit

T.KRISTOFFERSSON, W.RECZEK, J.RIEGER: Address Chain Optimization for Low Voltage Drams

R.OPARA : 1/f Noise Parameter Identification

J.TRONTELJ : Methodology for Automatic Schematic Generation from IC Layout

D.RAIČ : Towards a Faster and User Friendly Schematic Capture System

R.PORENTA, J.TRONTELJ : Methods for Handling Special Circuit Properties When Comparing Scheme and Layout Circuits

17:00 COFFEE BREAK

17:15 MIEL SESSION ON TECHNOLOGY

P.BELLUTTI, M.BOSCARDIN, A.LUI, G.SONCINI, M.ZEN, N.ZORZI : Bird's Beak Reduction by Dry Locos Technique

M.MAČEK, AL V.KORDESCH : Comparison of Thin Oxide Charge to Breakdown Measurement Techniques

D.RESNIK, P.POPOVIČ, D.VRTAČNIK, S.AMON : Characterization of Thermal SiO_2/LPCVD Si_3N_4 Double Layer Anti-reflective Coating

G.U.PIGNATEL, G.F.DALLA BETTA, G.SONCINI : Materials and Fabrication Technologies for Nuclear Radiation Detectors
T.ATHANAS, I.ŠORLI, Z.BELE, I.NEDEV : High Resistance Polysilicon Resistors for Analog-digital Design
U.ALJANČIČ, D.RESNIK, D.VRTAČNIK, S.AMON : Temperature Dependencies of Silicon Piezoresistive Pressure Sensor
M.MOZETIČ, M.KVEDER, M.DROBNIČ, A.PAULIN: Atomic Hydrogen Processing of Magnetron Surfaces

19:00 PRESENTATION OF LABORATORIES

20:00 COCKTAIL

THURSDAY, SEPTEMBER 29

08:30 INVITED PAPER

N.SETTER : Ferroelectric Thin Films for Microelectronics And Micromechanics Applications

09:30 SD SESSION ON THIN FILMS

M.GODEC, P.PANJAN, A.CVELBAR, B.NAVINŠEK, A.ZALAR : A Study of Titanium Silicide Growth
A.CVELBAR, P.PANJAN, B.NAVINŠEK, A.ZALAR, Ž.ŠMIT, M.BUDNAR, D.MANDRINO: A Comparative Study Of Ni/Si Interaction by Means of AES, XRD, RBS and Electrical Resistivity
A.CVELBAR, P.PANJAN, B.NAVINŠEK : In Situ Continuous Electrical Resistivity Measurement as an Analytical Method for Nickel Silicide Formation During Heating at a Constant Rate
U.DELALUT, M.KOSEC : Effect of Chemical Composition on Crystallization and Microstructure Development of Alkoxide Based PLZT Thin Films
A.KANDUŠER, P.PANJAN, D.MANDRINO, C.FILIPIČ, M.KOSEC, B.LAVRENČIČ : Dielectric and Crystallographic Properties of Sputtered $LiTaO_3$ Thin Films on Conducting and Semiconducting Substrates
M.STUBIČAR, G.BITELLI, S.LUGOMER, M.STIPANČIĆ : Formation of Ta-nitrides by High Power Pulsed CO_2 Laser in Pressurized N_2 Atmosphere
F.BRECELJ, M.MOZETIČ, K.ZUPAN, A.PREGELJ : Study of Barium Evaporation From Impregnated Cathode

11:15 COFFEE BREAK

11:30 SD SESSION ON CERAMICS, METALS AND COMPOSITES

R.KUŽEL, J.STEJSKAL : Electrical and Dielectric Properties of Polyanilline Composites
D.KUŠČER, M.HROVAT, J.HOLC, Z.SAMARDŽIJA, S.BERNIK, D.KOLAR : Investigation of Novel Sofc Cathode Materials
I.ZAJC, M.DROFENIK : New PTCR Ceramics
M.VALANT, D.SUVOROV : Microwave Dielectric Properties of the Bi-doped $Ba_{4.5}Nd_9Ti_{18}O_{54}$ Phase

12:30 LUNCH

14:30 INVITED PAPER

Z.SITAR : MBE in Ferroelectrics, Technique and Analysis

15:30 SD SESSION ON CERAMICS, METALS AND COMPOSITES

F.VODOPIVEC, B.BRESKVAR, B.ARZENŠEK, M.TORKAR, J.ŽVOKELJ : Effect of Deformation by Wire Drawing on Magnetic Properties of a $Fe_{28}Cr_{16}Co$ Alloy
M.JENKO, F.VODOPIVEC, M.GODEC, D.STEINER-PETROVIČ : Surface Activated Recrystallization of Non-oriented Electrical Steel Sheet
G.DRAŽIČ, S.KOBE-BESENIČAR, B.SAJE : A TEM-EDXS Study of Zirconia Doped Nd-Dy-Fe-B Magnets Fabricated from the HDDR Processed High Coercitivity Powders
B.ŠUŠTARŠIČ, B.BRESKVAR, V.LESKOVŠEK, A.RODIČ : Microstructural Characteristics of Water Atomized Cu-based Powders for Brazing

16:30 COFFEE BREAK

16:45 MIEL SESSION ON PHOTOVOLTAIC DEVICES

P.POPOVIĆ, E.BASSANESE, J.FURLAN, F.SMOLE : Calculating the Transient Response in Multilayer a-Si:H Structures
I.SKUBIC, J.FURLAN : Small Signal Capacitance of a NIN a-Si:H Structure
E.BASSANESE, P.POPOVIĆ, J.FURLAN : Transient Dark Currents in A-Si:h NIN and PIN Devices
M.TOPIČ, F.SMOLE, J.FURLAN, W.KUSIAN : Front TCO/a-Si:H Contact Heterojunction in p-i-n a-Si:H Solar Cells
F.SMOLE, M.TOPIČ, J.FURLAN : Effects of n(a-Si:H)/TCO Heterojunctions on p-i-n a-Si:H Solar Cell Performance
J.TOUŠKOVA, D.KINDL, J.KOVANDA, J.TOUŠEK : Characterization of CdS/CdTe Photovoltaic Cells
A.SUHADOLNIK : Distance Measurements Using Optical Fiber Sensors
A.BABNIK, A.SUHADOLNIK, J.MOŽINA : Fiber Optic Microphone

18:45 MIEL SESSION ON DEVICE PHYSICS AND MODELING

I.ZELINKA, J.TRONTELJ : Simulation of Large Scale Integrated Circuits with Spice
D.KRIŽAJ, S.AMON : Analytical Optimisation of Resurf LDMOS Transistor Breakdown Properties
S.SOKOLIF, S.AMON : Inconsistencies in Treatment of Heavy Doping Effects in General Purpose Device Simulators

20:00 CONFERENCE DINNER

FRIDAY, SEPTEMBER 30

08:30 INVITED PAPER

R.DELL'AQUA : Sensors : A Great Chance for Microelectronics Technologies

09:30 SD SESSION ON THICK FILMS

J.HOLC, J.SLUNEČKO, M.HROVAT : Temperature Characteristics of (Ba, Sr)TiO_3 Ceramics Thick Film Sensors
M.HROVAT, G.DRAŽIČ, J.HOLC, D.BELAVIČ : Microstructural Investigation of Thick Film Resistors for Strain Sensor Applications by TEM
D.ROČAK, V.STOPAR : New Fluxes and Organic Solvents for Hybrid Circuits Cleaning to Replace CFC Solvents
J.MAČEK, D.ARZENŠEK, M.MARINŠEK : Nickel Dispersions in Zirconium (Titanium) Dioxide Prepared by Gel Precipitation in Nonaqueous Media
J.MAČEK, A.DEGEN, B.NOVOSEL : Preparation of Metal Powders in Nonaqueus Media for Thick Film Applications
M.HROVAT, J.HOLC, D.KOLAR : An Evaluation of Thick Film Ruthenium Oxide Based Electrodes for Solid Oxide Fuel Cells

11:00 COFFEE BREAK

11:15 LATE PAPERS

12:15 CLOSING OF THE CONFERENCE

PREDSTAVLJAMO PODJETJE Z NASLOVNICE

Iskra Števci

Iskra Števci je samostojna družba, ki v zadnjih letih dosega izredno dobre rezultate. Uvršča se med vodilne evropske proizvajalce na področju merjenja in upravljanja z električno energijo. Izrazita je usmerjenost podjetja v izvoz. Od lanskoletnega prihodka v višini 100 milijonov DEM je okrog 90 odstotkov izvoza v 34 držav. Največ izvaža v Nemčijo, Benelux, Španijo, Malezijo, Kolumbijo in v Veliko Britanijo.

Proizvodni program obsega števce električne energije, tarifne naprave, statične precizijske števce, nove elektronske monolitne števce in sodobne merilne sisteme za merjenje, registracijo, obdelavo in prenos podatkov. Program je v celoti rezultat domačega znanja in dolgoletnih izkušenj strokovnjakov v Iskri Števci.

Iskra Števci uspešno izpolnjuje visoko postavljene zahteve domačih in tujih kupcev po kakovosti merilne opreme. Poslovanje in sistem zagotavljanja kakovosti sta prilagojena mednarodnim standardom ISO 9001.

Razvojna strategija Iskre Števci temelji na nenehnem uvajanju novih tehnologij in izdelkov, ki so nujno potrebni za obstanek na zahtevnih tujih trgih. Med take novosti sodijo tudi novi elektronski monolitni števci za gospodinjstva in industrijo.

Predzgodovina sedanjih elektronskih števcev se je začela že v zgodnjih sedemdesetih letih, ko so bili v Iskri Števci razviti prvi precizijski elektronski števci. Zelo velik tehnološki izziv, zlasti na področju mikroelektronike, je motiviral proizvajalce števcev, da so iskali možnost za razvoj novega števca za gospodinjstva prav v kombinaciji z elektronsko tehnologijo.

Ob sovlaganju v Iskrino tovarno mikroelektronike v 70. in 80. letih so strokovnjaki prišli do neprecenljivih znanj, ki so bila predpogoj, da je sploh prišlo do izvedljive zamisli o monolitnem števcu in da sta bili v nadaljevanju možni tudi raziskava in realizacija projekta, ki je pripeljal do proizvodnje elektronskih monolitnih števcev.

Specifika merilne smart senzorske tehnike je narekovala razvoj lastne proizvodne linije za profesionalno inkapsulacijo CER- PACK. Proste zmogljivosti nudimo tudi zunanjim zainteresiranim uporabnikom.

Izvozna uspešnost Iskre Števci je vedno temeljila na licenčni in patentni neodvisnosti lastnih izdelkov. Tudi originalna zasnova enočipnega merilnika električne energije na osnovi Hallovega senzorja potrjuje takšno generično sposobnost firme, ki se rezultira v uspešnem uvajanju novih izdelkov v monolitni tehniki.

S celovito ponudbo indukcijskih in elektronskih števcev ter sistemov za merjenje, registracijo in obdelavo podatkov o električni energiji Iskra Števci uspešno nastopa na domačem in tujem trgu. Njen glavni kapital je v inovativnem znanju in ljudeh, ki svoje delo prilagajajo času in novim zahtevam.

Pripravil: Alojz Boc, Iskra Števci,
Tržno komuniciranje

Industrija merilne in upravljalne tehnike Kranj, d.o.o.
Savska loka 4, 64001 Kranj
Tel. 064 221-321, faks: 221-312

POROČILA

SEMICON EVROPA 94
PALEXPO, ŽENEVA, ŠVICA 11.-14.APRIL

Že drugo leto zapored je bil ta izredno pomemben, če ne najpomembnejši dogodek za proizvajalce mikroelektronske procesne opreme in uporabnike v Ženevi na razstavnem prostoru Palexpo, kjer se odvijajo tudi mnoge druge razstave svetovnega pomena. Za razliko od prejšnjih let, ko je bila ta razstava v Zürichu v večih ločenih paviljonih, je na Palexpu vse združeno v enem velikem paviljonu. Glavni organizator te prireditve je SEMI (Semiconductor Equipment and Materials International), ki vsako leto zelo dobro poskrbi za informiranje obiskovalcev s svojimi brošurami.

Razstavni prostor je tematsko razdeljen v tri področja:
- testiranje in montaža
- kemikalije in plini
- procesna oprema

Struktura obiskovalcev je predvsem sestavljena iz ljudi, ki so neposredno vpleteni v delo na področju mikroelektronike in pridejo na razstavo z določenimi vprašanji tehnične narave, ki jih potem v neposrednem stiku s predstavniki proizvajalcev poskušajo skupno reševati in ustvariti temelje za nadaljnje sodelovanje. Vsekakor je tak sejem tudi vir povratnih informacij od uporabnikov k proizvajalcem. Nadalje je veliko obiskovalcev, ki se zanimajo za najnovejše dosežke na področju testirne ali procesne opreme in se na podlagi informacij iz prve roke nato laže odločijo za nabavo specifične opreme.

Istočasno s samo razstavo pa potekajo aktivnosti tudi na znanstveno strokovnem področju.

Tako so se letos že prvi dan sestale SEMI komisije za standarde v mikroelektroniki in pričele delo pri usklajevanju čedalje strožjih norm, ki naj bi bile temelj za vnaprej.

Obenem pa so vse tri dni potekala tudi strokovna posvetovanja iz naslednjih področij:

- trendi v CVD
- moderni fotolitografski postopki
- čiščenje silicijeve površine, ultračisto procesiranje

Ločeno so potekale tudi takoimenovane delavnice na naslednje teme:

- problemi varovanja okolja in varnosti v mikroelektronski industriji
- komunikacije pri koordiniranju SEMATECH in JESSI projektov
- standardizacijski procesi pri identifikaciji in kontroli mikroelektronskih materialov

Potekala pa je tudi okrogla miza na temo mikroelektromehanskih sistemov (MEMS), ki predstavlja danes ogromen potencialni trg, zato mu posvečajo čedalje več pozornosti.

Naslednja okrogla miza je bila na temo prikazovalnikov z ravnimi zasloni.

Ob opremi, ki jo uporabljamo v laboratoriju za elektronske elemente na Fakulteti za elektrotehniko in računalništvo in pri našem delu v polprevodniški tehnologiji se pojavljajo včasih težave tehničnega tipa, za katere je potrebno dostikrat konzultirati tehnično osebje proizvajalcev določene opreme in si pomagati z njihovimi izkušnjami. Obenem pa se je potrebno vedno znova spoznavati z novostmi, ki jih vpeljujejo v mikroelektronsko procesiranje, kot tudi nove merilne metode in instrumente za karakterizacijo elementov. Zato je bil obisk te razstave izpolnjen z mnogimi razgovori, na katere se je potrebno že vnaprej dobro pripraviti, da se v kratkem času izmenja čimveč koristnih informacij.

Pri merilni opremi smo se največ zadržali pri novem HP parametričnem analizatorju HP 4155a, ki predstavlja korak naprej od predhodnega modela HP4145, ki ga uporabljamo sedaj v našem laboratoriju in pri posebno prirejeni in oklopljeni merilni mizi firme Cascade Inc., ki vljučno z izpopolnjenimi merilnimi konicami dopušča ponovljive meritve tokov v razredu femtoamperov. Podobno smo se zanimali pri firmi MDC za kvazistatične CV meritve in ekstrakcijo parametrov, ki jo ponujajo s svojim programskim paketom. Take renomirane firme so pripravljene nuditi tudi brezplačno meritev vzorcev, kar je izredno dobrodošlo kot referenca v lastnem laboratoriju. Precej časa smo se zadržali tudi pri proizvajalcih opreme za čiščenje silicijevih rezin in sicer s postopki megasonic čiščenja in z recirkulacijskimi posodami za florovodično kislino. Poleg razgovora smo bili deležni tudi detajlnih razlag prednosti tega načina, podkrepljenih z rezultati mnogih neodvisnih eksperimentov, česar po pravilu ne dobiš v nobeni literaturi. Ker je danes mnogo dilem o učinkovitosti različnih tehnik čiščenja površine silicija, so bile informacije zelo koristne, dasiravno skoraj vse v prid proizvajalca. Nadalje so bili zanimivi razgovori o ozonatorjih, vgrajenih v sisteme superčiste vode za redukcijo TOC in bakterij z UV svetlobo, ki jih imamo namen vključiti v obstoječ sistem.Prav tako deluje tu tudi trg rabljene opreme in kar nekaj znanih "second hand" firm je bilo prisotnih s svojo ponudbo. Tencor je predstavljal novo serijo detektorjev delcev na rezini (surface scan serija 5000). Ravno tako smo se lahko pozanimali tudi za nabavo nekaterih rezervnih delov za starejše modele opreme, silicijeve rezine in za kvarčne izdelke, predvsem difuzijske cevi in pribor firm Heraeus in GE.

Poleg stalnih razstavljalcev je bilo opazno tudi nekaj predstavnikov evropskega vzhoda, predvsem inštitutov iz Rusije, ki so predstavljali svoj program, največkrat omejen na ponudbo eksotičnih materialov.

To je torej razstava, ki utrjuje stare stike, pomaga reševati tekoče tehnične prepreke, ki se pojavljajo pri delu in omogoča vpogled v trende in najnovejšo opremo oziroma postopke v svetu mikroelektronike in je kot taka izredno koristna in potrebna.

mag. Drago Resnik, dipl.ing.
Laboratorij za elektronske elemente
Fakulteta za elektrotehniko in računalništvo
Tržaška 25, 61000 Ljubljana

VESTI

China: technology's new frontier

In **The Book of Messer Marco Polo of Venice**, published at the end of the 13th century, Marco Polo described his travels in China: an enormous land with a thriving trade, full of exotic goods. Suddenly, the world Europe knew had doubled in size.

China, a nation of 1.2 billion people, is similar in size to the U. S. Geographically, the nation resembles the U. S. It lies between the same latitudes as the U. S., and, from Beijing to China's western border, the distance is about the same as from New York to San Francisco.

China's 1993 gross national product was around US$400 billion, growing at 8. 5% per year, according to the U. S. Department of Commerce. The top three investor nations are Honk Kong/Macao, Japan and Taiwan.

In a report issued by the U. S. Department of Commerce International Trade Administration, **China-Country Marketing Plan FY'93**, computers and peripherals, and communications were ranked fifth and seventh in the "China's best market prospect" listing.

According to the account, the Chinese spent around $1.3 billion in 1992 on computers and peripherals, an amount that it predicts will grow 10% per year.

Just what are the Chinese buying? Mostly workstations, personal computers and printers, the Commerce Department reports.

"China's imports of computer equipment increased by 50% in 1992 compared to 1991, to almost $1 billion, " a dispatch from the U. S. Embassy in Beijing in spring 1993 states. "We believe that the market for personal computers alone is worth about $750 million this year (1993) on the sale of about 300,000 units. Several domestic manufacturers offer Intel 386- and 486-based machines. "

Most PCs sold in China enter the country as components that are then assembled into final systems. Many components are smuggled. The U. S. Embassy dispatch notes, "Ministry of Machinery and Electronics officials admitted that 50% of all integrated circuits entering China are smuggled. "

Besides buying, China is also selling computer equipment. The February research study **Information Technology Market Opportunities in China**, from San Jose, Calif. -based Dataquest Inc., reports that China supplies floppy disks, PC motherboards, monitors, disk drive heads, mice, keyboards and more. The Dataquest report declares telecom to be the fastest growing sector of China's economy. Total revenue from postal and telecom services increased 40% in 1992 and 59% in 1993.

The research study expects the Chinese government to continue its heavy investment in communications infrastructure. More than 10 million phone lines were added to its communications infrastructure in 1993. The goal is for 400 million lines by 2010.

According to a dispatch issued by the American Embassy in Beijing on 24 Jan., China's Ministry of Posts and Telecommunications is building a national fiber-optic network to support that goal. As part of the eight five-year plan (1991-1995), the network will contain 22 trunk lines totalling 32, 000 kilometers by the end of 1995. Ten trunk lines were completed during 1993, and work began on another 10 trunk lines.

The number of cellular-phone subscribers jumped 200% since 1991, reaching 570,000 last year, reports Dataquest. Pager sales grew an amazing 1,500% from 437, 000 in 1990 to 7 milion in 1993.

By all accounts, China is the frontier for high technology capitalism. Procrastinators risk loosing big.

(ELECTRONICS, 28.2.1994)

Siemens grabs growing share of chip-card market

Within the last year, the Semiconductor Group of Munich-based **Siemens AG** has significantly increased its market share in the chip-card market. According to Peter Bauer, the new head of the Siemens chip-card department, his company currently serves about 28% of the world market for chip cards.

In this area, Siemens directly competes with **SGS Thomson Microelectronics NV** of Agrate Brianza, Italy and **Motorola Corp.** of Schaumburg, Ill. Together, these three companies are said to satisfy 83% of the world chip-card demand.

Bauer **claims to be the market leader in the intelligent memory card industry, with a market share of 56%. At an average annual growth rate of 30% in the intelligent memory card business, Bauer said Siemens expects to grab sales worth over DM500 milion (US$294 milion) by the year 2000.**

He said Siemens is a technology leader in the crypto-controller market. Ulrich Hamann, senior marketing manager of Siemens' chip- card department, said Siemens "will massively enter the controller-card market, " the fastes growing segment of the chip- card market in which Motorola leads.

TYPES OF CHIP CARDS

Intelligent memory cards contain security and access control logic, and an EEPROM of up to 8 kbytes. They are used as phone cards (less than 100-bit EEPROM) and health cards (256-byte EEPROM).

Microcontroller cards are comprised of an entire computer system with CPU, RAM, ROM, EEPROM, security logic and I/O. They are used as GSM network access cards and bank cards. A potential application is the "electronic purse"-cards that allow instant payments of small amounts for bus rides and at automated vending machines. The first field trial is the "carte bancaire" in France that allows banking transactions as well as shopping with the chip card.

Cryptocards are microcontroller cards with an additional math co- processor for cryptographic applications. They are used when a very high level of security is needed, such as for an electronic signature.

Identsystem cards are used for general access control-mainly as a contactless chip card. Main applications will be with public transport systems and for toll highways. -AV

(Electronics, 28.2.94)

Sony develops world's first UV solid-state laser

Sony Corp. of Tokyo has developed the world's first far ultraviolet, solid-state, high-power laser. The breakthrough by researchers at Sony Corporate Research Laboratories in Tokyo's Shinagawa ward was reported last week at the Advanced Solid State Lasers meeting in Salt Lake City, Utah. The experimental device can generate a 1-watt continuous wave beam at a wavelength of 266 nanometers. The result is achived by resonant doubling the 2. 7 W green output of a diode-pumped, intra-cavity-doubled neodymium yttrium-aluminum-garnet laser.

Commercial applications are between one and two years away. A. J. House in Sony's Tokyo headquarters, says the development **could replace costly excimer lasers in steppers for semiconductor production.** Sony researchers believe, says House, "that UV laser (steppers) would be capable of a design rule in the region of 0. 25 microns" at far lower installation and operating costs than excimer laser steppers.

Other possible applications cited by House include microsurgery or other high-precision etching or cutting operations. Consumer applications are unlikely because of the size of the equipment required for second harmonic generation lasers.

(ELECTRONICS, 28. 2. 1994)

Intel dedicates Fab 10 in Ireland

Long criticized for exporting U. S. -made semiconductors to Europe with no European presence, **Intel Corp.** of Santa Clara, Calif., early this month silenced its critics. On a 180 acre site in Leixlip, Ireland, where the Rye River joins River Liffey, Intel dedicated a 600,000 square foot fab.

With a 60,000 ft^2 classone clean room processing 8-inch wafers using 0.6-micron BiCMOS process rules, Intel will produce the Pentium and, eventually, its P6 processor.

Fab 10 will contribute to Intel's plan to manufacture over 6 million Pentium chips this year. It will also make the new 486DX4 the 3.3 volt, 100-MHz CPU with 16-kbyte cache for high-end notebook computers.

A US$750 million investment, Fab 10 is one of many Intel is building. Andrew S. Grove, Intel's president, says **the company will make $2.4 billion in capital investment in 1994, 26% more than 1993 - and again the largest in the industry.** The investments are part of a $7 billion five-year expansion program.

The facility is highly automated using an overhead monorail and floor-based robots to transport wafers during processing, and an automated on-line statistical and quality control system to monitor every step in the manufacturing process. Intel-based PCs act as station controllers for the wafer processing equipment in the fab.

(ELECTRONICS, 28. 2. 1994)

At IDEM, future ICs reach limits of theoretical physics

The **International Electron Devices Meeting (IEDM)** held last week (5-8 Dec.) in Washington was a showcase of integrated circuits with features sized of 0.1 micron and below. **Such developments promise circuits able to run on 1.5-volt power.** Three presentations illustrate the point.

AT&T Bell Laboratories of Holmdel, N. J., reported on a conventional silicon manufacturing process that can build an integrated circuit with a 0.1 micron feature size that operates at room temperature. Such devices previously had to be cooled.

Toshiba Corp.'s Research and Development Center in Kawasaki, Japan has succeeded in producing an IC with an even smaller feature size. At IEDM, it described its n-channel MOSFET with a gate length that is a mere 0.04 micron. It, too, operates at room temperature.

Finally, **Texas Instruments Inc.** went even further. At the conference, the Dallas-based company demonstrated **the first integrated circuits containing transistors with feature sizes of 0.02 micron.** At these dimensions electrons stop acting as particles and begin acting like waves.

MAKING 0.1 MICRON ICS WORK AT ROOM TEMPERATURE

Fabricating ever-smaller transistors in silicon is limited because of the chemical dopants, typically arsenic and boron, implanted in silicon to make it function as a transistor. At smaller feature sizes, the amount of dopants required would cause the transistor to act like a resistor.

The conventional solution has been to reduce the amount of dopants used. However, with this approach, the transistor leaks unwanted current and overheats the device. Until now, the solution has been to cool the transistor.

AT&T Bell Laboratories of Holmdel, N.J., solved the problem using a patented technique called vertical doping engineering. AT&T believes the technique will allow feature sizes as small as 0.05 micron.

Speed is another benefit of the technique. With vertical doping engineering, the 0.1-micron device can run at 116 GHz for n-channel MOS or 51 GHz for p-channel MOS. By contrast, cooled 0.1-micron circuits ran at 90 GHz for n-channel and 23G Hz for p-channel.

Changing the chemistry makes 0.05 micron transistors possible

In looking at the problem of creating sub-0.1 micron devices, **Toshiba Corp.'s** Research and Development Center in Kawasaki ,Japan, determined that changing the dopants used to create transistors was the best solution. Where conventional processes used boron, Toshiba substituted phosphorus.

The company has fabricated an n-channel MOSFET that has a gate length of 0.04 microns. The device is fabricated using phosporus source and drain junctions that are a mere 0.01 microns wide. Moreover, the gate functions at room temperature.

TI transistors obey quantum mechanics laws

Texas Instruments Inc. of Dallas has been experimenting with quantum effect transistors (QETs). Using a molecular beam epitaxy (MBE) process, more typically used in gallium arsenide manufacture, the company produces QETs using compounds of indium, phosphorus, gallium, aluminum and arsenic. The company is also trying to apply MBE to silicon.

Using MBE, TI researchers produce multiple layers of semiconductor materials each only a few atoms thick. Sandwiching the layers together creates barriers that stop the flow of electronics. Applying a voltage to a control terminal causes electron waves to tunnel through the barrier.

The technique works because electrons at these feature sizes behave like waves not particles. An electron demonstrates wavelike behavior when the barrier containing it has one dimension that approximates the electron's wavelength.

At room temperature, gallium arsnide - a semiconductor compound TI uses to build quantum effect transistors - has electrons whose wavelengths measure 0.02 microns. This is sufficiently close to the thickness of the barrier to allow the electron waves to tunnel through.

The logic circuit developed to demonstrate the viability of the process is a 1-bit adder that contains both bipolar and QETs. The adder has 17 transistors, two QETs and 15 bipolar transistors. **The circuit replaces 40 conventional transistors.**

QETs BOOST PERFORMANCE

Applications for Quantum-effect transistors includes:

- Communications: QETs in X-band analog-to-digital converters will boost performance of digital cellular telephones.
- Computers: will drive high-end computers to even higher performance.
- Consumer electronics: will provide high-bandwidth digital-video processing in high-definition television.
- Test equipment: will be used for high-speed triggering in instruments, such as oscilloscopes.

(ELECTRONICS, 13.12.1993)

Quantum-effect device called key to terabit memories

Fujitsu Ltd. of Tokyo has demonstrated a quantum-effect transistor which, according to the company, is "expected to pave the way for the development of 1-terabit-level memory and logic devices." Shown for the first time at this month's **International Solid-State Circuits Conference** in San Francisco, **the transistor is a second-generation ME (multi-emitter) RHET (resonant- tunneling hot electron transistor) that can execute complex logic functions.** The use of multiple emitters and the elimination of base electrodes makes this possible and also simplifies the fabrication process.

As an example of the potential of the new technology, Fujitsu researchers have formed a 3-input AND/NOR gate using only a single multi-emitter RHET and a resistor (see illustration). The two components replace the conventional configuration that requires a total of 18 transistors and resistors.

Although project scientists are convinced of the long-term potential of their research, Dr. Naoki Yokoyama, manager of the **Quantum Electron Devices Laboratory** in Atsugi, Japan, where the work is being carried out, concedes that commercial applications are still years in the future.

The RHET research is partially funded by the Ministry of International Trade and Industry's Quantum Device Project, which is also supporting the research efforts of five other firms, including **Motorola Corp.** of Schaumburg, Ill.

(ELECTRONICS, 28.2.1994)

M6805 compatible microprocessor core targetting a variety of ASIC processes

A process independent M6805 compatible ASIC microprocessor core, targetting a variety of double metal processes with geometries ranging from 0.8 to 2 microns has been launched by Austria Mikro Systeme International AG (AMS).

Similar to other AMS cores, the M6805 compatible device is implemented as a Microcore Design Kit, an approach welcomed by designers looking for more flexibility than is provided by the traditional "hardwired" approach. The kit consists of a six layer PCB featuring a fully scanable bond-out M6805 compatible microprocessor core including interrupt controller, breakpoint logic, JTAG-TAP interface, system PGA (Programmable Gate Array), usrer PGA, 128kB RAM, 64kB flash memory, 32k x 32 Bit signal recorder, PC TAP interface and PC parallel interface. By means of the user PGA, the developer can design his/her own peripherals and cu-

stom blocks. On completion of system evaluation, the microcore, together with the user's custom digital and analogue circuitry, is committed to silicon in a process and geometry selected by the user.

The M6805 compatible microprocessor core generated by the AMS design kit is based on the standard 8-Bit architecture and utilizes 100% compatible machine code. It features a byte efficient instruction set, with bit test and branch instructions, true bit manipulation, ROM-BIST, RAM-BIST and powerful indexed addressing modes. 8x8 multiplication is supported in many addressing modes. Other hardware features include a fully-static logic implementation, providing clock frequencies from DC to MHz.

The AMS M 6805 compatible microprocessor core is the latest example of an ASIC standard cell implemented by the company as a generator. These complex programmes automatically provide mask layout and simulation models, and allow the user considerable specifications flexibility. Generators are independent of the process technology used.

For further details please contact

Dr. Conrad Heberling, ext. 277
Schloß Premstätten
A-8141 Unterpremstätten, Austria
Telex 312547 ams a
Fax (03136) 52 501, 53 650
*tel: (03136) 500-0**

KOLEDAR PRIREDITEV 1994

JULY

04.07.-07.07.1994
INTERNATIONAL VACUUM MICROELECTRONICS CONFERENCE
Grenoble, France
(Info.:D:Celier, Tel.:33 1 42 78 15 82)

13.07.-15.07.1994
INTERNATIONAL ELECTRON DEVICES & MATERIALS SYMPOSIUM
Hsin Chu, Taiwan
(Info.:Chien Ping Lee, Tel.: 886-35-726100)

AUGUST

23.08.-26.08.1994
INTERNATIONAL CONFERENCE ON SOLID STATE DEVICES AND MATERIALS
Yokohama, Japan
(Info.: SSDM '94 Business Center, Tel.: 81-3-5814-5823)

29.08.-02.09.1994
INTERNATIONAL CONFERENCE ON HIGH SPEED PHOTOGRAPHY & PHOTONICS
Taejon, Korea
(Info.:Prof.Ung Kum, Dept.of physics, Yonsei University, Tel.:822-361-2617)

SEPTEMBER

05.09.-07.09.1994
ELECTROCERAMICS IV
INTERNATIONAL CONFERENCE ON ELECTRONIC CERAMICS & APPLICATIONS
RWTH Aachen, Germany

INTERNATIONAL SYMPOSIUM ON GALLIUM ARSENIDE & RELATED COMPONENTS

18.09.-22.09.1994
San Diego, CA, USA
(Info.: James Bell, Tel.: (908) 758-3386

28.09.-30.09.1994
22nd INTERNATIONAL CONFERENCE ON MICROELECTRONICS, MIEL '94
30th SYMPOSIUM ON DEVICES AND MATERIALS, SD '94
TERME ZREČE, Rogla, Slovenija(Info.:Meta Limpel, Tel.: 386 61 312 898)

OCTOBER

02.10.-05.10.1994
INTERNATIONAL CONFERENCE ON SYSTEM, MAN & CYBERNETICS
San antonio, TX, USA
(Info.: Dr.D.Y.Lee, Tel.: (518) 276-8174

04.10.-07.10.1994
ESREF '94
5th EUROPEAN SYMPOSIUM ON RELIABILITY OF ELECTRON DEVICES, FAILURE PHYSICS AND ANALYSIS
Glasgow, Scotland
(Info.: G.M.Brydon, Tel.: 44 604 408647)

10.10.-13.10.1994
INTERNATIONAL CONFERENCE ON COMPUTER DESIGN:VLSI IN COMPUTERS AND PROCESSORS
Cambridge, MA, USA
(Info.: IEEE Computer Society, Tel.:(202) 371-0101

NAVODILA AVTORJEM

Informacije MIDEM je znanstveno-strokovno-društvena publikacija Strokovnega društva za mikroelektroniko, elektronske sestavne dele in materiale-MIDEM. Časopis objavlja prispevke domačih in tujih avtorjev, še posebej članov MIDEM, s področja mikroelektronike, elektronskih sestavnih delov in materialov, ki so lahko:

izvirni znanstveni članki, predhodna sporočila, pregledni članki, razprave z znanstvenih in strokovnih posvetovanj in strokovni članki.

Članki bodo recenzirani.

Časopis objavlja tudi novice iz stroke, vesti iz delovnih organizacij, inštitutov in fakultet, obvestila o akcijah društva MIDEM in njegovih članov ter druge relevantne prispevke.

Strokovni prispevki morajo biti pripravljeni na naslednji način

- 1. Naslov dela, imena in priimki avtorjev brez titul.
- 2. Ključne besede in povzetek (največ 250 besed).
- 3. Naslov dela v angleščini.
- 4. Ključne besede v angleščini (Key words) in podaljšani povzetek (Extended Abstract) v angleščini.
- 5. Uvod, glavni del, zaključek, zahvale, dodatki in literatura.
- 6. Imena in priimki avtorjev, titule in naslovi delovnih organizacij, v katerih so zaposleni.

Ostala splošna navodila

1. V članku je potrebno uporabljati SI sistem enot oz. v oklepaju navesti alternativne enote.

2. Risbe je potrebno izdelati s tušem na pavs ali belem papirju. Širina risb naj bo do 7.5 oz. 15 cm. Vsaka risba, tabela ali fotografija naj ima številko in podnapis, ki označuje njeno vsebino. Risb, tabel in fotografij ni potrebno lepiti med tekst, ampak jih je potrebno ločeno priložiti članku. V tekstu je potrebno označiti mesto, kjer jih je potrebno vstaviti.

3. Delo je lahko napisano in bo objavljeno v kateremkoli jugoslovanskem jeziku v latinici in v angleščini.

Uredniški odbor ne bo sprejel strokovnih člankov, ki ne bodo poslani v dveh izvodih.

Avtorji, ki pripravljajo besedilo v urejevalnikih besedil, lahko pošljejo zapis datoteke na disketi (1.2 ali 1.44) v formatih ASCII, wordstar (3.4, 4.0), wordperfect, word, ker bo besedilo oblikovano v programu Ventura 2.0. Grafične datoteke so lahko v formatu HPL, SLD (AutoCAD), PCX ali IMG/GEM.

Avtorji so v celoti odgovorni za vsebino objavljenega sestavka. Rokopisov ne vračamo.

Rokopise pošljite na naslov

Uredništvo Informacije MIDEM
Elektrotehniška zveza Slovenije
Dunajska 10, 61000 Ljubljana

UPUTE AUTORIMA

Informacije MIDEM je znanstveno-stručno-društvena publikacija Stručnog društva za mikroelektroniku, elektronske sestavne dijelove i materijale - MIDEM. Časopis objavljuje priloge domaćih i stranih autora, naročito članova MIDEM, s područja mikroelektronike, elektronskih sastavnih dijelova in materijala koji mogu biti:

izvorni znanstveni članci, predhodna priopćenja, pregledni članci, izlaganja sa znanstvenih i stručnih skupova i stručni članci.

Članci će biti recenzirani.

Časopis također objavljuje novosti iz struke, obavijesti iz radnih organizacija, instituta i fakulteta, obavijesti o akcijama društva MIDEM i njegovih članova i druge relevantne obavijesti.

Stručni članci moraju biti pripremljeni kako slijedi

- 1. Naslov članka, imena i prezimena autora bez titula.
- 2. Ključne riječi i sažetak (najviše 250 riječi).
- 3. Naslov članka na engleskom jeziku.
- 4. Ključne riječi na engleskom jeziku (3Key Words) i produženi sažetak (Extended Abstract) na engleskom jeziku.
- 5. Uvod, glavni dio, zaključni dio, zahvale, dodaci i literatura.
- 6. Imena i prezimena autora, titule i naslovi institucija u kojima su zaposleni.

Ostale opšte upute

1. U prilogu treba upotrebljavati SI sistem jedinica od. u zagradi navesti alternativne jedinice.

2. Crteže treba izraditi tušem na pausu ili bijelom papiru. Širina crteža neka bude do 7.5 odnosno 15 cm. Svaki crtež, tablica ili fotografija treba imati broj i naziv koji označuje njen sadržaj. Crteže, tabele i fotografije nije potrebno lijepiti u tekst, već ih priložiti odvojeno, a u tekstu samo naznačiti mjesto gdje dolaze.

3. Rad može biti pisan i biti će objavljen na bilo kojem od jugoslavenskih jezika u latinici i na engleskom jeziku.

Autori mogu poslati radove na disketama (1.2 ili 1.44) u formatima tekst procesora ASCII, wordstar (3.4. i 4.0), word, wordperfect pošto će biti tekst dalje obrađen u Venturi 2.0. Grafičke datoteke mogu biti u formatu HPL, SLD (AutoCAD), PCX ili IMG/GEM.

Urednički odbor će odbiti sve radove koji neće biti poslani u dva primjerka.

Za sadržaj članaka autori odgovaraju u potpunosti. Rukopisi se na vraćaju.

Rukopise šaljite na adresu:

Uredništvo Informacije MIDEM
Elektrotehnična zveza Slovenije
Dunajska 10, 61000 Ljubljana
Slovenija

INFORMATION FOR CONTRIBUTORS

Informacije MIDEM is professional-scientific-social publication of Professional Society for Microelectronics, Electronic Components and Materials. In the Journal contributions of domestic and foreign authors, especially members of MIDEM, are published covering field of microelectronics, electronic components and materials. These contributions may be:

original scientific papers, preliminary communications, reviews, conference papers and professional papers.

All manuscripts are subject to reviews.

Scientific news, news from the companies, institutes and universities, reports on actions of MIDEM Society and its members as well as other relevant contributions are also welcome.

Each contribution should include the following specific components:

- 1. Title of the paper and authors' names.
- 2. Key Words and Abstract (not more than 250 words).
- 3. Introduction, main text, conclusion, acknowledgements, appendix and references.
- 4. Authors' names, titles and complete company or institution adress.

General information

1. Authors should use SI units and provide alternative units in parentheses wherever necessary.

2. Illustrations should be in black on white or tracing paper. Their width should be up to 7.5 or 15 cm. Each illustration, table or photograph should be numbered and with legend added. Illustrations, tables and photografphs are not to be placed into the text but added separatelly. Hower, their position in the text should be clearly marked.

3. Contributions may be written and will be published in any Yugoslav language and in english.

Authors may send their files on formatted diskettes (1.2 or 1.44) in ASCII, wordstar (3.4 or 4.0), word, wordperfect as text will be formated in Ventura 2.0. Graphics may be in HPL, SLD (AutoCAD), PCX or IMG/GEM formats.

Papers will not be accepted unless two copies are received.

Authors are fully responsible for the content of the paper. Manuscripts are not returned.

Contributions are to be sent to the address:

Uredništvo Informacije MIDEM
Elektrotehniška zveza Slovenije
Dunajska 10, 61000 Ljubljana,
Slovenia

2 Polprevodniške diode :

Zaporedna številka	Izrazi v jezikih jugoslovanskih narodov	Izrazi v tujih jezikih	D e f i n i c i j a
1	2	3	4
2.1	Signalne diode majhne moči (izrazi, ki se nanašajo na mejne vrednosti in karakteristike)		
2.1.1	• Konstantni (jednosmerni) inverzni napon • Konstantni (stalni) istosmjerni zaporni napon • Постојан инверзен напон • Trajna (enosmerna) zaporna napetost, trajna (enosmerna) inverzna napetost	147–0/IA–1.1 • Continuous (direct) reverse voltage • Tension inverse continue permanente	Vrednost trajne napetosti, ki je na diodi v zaporni smeri.
2.1.2	• Srednji inverzni napon • Srednji zaporni napon • Среден инверзен напон • Povprečna zaporna napetost, povprečna inverzna napetost	147–0/IA–1.2 • Mean reverse voltage • Tension inverse moyenne	Povprečna vrednost zaporne napetosti, ki je izračunana za določen čas.
2.1.3	• Vršni inverzni napon • Vršni zaporni napon • Врвен инверзен напон • Temenska zaporna napetost, temenska inverzna napetost	147–0/IA–1.3 • Peak reverse voltage • Tension inverse de crête	Maksimalna trenutna vrednost zaporne napetosti, ki se pojavlja na diodi vključujoč vse ponovitvene in neponovitvene prehodne pojave.

1	2	3	4
2.1.4	• Srednja direktna (propusna) struja • Srednja propusna struja • Средна директна струја • Povprečni prepustni tok	147–0/IA–1.4 • Mean forward current • Courant direct moyen	Povprečna vrednost prepustnega toka, izračunana za določen čas.
2.1.5	• Koeficijent detekcije (naponski) • Koeficijent detekcije (naponski) • Коефициент на детекција (по напон) • Učinkovitost napetostnega usmerjanja	147–0/IA–1.5 • Detector voltage efficiency • Efficacité de détection en tension	Razmerje med enosmerno napetostjo bremena in temensko vrednostjo sinusne vhodne napetosti ob določenih pogojih električnega vezja.
2.1.6	• Efikasnost detekcije (po snazi) • Efikasnost detekcije (po snazi) • Ефикасност на детекција (по моќност) • Učinkovitost močnostnega usmerjanja	147–0/IA–1.6 • Detector power efficiency • Efficacité de détection en puissance	Razmerje med spremembo enosmerne moči na obremenilnem uporu, ki ga povzroči izmenični signal, in razpoložljivo močjo iz generatorja sinusne napetosti, kadar dioda deluje pod določenimi pogoji.
2.1.7	• Naelektrisanje oporavka • Naboj oporavka • Полнеж на смирување • Nakopičena elektrina	147–0/IA–1.7 • Recovered charge • Charge recouvrée	Skupna elektrina, nakopičena v diodi po preklopu iz stanja določenega prepustnega toka v stanje označenega zapornega toka. Opomba: Ta naelektrenost vključuje komponente zaradi kopičenja nosilcev elektrine in zaradi kapacitivnosti osiromašene plasti.
2.1.8	• Dinamička (diferencijalna) otpornost • Dinamički otpor • Динамичка (диференцијална) отпорност • Diferencialna upornost	147–0/IA–1.8 • Differential resistance • Résistance différentielle	Diferencialna upornost, merjena med priključkoma diode pri določenih pogojih merjenja.

1	2	3	4
2.1.9	• Statička otpornost u direktnom smeru • Statički otpor u propusnom smjeru • Директна статичка отпорност • Enosmerna prepustna upornost	147–0/IA–1.9 • Foward D.C. resistance • Résistance direct en courant continu	Razmerje med enosmerno napetostjo v prepustne smeri, ki je priključena na diodo, in pripadajočim enosmernim tokom v prepustni smeri.
2.1.10	• Statička otpornost u inverznom smeru • Statički otpor u zapornom smjeru • Инверзна статичка отпорност • Enosmerna zaporna upornost, enosmerna inverzna upornost	147–0/IA–1.10 • Reverse D. C. resistance • Résistance inverse en courant continu	Razmerje med enosmerno zaporno napetostjo, ki je priključena na diodo, in pripadajočim enosmernim zapornim tokom.
2.1.11	• Kapacitivnost pri malom signalu • Kapacitivnost pri malom signalu • Динамичка капацитивност • Kapacitivnost pri majhnem signalu	147–0/IA–1.11 • Small-signal capacitance • Capacité différentielle	Diferencialna kapacitivnost med priključkoma diode, merjena pri podanih pogojih polarizacije.
2.1.12	• Vreme uključenja • Vrijeme uključenja • Време на вклучување • Prepustni vzpostavitveni čas	147–0/IA–1.12 • Forward recovery time • Temps de recouvrement direct	Čas, ki je potreben, da tok ali napetost doseže določeno vrednost po trenutni preklopitvi od nič ali od določene zaporne napetosti na določene prepustne polarizacijske pogoje.
2.1.13	• Vreme oporavka • Vrijeme oporavka • Време на исклучување • Zaporni vzpostavitveni čas	147–0/IA–1.13 • Reverse recovery time • Temps de recouvrement inverse	Čas, ki je potreben, da tok ali napetost doseže določeno vrednost po trenutni preklopitvi od določenih pogojev toka v prepustni smeri na določene zaporne polarizacijske pogoje.

MIKROIKS d.o.o.
Dunajska 5
61000 Ljubljana
SLOVENIJA

telefon: +386 (0)61 312 898
1332310
fax: +386 (0)61 319 170
odzivnik: 1332310

UGODNA PONUDBA RABLJENE OPREME IN KEMIKALIJ

Po zelo ugodni ceni in pod ugodnimi pogoji nudimo naslednjo rabljeno opremo:

1. Peč za temperaturno obdelavo vzorcev, Tempress M280

2. Kemično odporna jedkalna postaja z enim koritom, MicroAir

3. Delovna postaja z laminarnim pretokom zraka, 4", 6" in 8", MicroAir

4. Sistem za temperaturno staranje integriranih vezij, Marin Controls, System 25

5. Naparjevalnik za zlato in aluminij na silicijevih rezinah, MIPOT

6. Merilnik TOC (Total Organic Carbon) v vodi, Anatel A-100P

7. Elipsometer, Rudolph AutoEL III

8. Detektor vodika z ustrezno elektroniko in sondami, Auer

9. Avtomatski detektor arsina in fosfina, Matheson M8040

11. Ročni detektor strupenih plinov, Dräger

12. 572 Bayard Alpert Ionization Gauge

13. Avtomatski in ročni poravnalnik rezin (FLAT FINDER), H_2CO

14. Čistilnik plinov, Matheson 460 z vložki

15. Merilnik upornosti vode s sondo, Balsbaugh 900

16. Kemikalije in plini po seznamu

V kolikor se zanimate za katerega od naštetih izdelkov nas, prosim, pokličite!!!